DOCTORAL THESIS

The Virtual Photon Structure to the Next-to-next-to-leading Order in QCD

TAKAHIRO UEDA

Department of Physics, Faculty of Engineering
Yokohama National University

March 2007

Abstract

We investigate the spin-averaged virtual photon structure functions, which can be measured from two-photon processes in the future e^+e^- collider experiments. Especially we focus on $F_2^\gamma(x, Q^2, P^2)$ in the kinematical region $\Lambda^2 \ll P^2 \ll Q^2$, where $-Q^2$ and $-P^2$ are the mass squared of the probe and target photons, respectively, and Λ is the QCD scale parameter. In such a region, the photon structure functions can be calculated by the perturbative method without any experimental data input. The analysis is performed in massless QCD up to the order $\alpha\alpha_s$, which corresponds to the next-to-next-to-leading order (NNLO), and in leading twist approximation. We show that the NNLO contributions to F_2^γ are not small, particularly at large x. We also examine the longitudinal structure function $F_L^\gamma(x, Q^2, P^2)$ up to the order $\alpha\alpha_s$, which corresponds to the next-to-leading order (NLO).

Contents

List of Figures

List of Tables

Chapter 1

Introduction

The Large Hadron Collider (LHC) experiments will be started soon and it is much expected that signals for the new physics beyond the Standard Model (SM) will be discovered [1]. Once these signals are observed, it is preferable that they are examined more closely in a next generation electron-positron linear collider, i.e., the International Linear Collider (ILC) [2]. The outcomes of these experiments will open the door to deeper and wider understandings of the nature of our world, and will lead us to the next stage in the progress of the particle physics within a few decades.

However, to analyze these signals from the new physics and extract the maximum information from the experimental data, the knowledge of the SM, especially, of Quantum Chromodynamics (QCD) will be more important than ever before. It is important not only to explore the possibilities of the new physics but also to scrutinize phenomena arising from the known physics, because they can be sources of background in the high precision tests. For example, it is known that, in e^+e^- collision experiments, the cross section for the two-photon processes $e^+e^- \to e^+e^-\gamma\gamma \to e^+e^-X$ shown in Fig. 1.1 dominates at high energies over other processes such as the annihilation process $e^+e^- \to \gamma \to X$. In particular, the two-photon process, in which one of the virtual photon is very far off-shell (large $Q^2 = -q^2$) regarded as a probe photon, while the other is small $P^2 \ll Q^2$ (small $P^2 = -p^2$), can be viewed as a deep-inelastic electron-photon scattering where the target is a photon instead of a nucleon [3]. In this deep-inelastic scattering off photon targets, we can study the photon structure functions, which are the analogs of the nucleon structure functions. The photon structure functions are defined in the lowest order of the QED coupling constant $\alpha = e^2/(4\pi)$ and, in this work, they are of order α.

For the unpolarized (spin-averaged) structure function $F_2^\gamma(x, Q^2)$ in the case of the real photon target ($P^2 = 0$), the leading order (LO) corrections to the *point-like* parton model result [5, 6] were derived long

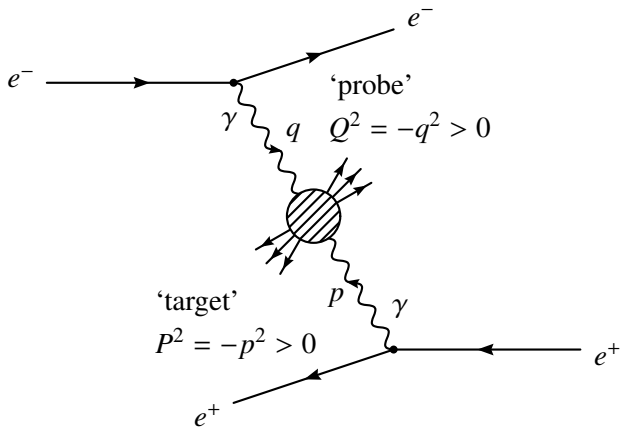

Figure 1.1: Deep inelastic scattering on a photon in the e^+e^- collider experiments.

ago [7], and the next-to-leading order (NLO) contributions were calculated a few years later [8], but only recently the next-to-next-to leading (NNLO) contributions have been completed [9].

A unique and interesting feature of the photon structure functions is that, in contrast with the nucleon case, the target mass squared $-P^2$ is not fixed but can take various values and that they show different behaviors depending on the values of P^2. The photon has two characters: The photon couples directly to quarks (pointlike nature) and sometimes it behaves as vector bosons (hadronic nature) [10]. Therefore the real photon structure function $F_2^\gamma(x, Q^2)$ may be decomposed as the pointlike piece and the hadronic piece. The former can be calculated, in principle, in a perturbative method, but the latter can only be computed by some non-perturbative method like lattice QCD, or estimated by vector meson dominance model (VDM) [10].

It was pointed out by Uematsu and Walsh [11] that the situation changes significantly when we consider the following kinematical region:

$$\Lambda^2 \ll P^2 \ll Q^2, \tag{1.1}$$

where Λ is the QCD scale parameter. In this kinematic region, the hadronic piece in $F_2^\gamma(x, Q^2, P^2)$ is negligible and decreases as powers of P^2. Therefore we can calculate whole structure functions, in principle, up to all orders in QCD by the perturbative method. Indeed, the spin-averaged virtual photon structure function $F_2^\gamma(x, Q^2, P^2)$ was studied before in the LO [11] and NLO [12, 13]. Meanwhile, the spin-dependent virtual structure functions $g_1^\gamma(x, Q^2, P^2)$ and $g_2^\gamma(x, Q^2, P^2)$ for the kinematical region Eq. (1.1) have been also studied in QCD [14, 15, 16]. Recently, the first moment of $g_1^\gamma(x, Q^2, P^2)$ was calculated up to the NNLO [17], and the transition of $g_1^\gamma(x, Q^2, P^2)$, when the target photon shifts from real to highly-virtual region, was investigated by using VDM for the estimation of the non-perturbative effects on the photon matrix elements [18].

In this thesis, the analysis of $F_2^\gamma(x, Q^2, P^2)$ in the kinematic region Eq. (1.1) is performed in massless perturbative QCD, up to the order $\alpha\alpha_s$, which corresponds to the NNLO, and in leading twist approximation. We use the operator product expansion (OPE) and the renormalization group (RG) approach. It is shown that the NNLO corrections are not small in comparison with the LO and NLO contributions, in particular at large x. We also discuss the longitudinal structure function $F_L^\gamma(x, Q^2, P^2)$ up to the order $\alpha\alpha_s$, which corresponds to the NLO.

This thesis is organized as follows. In the next chapter the photon structure functions for the virtual photon target are defined. Moreover some aspects of QCD are reviewed, for later use. In Chapter 3, using the operator product expansion (OPE) and the renormalization group (RG) method, we obtain the moment sum rules of the structure functions $F_2^\gamma(x, Q^2, P^2)$ and $F_L^\gamma(x, Q^2, P^2)$ up to the order $\alpha\alpha_s$. We also provide the necessary ingredients for the analysis, such as the coefficient functions and anomalous dimensions of the relevant operators, and photon matrix elements of these operators, all of which are calculated in the $\overline{\text{MS}}$ scheme [19]. In Chapter 4, we invert the moment sum rules to obtain the structure functions $F_2^\gamma(x, Q^2, P^2)$ and $F_L^\gamma(x, Q^2, P^2)$ as functions of x. Chapter 5 is devoted to the summary of our study and the future outlook.

Chapter 2

Preliminaries

In this chapter, we introduce the structure functions of the (virtual) photon, which is our subject in this thesis, through the discussion about the two-photon process in e^+e^- collision. Additionally, we review some aspect of tools for our analysis, for later use. More detailed arguments may be found in a number of textbooks and reviews; please refer to, for example, Refs. [20, 21].

2.1 Structure of the Photon

2.1.1 Two-photon Process in e^+e^- Collision

Let us consider the particle production in e^+e^- collision such as $e^+e^- \to e^+e^-X$. The dominant process at high energy is the two-photon process [3, 4]

$$e^-(l_1)e^+(l_2) \to e^-(l_1')e^+(l_2')\gamma(q)\gamma(p) \to e^-(l_1')e^+(l_2')X(P_X), \tag{2.1}$$

which is depicted in Fig. 2.1 [♯1]. The momenta of the incoming and outgoing leptons are denoted by l_1, l_2, l_1' and l_2', respectively, and the momenta of the photons are expressed as

$$\begin{aligned} q &= l_1 - l_1', \qquad q^2 = -Q^2 < 0, \\ p &= l_2 - l_2', \qquad p^2 = -P^2 < 0. \end{aligned} \tag{2.2}$$

Note that p and q are in general space-like for this process. For later use, we also define the Bjorken scaling variable x

$$x = \frac{Q^2}{2\nu}, \qquad \nu = p \cdot q. \tag{2.3}$$

Since $(p+q)^2 \geq 0$ for the physical particle production, x is in the range of $0 \leq x \leq 1$.

This process can be regarded as the deep inelastic electron-photon scattering and we can investigate $\gamma\gamma$ scattering through this process, using an analogy from the study of γp scattering via the experiments on the deep inelastic electron-proton scattering. P^2 shall be smaller than Q^2, $P^2 \leq Q^2$, and the *probe* photon and *target* photon refer to the photon with their virtuality P^2 and Q^2, respectively.

Differential Cross Section The differential cross section for the process Eq. (2.1) is given by

$$d\sigma = \frac{1}{4\sqrt{(l_1 \cdot l_2)^2 - m_e^4}} \frac{d^3l_1'}{(2\pi)^3 2E_1'} \frac{d^3l_2'}{(2\pi)^3 2E_2'} \sum_X |\mathcal{M}|^2 (2\pi)^4 \delta^4(p + q - P_X) d\Gamma, \tag{2.4}$$

[♯1] Potentially there exist the contributions from other diagrams, s- and t-channel bremsstrahlung diagrams where hadrons in the final states are produced by the bremsstrahlung photon, and Z boson exchange diagrams, can be ignored when appropriate cuts are used. At first, the s-channel diagram is suppressed by a factor E^{-2}. Secondly, the two-photon process has at least one more power of a collinear logarithm $\ln(E/m_e)$ than the t-channel diagram. Finally, Z boson exchange diagrams have no effect if the virtualities of the boson are not too large than the mass of the Z boson.

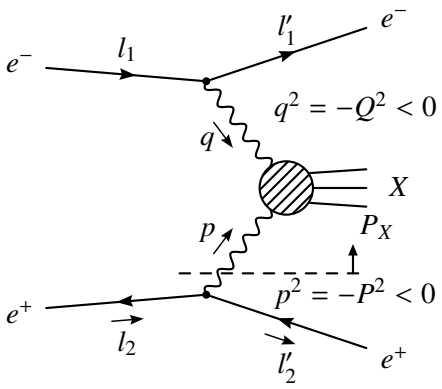

Figure 2.1: The particle production via two-photon process in the lepton-lepton scattering, $e^-(l_1)e^+(l_2) \to e^-(l'_1)e^+(l'_2)\gamma(q)\gamma(p) \to e^-(l'_1)e^+(l'_2)X(P_X)$. The subprocess above dashed line can be regarded as the deep inelastic scattering on a virtual photon. The mass squared of the probe and target photons are $-Q^2$ and $-P^2$, respectively.

where $E'_1 = l'^0_1$ and $E'_2 = l'^0_2$ are energy of the outgoing leptons, m_e is the electron mass, $\mathcal{M}$ is the invariant matrix element and

$$P_X = \sum_{i=1}^{n_X} p_i, \qquad d\Gamma = \prod_{i=1}^{n_X} \frac{d^3 p_i}{(2\pi)^3 2p_i^0}, \tag{2.5}$$

are the total momentum and the phase-space volume, respectively, of the produced hadron system X.

For the two-photon process, it is convenient to rewrite the cross section Eq. (2.4) as the following form, by separating into the leptonic part and the hadronic part (Fig. 2.2)

$$d\sigma = \frac{d^3 l'_1 d^3 l'_2}{2E'_1 2E'_2 (2\pi)^6} \frac{(4\pi\alpha)^3}{p^2 q^2} \frac{1}{4\sqrt{(l_1 \cdot l_2)^2 - m_e^4}} \rho_1^{\mu\nu} \rho_2^{\rho\tau} \cdot 2\pi W_{\mu\nu\rho\tau}. \tag{2.6}$$

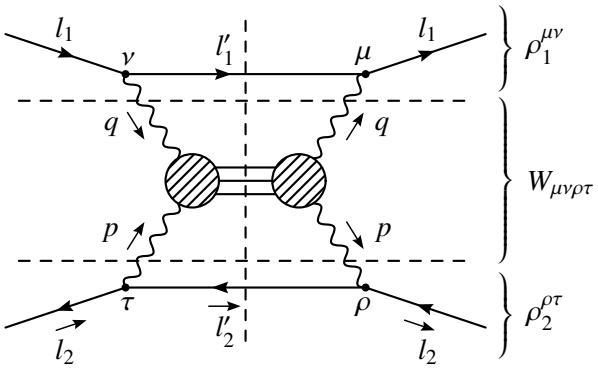

Figure 2.2: The squared amplitude for the two-photon process can be separated into the leptonic part and the hadronic part.

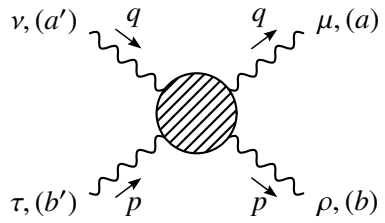

Figure 2.3: Forward scattering of a photon with momentum q and another photon with momentum p. a, b, a' and b' are the helicities of the final state and initial state photons, respectively.

In the leptonic part, the photon density matrix $\rho_1^{\mu\nu}$ and $\rho_2^{\rho\tau}$ are (summed over final spins)

$$\begin{aligned}\rho_1^{\mu\nu} &= \frac{1}{-q^2}\sum_{s_1'}\bar{u}(l_1,s_1)\gamma^\mu u(l_1',s_1')\bar{u}(l_1',s_1')\gamma^\nu u(l_1,s_1)\\ &= -\left(g^{\mu\nu}-\frac{q^\mu q^\nu}{q^2}\right)-\frac{(2l_1-q)^\mu(2l_1-q)^\nu}{q^2}-\frac{2im_e\epsilon^{\mu\nu\alpha\beta}s_{1\alpha}q_\beta}{q^2},\end{aligned} \tag{2.7a}$$

$$\begin{aligned}\rho_2^{\rho\tau} &= \frac{1}{-p^2}\sum_{s_2'}\bar{v}(l_2,s_2)\gamma^\tau v(l_2',s_2')\bar{v}(l_2',s_2')\gamma^\rho v(l_2,s_2)\\ &= -\left(g^{\rho\tau}-\frac{p^\rho p^\tau}{p^2}\right)-\frac{(2l_2-p)^\rho(2l_2-p)^\tau}{p^2}-\frac{2im_e\epsilon^{\rho\tau\alpha\beta}s_{2\alpha}p_\beta}{p^2},\end{aligned} \tag{2.7b}$$

where s_1, s_2, s_1' and s_2' are polarization vectors of the incoming and outgoing leptons, respectively, and normalized as $s_i^2=-1$. The hadronic tensor $W_{\mu\nu\rho\tau}$ is defined by[♯2]

$$(4\pi\alpha)W_{\mu\nu\rho\tau} = \frac{1}{2\pi}\sum_X\int d\Gamma\, M_{\mu\rho}^* M_{\nu\tau}\times(2\pi)^4\delta^4(p+q-P_X), \tag{2.8}$$

where $M_{\nu\tau}$ is the amplitude of the $\gamma(q)+\gamma(p)\to X$ subprocess.

2.1.2 Hadronic Tensor and Structure Functions

According to the optical theorem, the hadronic tensor $W_{\mu\nu\rho\tau}$ is related to the absorptive part of the photon-photon forward scattering amplitude for $\gamma(q)+\gamma(p)\to\gamma(q)+\gamma(p)$ (Fig. 2.3):

$$T_{\mu\nu\rho\tau}(p,q) = i\int d^4x\, d^4y\, d^4z\, e^{iq\cdot x}e^{ip\cdot(y-z)}\langle 0|T(J_\mu(x)J_\nu(0)J_\rho(y)J_\tau(z))|0\rangle, \tag{2.9}$$

(where J is the electromagnetic current) as follows

$$\begin{aligned}W_{\mu\nu\rho\tau}(p,q) &= \frac{1}{2\pi}\int d^4x\, d^4y\, d^4z\, e^{iq\cdot x}e^{ip\cdot(y-z)}\langle 0|T^*(J_\mu(x)J_\rho(y))T(J_\nu(0)J_\tau(z))|0\rangle\\ &= \frac{1}{\pi}\,\mathrm{Im}\,T_{\mu\nu\rho\tau}(p,q).\end{aligned} \tag{2.10}$$

In general, taking into account P-, T- and gauge-invariance, the tensor $W_{\mu\nu\rho\tau}$ can be decomposed in terms of the basis of eight independent tensors, which are constructed from the vectors q, p and the metric tensor g [22, 23, 24]. Here we construct $W_{\mu\nu\rho\tau}$ from eight structure functions along with Ref. [22].

[♯2]Note that, in our definition, the structure tensor $W_{\mu\nu\rho\tau}$ is proportional to α.

Helicity Amplitudes At first, let us define the helicity amplitudes as follows

$$W(a,b|a',b') = \epsilon^*_\mu(q,a)\epsilon^*_\rho(p,b)W^{\mu\nu\rho\tau}\epsilon_\nu(q,a')\epsilon_\tau(p,b'), \tag{2.11}$$

where $\epsilon^\mu(a)$ represents the photon polarization vector with helicity a, and $a = 0, \pm 1$. Similar ones for the other polarization vectors (See Fig. 2.3). There are constraints reducing the number of independent $W(a,b|a',b')$ to eight. $W(a,b|a',b')$ vanishes unless it satisfies the condition $a - b = a' - b'$ due to the angular momentum conservation. And parity conservation and time reversal invariance lead to

$$\begin{aligned} W(a,b|a',b') &= W(-a,-b|-a',-b') && \text{parity conservation} \\ &= W(a',b'|a,b). && \text{time reversal invariance} \end{aligned} \tag{2.12}$$

We may take eight independent helicity amplitudes as

$$\begin{aligned} &W(1,1|1,1), \quad W(1,-1|1,-1), \quad W(1,0|1,0), \quad W(0,1|0,1), \quad W(0,0|0,0), \\ &W(1,1|-1,-1), \quad W(1,1|0,0), \quad W(1,0|0,-1). \end{aligned} \tag{2.13}$$

The first five amplitudes are helicity-nonflip and the last three involve helicity flips. Note that the helicity-nonflip amplitudes are semipositive

$$W(a,b|a,b) \geq 0, \tag{2.14}$$

but not the helicity-flip ones. And besides, there are three independent positivity constraints on these amplitudes due to the Cauchy-Schwarz inequality [25]

$$|W(a,b|a',b')| \leq \sqrt{W(a,b|a,b)W(a',b'|a',b')}, \tag{2.15}$$

or explicitely

$$|W(1,1|,-1,-1)| \leq W(1,1|1,1), \tag{2.16a}$$

$$|W(1,1|0,0)| \leq \sqrt{W(1,1|1,1)W(0,0|0,0)}, \tag{2.16b}$$

$$|W(1,0|,0,-1)| \leq \sqrt{W(1,0|1,0)W(0,1|0,1)}. \tag{2.16c}$$

Construction of Hadronic Structure Tensor Due to the completeness and orthogonality relations for (space-like) polarized vectors in Eq. (2.11), $W_{\mu\nu\rho\tau}$ can be expressed in terms of the helicity amplitudes:

$$W_{\mu\nu\rho\tau} = \sum_{a,b,a',b'} \epsilon_\mu(q,a)\epsilon_\rho(p,b)W(a,b|a',b')\epsilon^*_\nu(q,a')\epsilon^*_\tau(p,b'). \tag{2.17}$$

The gauge-invariance is ensured by construction due to $q \cdot \epsilon(q) = p \cdot \epsilon(p) = 0$. We use the following eight structure functions instead of the helicity amplitudes:

$$W_{TT} = \frac{1}{2}\left[W(1,1|1,1) + W(1,-1|1,-1)\right] = \frac{\sqrt{X}}{4\pi^2\alpha}\sigma_{TT}, \tag{2.18a}$$

$$W_{ST} = W(0,1|0,1) = \frac{\sqrt{X}}{4\pi^2\alpha}\sigma_{ST}, \tag{2.18b}$$

$$W_{TS} = W(1,0|1,0) = \frac{\sqrt{X}}{4\pi^2\alpha}\sigma_{TS}, \tag{2.18c}$$

$$W_{SS} = W(0,0|0,0) = \frac{\sqrt{X}}{4\pi^2\alpha}\sigma_{SS}, \tag{2.18d}$$

$$W^a_{TT} = \frac{1}{2}\left[W(1,1|1,1) - W(1,-1|1,-1)\right] = \frac{\sqrt{X}}{4\pi^2\alpha}\tau^a_{TT}, \tag{2.18e}$$

$$W^\tau_{TT} = W(1,1|-1,-1) = \frac{\sqrt{X}}{4\pi^2\alpha}\tau_{TT}, \tag{2.18f}$$

$$W^\tau_{TS} = \frac{1}{2}\left[W(1,1|0,0) - W(1,0|0,-1)\right] = \frac{\sqrt{X}}{4\pi^2\alpha}\tau_{TS}, \tag{2.18g}$$

$$W^{\tau a}_{TS} = \frac{1}{2}\left[W(1,1|0,0) + W(1,0|0,-1)\right] = \frac{\sqrt{X}}{4\pi^2\alpha}\tau^a_{TS}, \tag{2.18h}$$

where σ_{ab}'s are the total cross section of $\gamma(q,a)\gamma(p,b) \to X(P_X)$ scattering with photon polarization a and b:

$$\sigma_{ab} = \frac{1}{4\sqrt{X}} \times (2\pi)(4\pi\alpha)W_{ab}, \tag{2.19}$$

with $X = (p\cdot q)^2 - p^2q^2$. Since the helicity-nonflip amplitudes are semipositive, the first four quantities are positive definite but the last four are not. Then it follows that $W_{\mu\nu\rho\tau}$ is written as [22, 26]

$$\begin{aligned} W_{\mu\nu\rho\tau} = {} & (P_{TT})^{\mu\nu\rho\tau}W_{TT} + (P^a_{TT})^{\mu\nu\rho\tau}W^a_{TT} + (P^\tau_{TT})^{\mu\nu\rho\tau}W^\tau_{TT} + (P_{ST})^{\mu\nu\rho\tau}W_{ST} \\ & + (P_{TS})^{\mu\nu\rho\tau}W_{TS} + (P_{SS})^{\mu\nu\rho\tau}W_{SS} - (P^\tau_{TS})^{\mu\nu\rho\tau}W^\tau_{TS} - (P^{\tau a}_{TS})^{\mu\nu\rho\tau}W^{\tau a}_{TS}, \end{aligned} \tag{2.20}$$

where P_i's are the following projection operators:

$$(P_{TT})^{\mu\nu\rho\tau} = R^{\mu\nu}R^{\rho\tau}, \tag{2.21a}$$

$$(P^a_{TT})^{\mu\nu\rho\tau} = R^{\mu\rho}R^{\nu\tau} - R^{\mu\tau}R^{\nu\rho}, \tag{2.21b}$$

$$(P^\tau_{TT})^{\mu\nu\rho\tau} = \frac{1}{2}(R^{\mu\rho}R^{\nu\tau} + R^{\mu\tau}R^{\nu\rho} - R^{\mu\nu}R^{\rho\tau}), \tag{2.21c}$$

$$(P_{ST})^{\mu\nu\rho\tau} = k_1^\mu k_1^\nu R^{\rho\tau}, \tag{2.21d}$$

$$(P_{TS})^{\mu\nu\rho\tau} = R^{\mu\nu}k_2^\rho k_2^\tau, \tag{2.21e}$$

$$(P_{SS})^{\mu\nu\rho\tau} = k_1^\mu k_1^\nu k_2^\rho k_2^\tau, \tag{2.21f}$$

$$(P^\tau_{TS})^{\mu\nu\rho\tau} = R^{\mu\rho}k_1^\nu k_2^\tau + R^{\mu\tau}k_1^\nu k_2^\rho + k_1^\mu k_2^\rho R^{\nu\tau} + k_1^\mu k_2^\tau R^{\nu\rho}, \tag{2.21g}$$

$$(P^{\tau a}_{TS})^{\mu\nu\rho\tau} = R^{\mu\rho}k_1^\nu k_2^\tau - R^{\mu\tau}k_1^\nu k_2^\rho + k_1^\mu k_2^\rho R^{\nu\tau} - k_1^\mu k_2^\tau R^{\nu\rho}, \tag{2.21h}$$

with

$$R^{\mu\nu} = -g^{\mu\nu} + \frac{1}{X}\left[\nu(q^\mu p^\nu + p^\mu q^\nu) - q^2p^\mu p^\nu - p^2q^\mu q^\nu\right], \tag{2.22}$$

$$k_1^\mu = \sqrt{\frac{-q^2}{X}}\left(p^\mu - \frac{\nu}{q^2}q^\mu\right), \qquad k_2^\mu = \sqrt{\frac{-p^2}{X}}\left(q^\mu - \frac{\nu}{p^2}p^\mu\right). \tag{2.23}$$

The (virtual) photon structure functions W_i in Eqs. (2.18) are functions of three invariants, i.e., ν, Q^2 and P^2, and have no kinematical singularities. The subscript "T" and "S" of the structure functions refer to the transverse photon ($a = \pm 1$) and time-like photon ($a = 0$), respectively. The first subscript corresponds to the probe photon and the second one corresponds to the target photon. The superscript "τ" implies amplitudes with spin-flip for each of the photons with total helicity conservation, and the superscript "a" implies polarized ones, i.e., these amplitudes appear in the antisymmetric part of $W_{\mu\nu\rho\tau}$ under the interchange of $\mu \leftrightarrow \nu$ and $\rho \leftrightarrow \tau$. Due to the fact that $W_{\mu\nu\rho\tau}$ is symmetric under the simultaneous interchange of $(q, \mu, \nu) \leftrightarrow (p, \rho, \tau)$ (just turn Fig. 2.3 upside-down), all photon structure functions are symmetric under interchange of $p \leftrightarrow q$, with exception of W_{ST} and W_{TS}, which satisfy $W_{ST}(p, q) = W_{TS}(q, p)$.

The unit vectors k_1, k_2 and the symmetric tensor $R^{\mu\nu}$, the *metric tensor* of the subspace which is orthogonal to q and p, satisfy the following relations:

$$\begin{aligned} &q \cdot k_1 = p \cdot k_2 = 0, \qquad k_1^2 = k_2^2 = 1. \\ &q^\mu R_{\mu\nu} = p^\mu R_{\mu\nu} = k_1^\mu R_{\mu\nu} = k_2^\mu R_{\mu\nu} = 0, \quad R^{\mu\rho} R_\rho{}^\nu = -R^{\mu\nu}, \quad R^{\mu\nu} R_{\mu\nu} = -g^{\mu\nu} R_{\mu\nu} = 2. \end{aligned} \tag{2.24}$$

With the aid of these relations, one can find the following orthogonality and normalization relations:

$$\begin{aligned} &(P_i)^{\mu\nu\rho\tau}(P_j)_{\mu\nu\rho\tau} = 0, \qquad \text{for} \quad i \neq j, \\ &(P_{TT})^{\mu\nu\rho\tau}(P_{TT})_{\mu\nu\rho\tau} = 4, \qquad (P^a_{TT})^{\mu\nu\rho\tau}(P^a_{TT})_{\mu\nu\rho\tau} = 4, \qquad (P^\tau_{TT})^{\mu\nu\rho\tau}(P^\tau_{TT})_{\mu\nu\rho\tau} = 2, \\ &(P_{ST})^{\mu\nu\rho\tau}(P_{ST})_{\mu\nu\rho\tau} = 2, \qquad (P_{TS})^{\mu\nu\rho\tau}(P_{TS})_{\mu\nu\rho\tau} = 2, \qquad (P_{SS})^{\mu\nu\rho\tau}(P_{SS})_{\mu\nu\rho\tau} = 1, \\ &(P^\tau_{TS})^{\mu\nu\rho\tau}(P^\tau_{TS})_{\mu\nu\rho\tau} = 8, \qquad (P^{\tau a}_{TS})^{\mu\nu\rho\tau}(P^{\tau a}_{TS})_{\mu\nu\rho\tau} = 8. \end{aligned} \tag{2.25}$$

2.1.3 Spin-averaged Structure Functions and Unpolarized Cross Section

The hadronic structure $W_{\mu\nu\rho\tau}$ essentially represents the scattering of a probe photon on a target photon. For unpolarized target photon, as usual, one can average over spins of the target photon and introduce the structure functions for the spin-averaged target photon. This is done by contracting (4th. rank) hadronic tensor $W_{\mu\nu\rho\tau}$ with the polarization vectors of the target photon, and then we obtain the 2nd. rank tensor $W_{\mu\nu}$. This tensor can be decomposed into two functions[♯3] just as familiar structure functions of spin-1/2 targets, e.g., protons and neutrons.

Spin-averaged Structure Functions We take the spin average for the target photon and define the spin-averaged structure tensor:

$$\begin{aligned} W^\gamma_{\mu\nu}(p, q) &= \frac{1}{2} \sum_a \epsilon^{\rho *}(p, a) W_{\mu\nu\rho\tau}(p, q) \epsilon^\tau(p, a) \\ &= -\frac{1}{2} g^{\rho\tau} W_{\mu\nu\rho\tau}(p, q) \\ &= \frac{1}{2\pi} \int d^4x\, e^{iq\cdot x} \langle \gamma(p)| J_\mu(x) J_\nu(0) |\gamma(p)\rangle_{\text{spin ave}}. \end{aligned} \tag{2.26}$$

It relates to the absorptive part of the corresponding forward scattering amplitude

$$T_{\mu\nu}(p, q) = i \int d^4x\, e^{iq\cdot x} \langle \gamma(p)| T(J_\mu(x) J_\nu(0)) |\gamma(p)\rangle_{\text{spin ave}}, \tag{2.27}$$

such as

$$W^\gamma_{\mu\nu}(p, q) = \frac{1}{\pi} \operatorname{Im} T_{\mu\nu}. \tag{2.28}$$

[♯3] The spin-1 structure tensor (which consists of eight functions) can be decomposed into a spin-averaged (two functions), a spin-dependent symmetric (singly-polarized; four functions) and a spin-dependent antisymmetric part (two functions) [27, 28].

From the expression of $W_{\mu\nu\rho\tau}$ given in Eq. (2.20), we obtain

$$\begin{aligned} W^{\gamma}_{\mu\nu} &= R_{\mu\nu}\left[W_{TT} - \frac{1}{2}W_{TS}\right] + k_{1\mu}k_{1\nu}\left[W_{ST} - \frac{1}{2}W_{SS}\right] \\ &= -\left(g_{\mu\nu} - \frac{q_\mu q_\nu}{q^2}\right)\left[W_{TT} - \frac{1}{2}W_{TS}\right] \\ &\quad + \left(p_\mu - \frac{\nu}{q^2}q_\mu\right)\left(p_\nu - \frac{\nu}{q^2}q_\nu\right)\frac{Q^2}{X}\left[W_{TT} + W_{ST} - \frac{1}{2}W_{TS} - \frac{1}{2}W_{SS}\right]. \end{aligned} \tag{2.29}$$

On the other hand, the spin-averaged tensor $W^{\gamma}_{\mu\nu}$ can be expressed in the standard form in terms of the structure functions $F_1 = W_1$ and $2F_2 = \nu W_2$ as spin-1/2 targets:

$$W^{\gamma}_{\mu\nu} = -\left(g_{\mu\nu} - \frac{q_\mu q_\nu}{q^2}\right)F^{\gamma}_1 + \left(p_\mu - \frac{\nu}{q^2}q_\mu\right)\left(p_\nu - \frac{\nu}{q^2}q_\nu\right)\frac{2F^{\gamma}_2}{\nu}. \tag{2.30}$$

By comparing Eqs. (2.29) with (2.30), we find

$$F^{\gamma}_1 = W_{TT} - \frac{1}{2}W_{TS}, \tag{2.31a}$$

$$F^{\gamma}_2 = \frac{x}{\tilde{\beta}^2}\left[W_{TT} + W_{ST} - \frac{1}{2}W_{TS} - \frac{1}{2}W_{SS}\right], \tag{2.31b}$$

where

$$\tilde{\beta} = \sqrt{1 - 4x^2\frac{P^2}{Q^2}}. \tag{2.32}$$

The longitudinal structure function W_L is given by

$$W^{\gamma}_L = k^{\mu}_1 k^{\nu}_1 W^{\gamma}_{\mu\nu} = W_{ST} - \frac{1}{2}W_{SS}, \tag{2.33}$$

and F^{γ}_L with the appropriate normalization satisfies the usual relation when $P^2 \ll Q^2$ ($\tilde{\beta} \approx 1$):

$$F^{\gamma}_L = xW^{\gamma}_L = \tilde{\beta}^2 F^{\gamma}_2 - xF^{\gamma}_1 \approx F^{\gamma}_2 - xF^{\gamma}_1, \tag{2.34}$$

and then our expression for the spin-averaged structure tensor is

$$W^{\gamma}_{\mu\nu} = \left(g_{\mu\nu} - \frac{q_\mu q_\nu}{q^2}\right)\frac{F^{\gamma}_L}{x} + \left(-g_{\mu\nu} + \frac{q_\mu p_\nu + p_\mu q_\nu}{\nu} - \frac{p_\mu p_\nu}{\nu^2}q^2\right)\frac{F^{\gamma}_2}{x}. \tag{2.35}$$

Unpolarized Differential Cross Section Next let us see how the structure functions appear in the differential cross section of $e^+e^- \to e^+e^-X$. For unpolarized e^+e^- beams, the photon density matrix $\rho^{\mu\nu}_1$ and $\rho^{\rho\tau}_2$ Eqs. (2.7) becomes (averaged over initial spins)

$$\rho^{\mu\nu}_{1(\text{unpol})} = -\left(g^{\mu\nu} - \frac{q^\mu q^\nu}{q^2}\right) - \frac{(2l_1 - q)^\mu (2l_1 - q)^\nu}{q^2}, \tag{2.36a}$$

$$\rho^{\rho\tau}_{2(\text{unpol})} = -\left(g^{\rho\tau} - \frac{p^\rho p^\tau}{p^2}\right) - \frac{(2l_2 - p)^\rho (2l_2 - p)^\tau}{p^2}, \tag{2.36b}$$

and finally one can obtain the $ee \to eeX$ cross section for unpolarized beams in terms of $\gamma\gamma \to X$ cross sections [20, 22-b, 29, 30]

$$\begin{aligned} d^6\sigma_{(\text{unpol})}(ee \to eeX) = \frac{d^3l'_1 d^3l'_2}{l'^0_1 l'^0_2}\frac{\alpha^2}{16\pi^4 Q^2 P^2}\sqrt{\frac{(p\cdot q)^2 - Q^2P^2}{(l_1\cdot l_2)^2 - m_e^4}} \\ \times\Big[4\rho^{++}_1\rho^{++}_2\sigma_{TT} + 2\rho^{00}_1\rho^{++}_2\sigma_{ST} + 2\rho^{++}_1\rho^{00}_2\sigma_{TS} + \rho^{00}_1\rho^{00}_2\sigma_{SS} \\ + 2|\rho^{+-}_1\rho^{+-}_2|\tau_{TT}\cos 2\phi - 8|\rho^{+0}_1\rho^{+0}_2|\tau_{TS}\cos\phi\Big], \end{aligned} \tag{2.37}$$

where ϕ is the angle between the scattering planes of the scattered e^+ and e^- in the center-of-mass system of the colliding photons, and ρ_i^{ab}'s are elements of the photon density matrix:

$$\begin{aligned} 2\rho_1^{++} &= \frac{1}{X}(2l_1\cdot p-\nu)^2+1-4\frac{m_e^2}{Q^2}, \qquad 2\rho_2^{++} = \frac{1}{X}(2l_2\cdot q-\nu)^2+1-4\frac{m_e^2}{P^2}, \\ \rho_1^{00} &= 2\rho_1^{++}-2+4\frac{m_e^2}{Q^2}, \qquad \rho_2^{00} = 2\rho_2^{++}-2+4\frac{m_e^2}{P^2}, \\ |\rho_i^{+-}| &= \rho_i^{++}-1, \qquad |\rho_i^{+0}| = \sqrt{(\rho_i^{00}+1)|\rho_i^{+-}|}. \end{aligned} \tag{2.38}$$

Note that $\gamma\gamma \to X$ cross sections σ_{ab} relates photon structure functions W_{ab} by Eqs. (2.18) and spin-averaged structure functions are related to some of them by Eqs. (2.31). It is noted that all these quantities are expressed in terms of the measurable momenta l_1, l_2, l_1' and l_2' only, and hence are completely known.

2.2 Quantum Chromodynamics and Related Topics

2.2.1 Quantum Chromodynamics

Quantum Chromodynamics (QCD) [31] is the non-Abelian gauge theory which describes the strong interaction between quarks via exchanging the gauge boson called gluon, and one of the constituents of the standard model of particle physics together with the Weinberg-Salam model of electroweak interactions [32, 33].

Let the quark field ψ_i transform in the fundamental representation of SU(N) where i is the color index running over $i = 1, \cdots, N$, with $N = 3$ for QCD. It transforms as

$$\psi_i(x) \to U_{ij}(x)\psi_j(x), \tag{2.39}$$

where U_{ij} is an group element of SU(N), i.e., U is $N \times N$ matrix satisfying $UU^\dagger = 1$ and $\det(U) = 1$, and can be parameterized as

$$U_{ij}(x) = \left(e^{i\theta^a(x)t^a}\right)_{ij}. \tag{2.40}$$

Here $\theta^a(x)$ is an real parameter (for the local gauge transformation, it depend on x) and t^a is the generator of this transformation. The generators of SU(N) group are represented by N^2-1, $N \times N$ matrices which are Hermitian and traceless. The Lie algebra is defined by the commutation relations of t^a,

$$[t^a, t^b] = if^{abc}t^c, \tag{2.41}$$

where f^{abc} is the structure constant. The basis for the generators t^a can be chosen as the trace of two generators satisfy

$$\mathrm{tr}(t^a t^b) = T_F\delta^{ab}, \tag{2.42}$$

and we take $T_F = 1/2$. In this basis f^{abc} is totally antisymmetric.

Lagrangian The classical Lagrangian of QCD is of the form which was originally written down by Yang and Mills [34]

$$\mathcal{L}_{\mathrm{CL}} = \sum_f \bar{\psi}_f(i\not{D}-m_f)\psi_f - \frac{1}{4}(F_{\mu\nu}^a)^2. \tag{2.43}$$

Here ψ_f is a quark field with its mass m_f and f labels distinct quark fields (quark flavor u, d, c, s, t, b). The covariant derivative D_μ is given by

$$D_\mu = \partial_\mu - igA^a_\mu t^a, \tag{2.44}$$

with the strong coupling g and the gluon field A^a_μ. $F^a_{\mu\nu}$ is the field strength which consists of A^a_μ as

$$F^a_{\mu\nu} = \partial_\mu A^a_\nu - \partial_\nu A^a_\mu + g f^{abc} A^b_\mu A^c_\nu. \tag{2.45}$$

Then it is easy to see that the Lagrangian Eq. (2.43) is invariant under local gauge transformations[♯4]:

$$\psi_f \to \psi'_f = U\psi_f, \tag{2.46}$$

$$A^a_\mu t^a \to A^{a\prime}_\mu t^a = U\left[A^a_\mu t^a - \frac{i}{g}U^\dagger(\partial_\mu U)\right]U^\dagger. \tag{2.47}$$

Note that the introduction of the quark-gluon interaction via the covariant derivative D_μ is inevitable for maintaining local gauge invariance, canceling troublesome term $\partial_\mu U$ which appears in the transformation of the quark kinetic term $\bar{\psi}_f(i\partial\!\!\!/)\psi_f$.

However, the gauge invariance of the classical Lagrangian $\mathcal{L}_{CL}$ actually triggers some troubles in the quantization. The solution to this problem is adding the gauge-fixing terms $\mathcal{L}_{GF}$ to break this invariance. The most common choice of $\mathcal{L}_{GF}$ is so-called covariant gauges

$$\mathcal{L}_{GF} = -\frac{1}{2\xi}(\partial \cdot A^a)^2, \tag{2.48}$$

where ξ is the gauge parameter, most familiar choice of which is the Feynman gauge, $\xi = 1$.

Furthermore, in the covariant gauges, we must add the Faddeev-Popov Lagrangian [35]

$$\mathcal{L}_{FP} = \bar{c}^a(-\partial \cdot D^{ac})c^c, \tag{2.49}$$

where c^a and $\bar{c}^a$ are scalar ghost and antighost fields, respectively, and D^{ac}_μ is given by

$$D^{ac}_\mu = \partial_\mu \delta^{ac} + g f^{abc} A^b_\mu. \tag{2.50}$$

These ghost fields anticommute in the quantization procedure, despite their spin. In a quantized non-Abelian theory, the ghost fields are needed for canceling the unphysical states of the gauge bosons, which preserves the unitarity of the S-matrix.

2.2.2 Renormalization

In tree-level calculation, the dynamical behavior of quark-gluon processes in QCD does not appear, which is fundamentally linked to the properties of QCD. So the evaluation of the loop diagrams is needed, but beyond the tree-level, we often suffer a sever problem. These are the ultraviolet divergences, which have originated as infinite loop momentum.

[♯4] It is useful to note that D_μ and $F^a_{\mu\nu}$ transform as

$$D_\mu \to U D_\mu U^\dagger, \qquad F^a_{\mu\nu} t^a = \frac{i}{g}[D_\mu, D_\nu] \to U(F^a_{\mu\nu} t^a)U^\dagger,$$

and the second term in Eq. (2.43) can be written as

$$-\frac{1}{4}(F^a_{\mu\nu})^2 = -\frac{1}{4T_F}\,\mathrm{tr}\left[(F^a_{\mu\nu}t^a)^2\right].$$

The essential point for solving this problem is, a physical parameter A_{obs}which can be observed in the actual experiment is the sum of a bare paramter A_{bare} which is contained in the tree-level contributions and a loop correction A_{loop} which may be infinite:

$$A_{\text{obs}} = A_{\text{bare}} + A_{\text{loop}}, \tag{2.51}$$

and we cannot separately observe A_{bare} or A_{loop}. Therefore if we can absorb the divergences from the loop contributions into the bare parameter in a consistent fashion (renormalization), we are left with the physical, renormalized parameter which is finite and measurable.

Since divergent integrals are not mathematically manageable, in the intermediate stage before the renormalization, we need the process which makes divergent integrals suitably convergent ones (regularization). To give an actual example of the regularization method:

1. *Cut-off method*
   One of the simplest and naïve regularization is the cut-off method in which the large momentum region is cut off in the divergent region:

$$\int_0^\infty dk \to \int_0^\Lambda dk. \tag{2.52}$$

   The original integral is recovered as $\Lambda \to \infty$. It, however, breaks translation invariance and rough treatment for the surface term often leads puzzling results. Also gauge invariance breaks in this regularization. Therefore the cut-off method is not suitable for the regularization of gauge theories.

2. *Pauli-Villas regulator method*
   In this regularization, the propagator in the integrand of the divergent integral may be replaced by

$$\frac{1}{k^2 - m^2} \to \frac{1}{k^2 - m^2} - \frac{1}{k^2 - M^2} = \frac{M^2 - m^2}{(k^2 - m^2)(k^2 - M^2)}. \tag{2.53}$$

   Then, the large momentum behavior of the modified propagator Eq. (2.53) is better ($O(1/k^4)$) than that of the original one ($O(1/k^2)$). The additional term in Eq. (2.53) is called the Pauli-Villas regulator [36]. The original propagator is recovered as $M \to \infty$. This method respects translation and Lorentz invariance and, in fact, gauge invariance is preserved in the quantum electrodynamics. However, in this method, the proof of the unitarity of the massless Yang-Mills theory is found to be rather difficult. Furthermore, in the massive Yang-Mills theory such as Weinberg-Salam theory, the Pauli-Villas regulator method does not maintain gauge invariance in a consistent way.

3. *Dimensional regularization*
   In this regularization, the integral is regarded as a function of the number of the space-time dimension $d = 4 - 2\epsilon$:

$$\int d^4k \to \int d^dk. \tag{2.54}$$

   The original divergence will show up as a pole at $d = 4$. Since in this regularization, nothing is violated except that space-time is not 4-dimensional, Lorentz invariance, gauge invariance, unitarity, etc. are preserved. Therefore the dimensional regularization is the most suitable for gauge theories in a lot of cases.

After the regularization process, the renormalized quantity $A_{\rm ren}$ and unrenormalized quantitiy $A_{\rm un}$, which is regularized by some cut-off parameter λ (e.g., ϵ in the dimensional regularization), is connected as

$$A_{\rm ren}(p,\mu) = Z^{-1}(\lambda,\mu)A_{\rm un}(p,\lambda), \tag{2.55}$$

where Z is the renormalization constant, p denotes the momenta of the external lines, and μ is the renormalization scale, a new mass, at which the infinities are absorbed into Z, and which is not included as a parameter in the original unrenormalized theory. To begin with, μ can be taken arbitrary scale absolutely, and may differ from integral to integral. Moreover,

Since $A_{\rm ren}(p,\mu)$ in Eq. (2.55) is renormalized and thus finite, all infinities in $A_{\rm un}(p,\lambda)$ are absorbed into the renormalization constant $Z(\lambda,\mu)$. However, there is still freedom to choose the finite term in $Z(\lambda,\mu)$. In order to fix this arbitrary finite term, we need an additional requirement which sets up a renormalization scheme. There are two basic classes of schemes widely used:

1. *Momentum subtraction scheme*
   In this scheme, we choose

   $$A_{\rm rem}(p_0,\mu_0) = A_0, \tag{2.56}$$

   with p_0 being some fixed set of external momenta, i.e., we fix $A_{\rm rem}$ such as that it has a specific form at some point.

2. *Minimum subtraction (MS) scheme*
   This scheme is due to 't Hooft [37] and is specific to the dimensional regularization. In this scheme, we eliminate only the pole terms $1/\epsilon$. Because of its simplicity, this scheme is used in many QCD calculations. In practice, the combination $1/\epsilon - \gamma_E + \ln(4\pi)$ always appear. Therefore it is usuful to eliminate these constants together; such a scheme is called by $\overline{\rm MS}$ scheme [19].

Now, because $A_{\rm rem}(p,\mu)$ is a physical quantity, it should be independent of our choise of μ, and this leads renormalization group (RG) equation:

$$\mu\frac{d}{d\mu}A_{\rm rem}(p,\mu) = 0 \tag{2.57}$$

This equation holds exactly if we have the exact solution of the theory, but we usually use perturbative series expansion, then there are errors of the order of the first uncomputed perturbation expansion. This will be a useful approximation if the coupling is small, which leads us to our next topic, asymptotic freedom.

2.2.3 Asymptotic Freedom

The notable characteristic of the strong interaction is twofold. Hadron spectra are very well described by the quark model, but quarks have never been seen in isolation. All attempt to detect a single quark failed. Evidently, the forces between quarks are strong. Paradoxically, however, certain high energy phenomena are quite successfully described by the parton model, in which quarks behave as they do not interact at all. *Asymptotic freedom* refers to the weakness of the short-distance interaction, while the *confinement* of quarks follows from its strength at long distance.

An amazing feature of QCD is its ability to describe both kinds of behavior. To see these feature, it is useful to introduce the renormalization group equation for the QCD coupling constant g,

$$\mu\frac{dg(\mu)}{d\mu} = \beta(g(\mu)), \tag{2.58}$$

where $\beta(g(\mu))$ can be calculated by perturbation. Up to the one-loop level we have [38, 39]

$$\beta(g) = -\frac{g^3}{16\pi^2}\beta_0 + O(g^5), \qquad \beta_0 = \frac{11}{3}C_A - \frac{2}{3}n_f, \tag{2.59}$$

where $C_A = 3$ in QCD, and n_f is the number of quark flavors. The positiveness of β_1 means that as μ increases, the observed coupling decreases. This is what we mean by asymptotic freedom. At the same time, as μ decreases, the coupling decreases. This shows that perturbation theory will not be applied at low energies, where obviously the interaction force is strong. In this fashion, a perturbative description at high energies is compatible with confinement at low energies.

Note that by changing the color factors $C_A \to 0$, $n_f/2 \to 3n_f\langle e^2\rangle$, we can obtain β_0 for the quantum electrodynamics, which is negative. Indeed, among the known renormalizable quantum field theories in four dimensions, only non-Abelian Yang-Mills theories have the property of asymptotic freedom [40, 41].

2.2.4 Operator product expansion

It is often useful to consider how the product of the two fields $A(x)B(y)$ behaves when $x \to y$ (or near lightcone $(x-y)^2 \to 0$). Wilson suggested that there is a convergent expansion of such products as a sum (possibly infinite) of local fields [42]:

$$A(x)B(y) \sim \sum_i C^i(x-y)O_i\left(\frac{x+y}{2}\right), \qquad \text{for } x \to y, \tag{2.60}$$

where O_i is a local operator which is regular when $x \to y$, and C^i is a corresponding coefficient which is singular when $x \to y$. This operator identity was justified in the framework of the perturbation theory by Zimmermann [43].

Let d_A, d_B and d_i be the mass dimension of the operators A, B and O_i, respectively. Then C^i must behave as

$$C^i(x-y) \sim \left(\frac{1}{x-y}\right)^{d_A+d_B-d_i}, \qquad \text{for } x \to y. \tag{2.61}$$

Therefore the terms which contains lower dimension operators in the right-hand side of Eq. (2.60) are dominant, and we should consider only such operators. More realistic application of the operator product expansion (near lightcone) appears in the next chapter.

Chapter 3

Theoretical Framework

As we have seen in the previous chapter, the spin-averaged virtual photon structure tensor $W^{\gamma}_{\mu\nu}$ is given by

$$\begin{aligned} W^{\gamma}_{\mu\nu}(p,q) &= \frac{1}{2}\sum_{a}\epsilon^{\rho *}(p,a)W_{\mu\nu\rho\tau}(p,q)\epsilon^{\tau}(p,a) \\ &= -\frac{1}{2}g^{\rho\tau}W_{\mu\nu\rho\tau}(p,q) \\ &= \frac{1}{2\pi}\int d^4x\, e^{iq\cdot x}\langle\gamma(p)|J_{\mu}(x)J_{\nu}(0)|\gamma(p)\rangle_{\text{spin ave}}, \end{aligned} \tag{3.1}$$

and it relates to the absorptive part of the corresponding forward scattering amplitude

$$T_{\mu\nu}(p,q) = i\int d^4x\, e^{iq\cdot x}\langle\gamma(p)|T(J_{\mu}(x)J_{\nu}(0))|\gamma(p)\rangle_{\text{spin ave}}, \tag{3.2}$$

such as

$$W^{\gamma}_{\mu\nu}(p,q) = \frac{1}{\pi}\,\text{Im}\,T_{\mu\nu}. \tag{3.3}$$

On the other hand, in terms of two independent structure functions F^{γ}_2 and F^{γ}_L, $W^{\gamma}_{\mu\nu}$ can be written as

$$W^{\gamma}_{\mu\nu}(p,q) = e_{\mu\nu}\frac{1}{x}F^{\gamma}_L(x,Q^2,P^2) + d_{\mu\nu}\frac{1}{x}F^{\gamma}_2(x,Q^2,P^2). \tag{3.4}$$

and the tensors $e_{\mu\nu}$ and $d_{\mu\nu}$ are given by

$$e_{\mu\nu} = g_{\mu\nu} - \frac{q_{\mu}q_{\nu}}{q^2}, \qquad d_{\mu\nu} = -g_{\mu\nu} + \frac{q_{\mu}p_{\nu}+p_{\mu}q_{\nu}}{p\cdot q} - \frac{p_{\mu}p_{\nu}}{(p\cdot q)^2}q^2. \tag{3.5}$$

In this chapter, we analyze the photon structure function $F^{\gamma}_2(x,Q^2,P^2)$ and $F^{\gamma}_L(x,Q^2,P^2)$, using the theoretical framework based on the operator product expansion (OPE) and the renormalization group (RG) method, in the kinematical region $\Lambda^2 \ll P^2 \ll Q^2$, where Λ is the QCD scale parameter. In the kinematical region $\Lambda^2 \ll P^2$, the photon matrix elements can be calculated in the perturbation, and for $P^2 \ll Q^2$ we can neglect corrections from kinematical mass effects and from higher twist corrections, which have the form $(P^2/Q^2)^k$ $(k = 1, 2, \cdots)$.

3.1 Moment Sum Rules From OPE and RG

Moment Sum Rules By applying OPE for the product of two electromagnetic currents at short distance we obtain

$$\begin{aligned} & i\int d^4x\, e^{iq\cdot x} T(J_\mu(x)J_\nu(0)) \\ &= \sum_{n,i}\left(\frac{2}{Q^2}\right)^n \left[\left(g_{\mu\nu}-\frac{q_\mu q_\nu}{q^2}\right) q_{\mu_1}q_{\mu_2} C^n_{L,i}\left(\frac{Q^2}{\mu^2},\bar{g}(\mu^2),\alpha\right)\right. \\ &\qquad \left. + \left(-g_{\mu\mu_1}g_{\nu\mu_2}q^2 + g_{\mu\mu_1}q_\nu q_{\mu_2} + g_{\nu\mu_2}q_\mu q_{\mu_1} - g_{\mu\nu}q_{\mu_1}q_{\mu_2}\right) C^n_{2,i}\left(\frac{Q^2}{\mu^2},\bar{g}(\mu^2),\alpha\right)\right] \\ &\qquad \times q_{\mu_3}\cdots q_{\mu_n} O_i^{\mu_1\cdots\mu_n}(\mu^2) + \cdots . \end{aligned} \tag{3.6}$$

Here all quantities are assumed to be renormalized at the renormalization scale μ and $\bar{g}(\mu^2)$ is the effective running QCD coupling constant at this point. α is the fine structure constant. $O_i^{\mu_1\cdots\mu_n}$ are spin-n twist-2 irreducible operators (hereafter we often refer to $O_i^{\mu_1\cdots\mu_n}$ as O_i^n). $C^n_{L,i}$ and $C^n_{2,i}$ are the coefficient functions corresponding these operators and contributing to the structure functions F_L^γ and F_2^γ, respectively. The sum on i runs over the possible twist-2 operators and "$\cdots$" represents other terms with irrelevant operators and coefficient functions. Actually, the relevant operators O_i^n are flavor singlet quark (ψ), gluon (G), flavor nonsinglet quark (NS) and photon (γ) operators as follows:

$$O_\psi^{\mu_1\cdots\mu_n} = \frac{1}{2} i^{n-1}\bar{\psi}\gamma^{\{\mu_1}D^{\mu_2}\cdots D^{\mu_n\}}\mathbf{1}\psi, \tag{3.7a}$$

$$O_G^{\mu_1\cdots\mu_n} = \frac{1}{2} i^{n-2} G_\alpha{}^{\{\mu_1}D^{\mu_2}\cdots D^{\mu_{n-1}}G^{\alpha\mu_n\}}, \tag{3.7b}$$

$$O_{NS}^{\mu_1\cdots\mu_n} = \frac{1}{2} i^{n-1}\bar{\psi}\gamma^{\{\mu_1}D^{\mu_2}\cdots D^{\mu_n\}}\left(Q^2_{ch} - \langle e^2\rangle\mathbf{1}\right)\psi, \tag{3.7c}$$

$$O_\gamma^{\mu_1\cdots\mu_n} = \frac{1}{2} i^{n-2} F_\alpha{}^{\{\mu_1}\partial^{\mu_2}\cdots\partial^{\mu_{n-1}}F^{\alpha\mu_n\}}. \tag{3.7d}$$

Here D^μ denotes the covariant derivative and it is understood that the symmetrical and traceless part is taken with respect to the Lorentz indices $\mu_1\cdots\mu_n$ in the curly bracket. In quark operators O_ψ^n and O_{NS}^n, $\mathbf{1}$ is $n_f\times n_f$ unit matrix, Q^2_{ch} is the square of the $n_f\times n_f$ quark-charge matrix, with n_f being the number of the active quark (i.e., effectively massless quark) flavors, and $\langle e^2\rangle = (\sum_{i=1}^{n_f} e_i^2)/n_f$ is the average charge squared where e_i is the electromagnetic charge of the active quark with flavor i in the unit of proton charge. It is noted that we have a relation $\mathrm{tr}(Q^2_{ch} - \langle e^2\rangle\mathbf{1}) = 0$. The essential feature in the analysis of the photon structure functions, in contrast to the case of the nucleon counterparts, is that the photon operators O_γ^n appear in addition to the familiar hadronic operators O_ψ^n, O_G^n and O_{NS}^n [7].

The spin-averaged matrix elements of these operators sandwiched by the photon states with momentum p are expressed as

$$\langle\gamma(p)|O_i^{\mu_1\cdots\mu_n}|\gamma(p)\rangle_{\text{spin ave}} = A_i^n\left(\frac{P^2}{\mu^2},\bar{g}(\mu^2),\alpha\right)p^{\{\mu_1}\cdots p^{\mu_n\}}, \qquad \text{for} \quad i=\psi,G,NS,\gamma, \tag{3.8}$$

Using the OPE in Eq.(3.6) with the photon matrix elements in Eq. (3.8), we can write the forward scattering amplitude $T_{\mu\nu}$ in Eq. (3.2) as

$$T_{\mu\nu} = \sum_{n,i}\left(\frac{1}{x}\right)^n \left(e_{\mu\nu}C^n_{L,i} + d_{\mu\nu}C^n_{2,i}\right)A_i^n, \tag{3.9}$$

which is an expansion in terms of $1/x$ for unphysical $x \to \infty$. The continuation of this result to the physical region $0 < x < 1$ is done by a dispersion relation in the complex x-plane, and using the relation Eq. (3.3) we finally obtain the moment sum rules for F_2^γ and F_L^γ as follows [44]:

$$\frac{1+(-1)^n}{2}\int_0^1 dx\, x^{n-2} F_2^\gamma(x,Q^2,P^2) = \sum_{i=\psi,G,NS,\gamma} C_{2,i}^n\left(\frac{Q^2}{\mu^2},\bar{g}(\mu^2),\alpha\right) A_i^n\left(\frac{P^2}{\mu^2},\bar{g}(\mu^2),\alpha\right), \tag{3.10a}$$

$$\frac{1+(-1)^n}{2}\int_0^1 dx\, x^{n-2} F_L^\gamma(x,Q^2,P^2) = \sum_{i=\psi,G,NS,\gamma} C_{L,i}^n\left(\frac{Q^2}{\mu^2},\bar{g}(\mu^2),\alpha\right) A_i^n\left(\frac{P^2}{\mu^2},\bar{g}(\mu^2),\alpha\right), \tag{3.10b}$$

We can freely choose the renormalization point μ due to the fact that the left-hand side of Eqs. (3.10) does not depend on it. We later take $\mu^2 = -p^2 = P^2$ as a matter of practical convenience. Note that because F_2^γ and F_L^γ are symmetric function in $p \cdot q$, this moment sum rules apply only for even n.

The photon structure functions are defined in the lowest order of α and, through this work, they are of order α. Since the coefficient functions $C_{2,\gamma}^n$ and $C_{L,\gamma}^n$ are $O(\alpha)$, it is sufficient to evaluate A_γ^n at $O(1)$, and thus we have

$$A_\gamma^n\left(\frac{P^2}{\mu^2},\bar{g}(\mu^2),\alpha\right) = 1. \tag{3.11}$$

On the other hand, the matrix elements A_i^n ($i = \psi, G, NS$) for the hadronic operators start at $O(\alpha)$. For $-p^2 = P^2 \gg \Lambda^2$, we can calculate these photon matrix elements of the hadronic operators perturbatively, in each power of g^2. Choosing μ^2 at P^2, we get them in the form as

$$A_i^n(\bar{g}(P^2),\alpha) \equiv A_i^n\left(\frac{P^2}{\mu^2},\bar{g}(\mu^2),\alpha\right)\Big|_{\mu^2=P^2} = \frac{\alpha}{4\pi}\left[A_i^{(1),n} + \frac{\bar{g}^2(P^2)}{16\pi^2}A_i^{(2),n} + O(\bar{g}^4(P^2))\right], \qquad \text{for} \quad i = \psi, G, NS. \tag{3.12}$$

Let us analyze the structure function $F_2^\gamma(x,Q^2,P^2)$. We will evaluate its moment sum rule up to the NNLO ($\alpha\alpha_s$). The longitudinal structure function $F_L^\gamma(x,Q^2,P^2)$ can be evaluated in a similar manner. To the lowest order in α, the Q^2-dependence of the coefficient functions $C_{2,i}^n(Q^2/\mu^2,\bar{g}(\mu^2),\alpha)$ in Eq. (3.10a) is governed by the RG equations.

$$\left(\mu\frac{\partial}{\partial\mu} + \beta(g)\frac{\partial}{\partial g}\right) C_{2,i}^n\left(\frac{Q^2}{\mu^2},g,\alpha\right) = \gamma_{ij}^n(g,\alpha) C_{2,j}^n\left(\frac{Q^2}{\mu^2},g,\alpha\right), \tag{3.13}$$

with $i, j = \psi, G, NS$ and γ. Here $\beta(g)$ is the QCD beta function and $\gamma^n(g,\alpha)$ is the anomalous dimension matrix. To the lowest order in α, this matrix has the following form:

$$\gamma^n(g,\alpha) = \left(\begin{array}{c|c} \hat{\gamma}^n(g) & \mathbf{0} \\ \hline \boldsymbol{K}^n(g,\alpha) & 0 \end{array}\right), \tag{3.14}$$

where $\hat{\gamma}^n(g)$ is the usual 3×3 anomalous dimension matrix in the hadronic sector

$$\hat{\gamma}^n(g) = \begin{pmatrix} \gamma_{\psi\psi}^n(g) & \gamma_{G\psi}^n(g) & 0 \\ \gamma_{\psi G}^n(g) & \gamma_{GG}^n(g) & 0 \\ 0 & 0 & \gamma_{NS}^n(g) \end{pmatrix}, \tag{3.15}$$

and $\boldsymbol{K}^n(g,\alpha)$ is the three-component row vector

$$\boldsymbol{K}^n(g,\alpha) = \begin{pmatrix} K_\psi^n(g,\alpha) & K_G^n(g,\alpha) & K_{NS}^n(g,\alpha) \end{pmatrix}, \tag{3.16}$$

which represent the mixing between photon operators and remaining three hadronic operators.

If we choose $\mu^2 = -p^2 = P^2$, the solution of Eq. (3.13) is given by

$$C^n_{2,i}\left(\frac{Q^2}{P^2}, \bar{g}(P^2), \alpha\right) = \left(T \exp\left[\int_{\bar{g}(Q^2)}^{\bar{g}(P^2)} dg \frac{\boldsymbol{\gamma}^n(g,\alpha)}{\beta(g)}\right]\right)_{ij} C^n_{2,j}\left(\frac{Q^2}{P^2} = 1, \bar{g}(Q^2), \alpha\right). \tag{3.17}$$

The T-ordering in Eq. (3.17) is necessary since $[\boldsymbol{\gamma}^n(g,\alpha), \boldsymbol{\gamma}^n(g',\alpha)] \neq 0$, and is defined as

$$T \exp\left[\int_{g_2}^{g_1} dg \frac{\boldsymbol{\gamma}^n(g,\alpha)}{\beta(g)}\right] = 1 + \int_{g_2}^{g_1} dg \frac{\boldsymbol{\gamma}^n(g,\alpha)}{\beta(g)} + \int_{g_2}^{g_1} dg \int_{g}^{g_1} dg' \frac{\boldsymbol{\gamma}^n(g,\alpha)}{\beta(g)} \frac{\boldsymbol{\gamma}^n(g',\alpha)}{\beta(g')} + \cdots. \tag{3.18}$$

With the aid of Eq. (3.17), for even n, the moment sum rule for F_2^γ in Eq. (3.10a) becomes

$$\int_0^1 dx\, x^{n-2} F_2^\gamma(x, Q^2, P^2) = \sum_{i=\psi,G,NS,\gamma} A_i^n(\bar{g}(P^2), \alpha) \left(T \exp\left[\int_{\bar{g}(Q^2)}^{\bar{g}(P^2)} dg \frac{\boldsymbol{\gamma}^n(g,\alpha)}{\beta(g)}\right]\right)_{ij} C^n_{2,j}\left(1, \bar{g}(Q^2), \alpha\right). \tag{3.19}$$

Furthermore, the T-ordered exponential in Eq. (3.19) has the form as [8]

$$T \exp\left[\int_{\bar{g}(Q^2)}^{\bar{g}(P^2)} dg \frac{\boldsymbol{\gamma}^n(g,\alpha)}{\beta(g)}\right] = \left(\begin{array}{c|c} \boldsymbol{M}^n & \mathbf{0} \\ \hline \boldsymbol{X}^n & 1 \end{array}\right), \tag{3.20}$$

where $\boldsymbol{M}^n$ is a 3×3 matrix and $\boldsymbol{X}^n$ is a three-component row vector, one can find from Eqs. (3.14) and (3.20),

$$\boldsymbol{M}^n\left(\frac{Q^2}{P^2}, \bar{g}(P^2)\right) = T \exp\left[\int_{\bar{g}(Q^2)}^{\bar{g}(P^2)} dg \frac{\hat{\boldsymbol{\gamma}}^n(g)}{\beta(g)}\right], \tag{3.21a}$$

$$\boldsymbol{X}^n\left(\frac{Q^2}{P^2}, \bar{g}(P^2), \alpha\right) = \int_{\bar{g}(Q^2)}^{\bar{g}(P^2)} dg \frac{\boldsymbol{K}^n(g,\alpha)}{\beta(g)} T \exp\left[\int_{\bar{g}(Q^2)}^{g} dg' \frac{\hat{\boldsymbol{\gamma}}^n(g')}{\beta(g')}\right]. \tag{3.21b}$$

Therefore, with the following notations:

$$\boldsymbol{A}^n(g,\alpha) = \begin{pmatrix} A^n_\psi(g,\alpha) & A^n_G(g,\alpha) & A^n_{NS}(g,\alpha) \end{pmatrix}, \tag{3.22}$$

and

$$\boldsymbol{C}^n_2(g) = \begin{pmatrix} C^n_{2,\psi}(1,g) \\ C^n_{2,G}(1,g) \\ C^n_{2,NS}(1,g) \end{pmatrix}, \qquad C^n_{2,\gamma}(g,\alpha) = C^n_{2,\gamma}(1,g,\alpha), \tag{3.23}$$

we finally write down Eq. (3.19) as

$$\begin{aligned} \int_0^1 dx\, x^{n-2} F_2^\gamma(x, Q^2, P^2) = {} & \boldsymbol{A}^n\left(\bar{g}(P^2), \alpha\right) \cdot \boldsymbol{M}^n\left(\frac{Q^2}{P^2}, \bar{g}(P^2)\right) \cdot \boldsymbol{C}^n_2\left(\bar{g}(Q^2)\right) \\ & + \boldsymbol{X}^n\left(\frac{Q^2}{P^2}, \bar{g}(P^2), \alpha\right) \cdot \boldsymbol{C}^n_2\left(\bar{g}(Q^2)\right) + C^n_{2,\gamma}\left(\bar{g}(Q^2), \alpha\right). \end{aligned} \tag{3.24}$$

This expression is valid to any order in the effective running QCD coupling constant $\bar{g}^2$ and to the first order in α.

Expanding Moment Sum Rules up to NNLO To evaluate $M^n(Q^2/P^2, \bar{g}(P^2))$ in Eq. (3.21a), we first expand $\hat{\gamma}^n(g)$ in powers of g^2 up to three-loop level as follows:

$$\begin{aligned}\hat{\gamma}^n(g) &= \hat{\gamma}^{(0),n}(g) + \hat{\gamma}^{(1),n}(g) + \hat{\gamma}^{(2),n}(g) + \cdots \\ &= \frac{g^2}{16\pi^2}\hat{\gamma}^{(0),n} + \frac{g^4}{(16\pi^2)^2}\hat{\gamma}^{(1),n} + \frac{g^6}{(16\pi^2)^3}\hat{\gamma}^{(2),n} + O(g^8).\end{aligned} \tag{3.25}$$

Then the T-ordered exponential of $M^n(Q^2/P^2, \bar{g}(P^2))$ can be expanded such as

$$\begin{aligned}&T\exp\left[\int_{g_2}^{g_1} dg \frac{\hat{\gamma}^n(g)}{\beta(g)}\right] \\ &\quad= \exp\left[\int_{g_2}^{g_1} dg \frac{\hat{\gamma}^{(0),n}(g)}{\beta(g)}\right] \\ &\qquad+ \int_{g_2}^{g_1} dg\, \exp\left[\int_{g}^{g_1} dg' \frac{\hat{\gamma}^{(0),n}(g')}{\beta(g')}\right] \frac{\hat{\gamma}^{(1),n}(g)}{\beta(g)} \exp\left[\int_{g_2}^{g} dg' \frac{\hat{\gamma}^{(0),n}(g')}{\beta(g')}\right] \\ &\qquad+ \int_{g_2}^{g_1} dg\, \exp\left[\int_{g}^{g_1} dg' \frac{\hat{\gamma}^{(0),n}(g')}{\beta(g')}\right] \frac{\hat{\gamma}^{(2),n}(g)}{\beta(g)} \exp\left[\int_{g_2}^{g} dg' \frac{\hat{\gamma}^{(0),n}(g')}{\beta(g')}\right] \\ &\qquad+ \int_{g_2}^{g_1} dg\, \exp\left[\int_{g}^{g_1} dg'' \frac{\hat{\gamma}^{(0),n}(g'')}{\beta(g'')}\right] \frac{\hat{\gamma}^{(1),n}(g)}{\beta(g)} \int_{g_2}^{g} dg' \exp\left[\int_{g'}^{g} dg'' \frac{\hat{\gamma}^{(0),n}(g'')}{\beta(g'')}\right] \\ &\qquad\qquad\times \frac{\hat{\gamma}^{(1),n}(g')}{\beta(g')} \exp\left[\int_{g_2}^{g'} dg'' \frac{\hat{\gamma}^{(0),n}(g'')}{\beta(g'')}\right] + \cdots .\end{aligned} \tag{3.26}$$

To evaluate these integrals, we make a full use of the projection operators obtained from the one-loop anomalous dimension matrix $\hat{\gamma}^{(0),n}$ in the second line of Eq. (3.25) [8]:

$$\hat{\gamma}^{(0),n} = \sum_{i=+,-,NS} \lambda_i^n \boldsymbol{P}_i^n, \tag{3.27}$$

where λ_i^n ($i = +, -, NS$) and $\boldsymbol{P}_i^n$ are eigenvalues of $\hat{\gamma}^{(0),n}$ and the corresponding projection operators, respectively. Explicitly,

$$\lambda_\pm^n = \frac{1}{2}\left[\gamma_{\psi\psi}^{(0),n} + \gamma_{GG}^{(0),n} \pm \sqrt{\left(\gamma_{\psi\psi}^{(0),n} - \gamma_{GG}^{(0),n}\right)^2 + 4\gamma_{\psi G}^{(0),n}\gamma_{G\psi}^{(0),n}}\right], \qquad \lambda_{NS}^n = \gamma_{NS}^{(0),n}, \tag{3.28}$$

and

$$\boldsymbol{P}_\pm^n = \frac{1}{\lambda_\pm^n - \lambda_\mp^n}\begin{pmatrix} \gamma_{\psi\psi}^{(0),n} - \lambda_\mp^n & \gamma_{G\psi}^{(0),n} & 0 \\ \gamma_{\psi G}^{(0),n} & \gamma_{GG}^{(0),n} - \lambda_\mp^n & 0 \\ 0 & 0 & 0 \end{pmatrix}, \qquad \boldsymbol{P}_{NS}^n = \begin{pmatrix} 0 & 0 & 0 \\ 0 & 0 & 0 \\ 0 & 0 & 1 \end{pmatrix}, \tag{3.29}$$

which have the following properties:

$$\boldsymbol{P}_i^n \boldsymbol{P}_j^n = \delta_{ij}\boldsymbol{P}_i^n, \qquad \sum_{i=+,-,NS} \boldsymbol{P}_i^n = 1. \tag{3.30}$$

Expanding $\beta(g)$ in powers of g^2 up to the three-loop level as

$$\beta(g) = -\frac{g^3}{16\pi^2}\beta_0 - \frac{g^5}{(16\pi^2)^2}\beta_1 - \frac{g^7}{(16\pi^2)^3}\beta_2 + O(g^9), \tag{3.31}$$

we find that the exponential in the Eq. (3.26) can be reduced to, up to desired order,

$$\exp\left[\int_{g_2}^{g_1} dg \frac{\hat{\gamma}^{(0),n}(g)}{\beta(g)}\right] = \sum_i \boldsymbol{P}_i^n \left(\frac{g_2^2}{g_1^2}\right)^{d_i^n} \left[1 + \frac{g_1^2 - g_2^2}{16\pi^2}\frac{\beta_1}{\beta_0} d_i^n - \frac{g_1^4 - g_2^4}{(16\pi^2)^2}\left(\frac{\beta_1^2}{\beta_0^2} - \frac{\beta_2}{\beta_0}\right)\frac{d_i^n}{2} + \frac{(g_1^2 - g_2^2)^2}{(16\pi^2)^2}\frac{\beta_1^2}{\beta_0^2}\frac{\left(d_i^n\right)^2}{2}\right], \tag{3.32}$$

where

$$d_i^n = \frac{\lambda_i^n}{2\beta_0}. \tag{3.33}$$

Then it is a straightforward task to expand Eq. (3.26), or $\boldsymbol{M}^n(Q^2/P^2, \bar{g}(P^2))$ up to the NNLO. The final form of $\boldsymbol{M}^n(Q^2/P^2, \bar{g}(P^2))$ is given in Eq. (A.1) in Appendix A. Similarly, expanding $\boldsymbol{K}^n(g, \alpha)$ in powers of g^2 up to three-level as

$$\boldsymbol{K}^n(g, \alpha) = -\frac{\alpha}{4\pi}\left[\boldsymbol{K}^{(0),n} + \frac{g^2}{16\pi^2}\boldsymbol{K}^{(1),n} + \frac{g^4}{(16\pi^2)^2}\boldsymbol{K}^{(2),n} + O(g^6)\right], \tag{3.34}$$

one can evaluate $\boldsymbol{X}^n(Q^2/P^2, \bar{g}(P^2), \alpha)$ in Eq. (3.21b) up to the NNLO, which is given in Eq. (A.2).

Finally, expansions are made for the photon matrix elements of the hadronic operators $\boldsymbol{A}^n(g, \alpha)$ as well as the coefficient functions $\boldsymbol{C}_2^n(g)$ and $\boldsymbol{C}_{2,\gamma}^n(g, \alpha)$ up to the two-loop level as follows:

$$\boldsymbol{A}^n(g, \alpha) = \frac{\alpha}{4\pi}\left[\boldsymbol{A}^{(1),n} + \frac{g^2}{16\pi^2}\boldsymbol{A}^{(2),n} + O(g^4)\right], \tag{3.35a}$$

$$\boldsymbol{C}_2^n(g) = \boldsymbol{C}_2^{(0),n} + \frac{g^2}{16\pi^2}\boldsymbol{C}_2^{(1),n} + \frac{g^4}{(16\pi^2)^2}\boldsymbol{C}_2^{(2),n} + O(g^6), \tag{3.35b}$$

$$\boldsymbol{C}_{2,\gamma}^n(g, \alpha) = \frac{\alpha}{4\pi}\left[\boldsymbol{C}_{2,\gamma}^{(1),n} + \frac{g^2}{16\pi^2}\boldsymbol{C}_{2,\gamma}^{(2),n} + O(g^4)\right]. \tag{3.35c}$$

Then putting Eqs. (A.1), (A.2) and (3.35) into Eq. (3.24), we find that the expression for the moment sum rule of $F_2^\gamma(x, Q^2, P^2)$ up to the NNLO ($\alpha\alpha_s$) corrections is summarized as follows:

$$\begin{aligned}
&\int_0^1 dx\, x^{n-2} F_2^\gamma(x, Q^2, P^2) \\
&\quad = \frac{\alpha}{4\pi}\frac{1}{2\beta_0}\Bigg\{\frac{4\pi}{\alpha_s(Q^2)}\sum_i \mathcal{L}_i^n\left[1 - \left(\frac{\alpha_s(Q^2)}{\alpha_s(P^2)}\right)^{d_i^n+1}\right] \\
&\qquad + \sum_i \mathcal{A}_i^n\left[1 - \left(\frac{\alpha_s(Q^2)}{\alpha_s(P^2)}\right)^{d_i^n}\right] + \sum_i \mathcal{B}_i^n\left[1 - \left(\frac{\alpha_s(Q^2)}{\alpha_s(P^2)}\right)^{d_i^n+1}\right] + \mathcal{C}^n \\
&\qquad + \frac{\alpha_s(Q^2)}{4\pi}\Bigg(\sum_i \mathcal{D}_i^n\left[1 - \left(\frac{\alpha_s(Q^2)}{\alpha_s(P^2)}\right)^{d_i^n-1}\right] + \sum_i \mathcal{E}_i^n\left[1 - \left(\frac{\alpha_s(Q^2)}{\alpha_s(P^2)}\right)^{d_i^n}\right] \\
&\qquad\quad + \sum_i \mathcal{F}_i^n\left[1 - \left(\frac{\alpha_s(Q^2)}{\alpha_s(P^2)}\right)^{d_i^n+1}\right] + \mathcal{G}^n\Bigg) + O(\alpha_s^2)\Bigg\},
\end{aligned} \tag{3.36}$$

with $i = +, -, NS$. The coefficients $\mathcal{L}_i^n$, $\mathcal{A}_i^n$, $\mathcal{B}_i^n$, $\mathcal{C}^n$, $\mathcal{D}_i^n$, $\mathcal{E}_i^n$, $\mathcal{F}_i^n$ and $\mathcal{G}^n$ are given by

$$\mathcal{L}_i^n = \boldsymbol{K}^{(0),n}\boldsymbol{P}_i^n\boldsymbol{C}_2^{(0),n}\frac{1}{d_i^n+1}, \tag{3.37a}$$

$$\begin{aligned}\mathcal{A}_i^n = &-\boldsymbol{K}^{(0),n}\sum_j \frac{\boldsymbol{P}_j^n\hat{\boldsymbol{\gamma}}^{(1),n}\boldsymbol{P}_i^n}{\lambda_j^n-\lambda_i^n+2\beta_0}\boldsymbol{C}_2^{(0),n}\frac{1}{d_i^n} + \boldsymbol{K}^{(0),n}\boldsymbol{P}_i^n\boldsymbol{C}_2^{(0),n}\frac{\beta_1}{\beta_0}\frac{d_i^n-1}{d_i^n}\\ &+ \boldsymbol{K}^{(1),n}\boldsymbol{P}_i^n\boldsymbol{C}_2^{(0),n}\frac{1}{d_i^n} - 2\beta_0\boldsymbol{A}^{(1),n}\boldsymbol{P}_i^n\boldsymbol{C}_2^{(0),n},\end{aligned} \tag{3.37b}$$

$$\begin{aligned}\mathcal{B}_i^n = &\boldsymbol{K}^{(0),n}\sum_j \frac{\boldsymbol{P}_i^n\hat{\boldsymbol{\gamma}}^{(1),n}\boldsymbol{P}_j^n}{\lambda_i^n-\lambda_j^n+2\beta_0}\boldsymbol{C}_2^{(0),n}\frac{1}{d_i^n+1} + \boldsymbol{K}^{(0),n}\boldsymbol{P}_i^n\boldsymbol{C}_2^{(1),n}\frac{1}{d_i^n+1}\\ &- \boldsymbol{K}^{(0),n}\boldsymbol{P}_i^n\boldsymbol{C}_2^{(0),n}\frac{\beta_1}{\beta_0}\frac{d_i^n}{d_i^n+1},\end{aligned} \tag{3.37c}$$

$$\mathcal{C}^n = 2\beta_0\left(C_{2,\gamma}^{(1),n} + \boldsymbol{A}^{(1),n}\cdot\boldsymbol{C}_2^{(0),n}\right), \tag{3.37d}$$

$$\begin{aligned}\mathcal{D}_i^n = &-\boldsymbol{K}^{(0),n}\boldsymbol{P}_i^n\boldsymbol{C}_2^{(0),n}\left(\frac{\beta_1^2}{\beta_0^2}+\frac{\beta_2}{\beta_0}\frac{1}{d_i^n-1}\right)\left(1-\frac{d_i^n}{2}\right) - \boldsymbol{K}^{(0),n}\sum_j\frac{\boldsymbol{P}_j^n\hat{\boldsymbol{\gamma}}^{(1),n}\boldsymbol{P}_i^n}{\lambda_j^n-\lambda_i^n+2\beta_0}\boldsymbol{C}_2^{(0),n}\frac{\beta_1}{\beta_0}\frac{d_j^n-1}{d_i^n-1}\\ &- \boldsymbol{K}^{(0),n}\sum_j\frac{\boldsymbol{P}_j^n\hat{\boldsymbol{\gamma}}^{(1),n}\boldsymbol{P}_i^n}{\lambda_j^n-\lambda_i^n+4\beta_0}\boldsymbol{C}_2^{(0),n}\frac{\beta_1}{\beta_0}\left(1-\frac{d_j^n}{d_i^n-1}\right) - \boldsymbol{K}^{(0),n}\sum_j\frac{\boldsymbol{P}_j^n\hat{\boldsymbol{\gamma}}^{(2),n}\boldsymbol{P}_i^n}{\lambda_j^n-\lambda_i^n+4\beta_0}\boldsymbol{C}_2^{(0),n}\frac{1}{d_i^n-1}\\ &+ \boldsymbol{K}^{(0),n}\sum_{j,k}\frac{\boldsymbol{P}_k^n\hat{\boldsymbol{\gamma}}^{(1),n}\boldsymbol{P}_j^n\hat{\boldsymbol{\gamma}}^{(1),n}\boldsymbol{P}_i^n}{(\lambda_j^n-\lambda_i^n+2\beta_0)(\lambda_k^n-\lambda_i^n+4\beta_0)}\boldsymbol{C}_2^{(0),n}\frac{1}{d_i^n-1} + \boldsymbol{K}^{(1),n}\boldsymbol{P}_i^n\boldsymbol{C}_2^{(0),n}\frac{\beta_1}{\beta_0}\\ &- \boldsymbol{K}^{(1),n}\sum_j\frac{\boldsymbol{P}_j^n\hat{\boldsymbol{\gamma}}^{(1),n}\boldsymbol{P}_i^n}{\lambda_j^n-\lambda_i^n+2\beta_0}\boldsymbol{C}_2^{(0),n}\frac{1}{d_i^n-1} + \boldsymbol{K}^{(2),n}\boldsymbol{P}_i^n\boldsymbol{C}_2^{(0),n}\frac{1}{d_i^n-1}\\ &+ 2\beta_0\boldsymbol{A}^{(1),n}\sum_j\frac{\boldsymbol{P}_j^n\hat{\boldsymbol{\gamma}}^{(1),n}\boldsymbol{P}_i^n}{\lambda_j^n-\lambda_i^n+2\beta_0}\boldsymbol{C}_2^{(0),n} - 2\beta_0\boldsymbol{A}^{(1),n}\boldsymbol{P}_i^n\boldsymbol{C}_2^{(0),n}\frac{\beta_1}{\beta_0}d_i^n - 2\beta_0\boldsymbol{A}^{(2),n}\boldsymbol{P}_i^n\boldsymbol{C}_2^{(0),n},\end{aligned} \tag{3.37e}$$

$$\begin{aligned}\mathcal{E}_i^n = &\boldsymbol{K}^{(0),n}\boldsymbol{P}_i^n\boldsymbol{C}_2^{(1),n}\frac{\beta_1}{\beta_0}\frac{d_i^n-1}{d_i} - \boldsymbol{K}^{(0),n}\sum_j\frac{\boldsymbol{P}_j^n\hat{\boldsymbol{\gamma}}^{(1),n}\boldsymbol{P}_i^n}{\lambda_j^n-\lambda_i^n+2\beta_0}\boldsymbol{C}_2^{(1),n}\frac{1}{d_i^n} + \boldsymbol{K}^{(1),n}\boldsymbol{P}_i^n\boldsymbol{C}_2^{(1),n}\frac{1}{d_i^n}\\ &- \boldsymbol{K}^{(0),n}\boldsymbol{P}_i^n\boldsymbol{C}_2^{(0),n}\frac{\beta_1^2}{\beta_0^2}(d_i^n-1) + \boldsymbol{K}^{(0),n}\sum_j\frac{\boldsymbol{P}_i^n\hat{\boldsymbol{\gamma}}^{(1),n}\boldsymbol{P}_j^n}{\lambda_i^n-\lambda_j^n+2\beta_0}\boldsymbol{C}_2^{(0),n}\frac{\beta_1}{\beta_0}\frac{d_i^n-1}{d_i^n}\\ &+ \boldsymbol{K}^{(0),n}\sum_j\frac{\boldsymbol{P}_j^n\hat{\boldsymbol{\gamma}}^{(1),n}\boldsymbol{P}_i^n}{\lambda_j^n-\lambda_i^n+2\beta_0}\boldsymbol{C}_2^{(0),n}\frac{\beta_1}{\beta_0} - \boldsymbol{K}^{(0),n}\sum_{j,k}\frac{\boldsymbol{P}_j^n\hat{\boldsymbol{\gamma}}^{(1),n}\boldsymbol{P}_i^n\hat{\boldsymbol{\gamma}}^{(1),n}\boldsymbol{P}_k^n}{(\lambda_i^n-\lambda_k^n+2\beta_0)(\lambda_j^n-\lambda_i^n+2\beta_0)}\boldsymbol{C}_2^{(0),n}\frac{1}{d_i^n}\\ &- \boldsymbol{K}^{(1),n}\boldsymbol{P}_i^n\boldsymbol{C}_2^{(0),n}\frac{\beta_1}{\beta_0} + \boldsymbol{K}^{(1),n}\sum_j\frac{\boldsymbol{P}_i^n\hat{\boldsymbol{\gamma}}^{(1),n}\boldsymbol{P}_j^n}{\lambda_i^n-\lambda_j^n+2\beta_0}\boldsymbol{C}_2^{(0),n}\frac{1}{d_i^n}\\ &- 2\beta_0\boldsymbol{A}^{(1),n}\sum_j\frac{\boldsymbol{P}_i^n\hat{\boldsymbol{\gamma}}^{(1),n}\boldsymbol{P}_j^n}{\lambda_i^n-\lambda_j^n+2\beta_0}\boldsymbol{C}_2^{(0),n} + 2\beta_0\boldsymbol{A}^{(1),n}\boldsymbol{P}_i^n\boldsymbol{C}_2^{(0),n}\frac{\beta_1}{\beta_0}d_i^n - 2\beta_0\boldsymbol{A}^{(1),n}\boldsymbol{P}_i^n\boldsymbol{C}_2^{(1),n},\end{aligned} \tag{3.37f}$$

$$\begin{aligned}\mathcal{F}_i^n = &\boldsymbol{K}^{(0),n}\boldsymbol{P}_i^n\boldsymbol{C}_2^{(2),n}\frac{1}{d_i^n+1} - \boldsymbol{K}^{(0),n}\boldsymbol{P}_i^n\boldsymbol{C}_2^{(1),n}\frac{\beta_1}{\beta_0}\frac{d_i^n}{d_i^n+1} + \boldsymbol{K}^{(0),n}\sum_j\frac{\boldsymbol{P}_i^n\hat{\boldsymbol{\gamma}}^{(1),n}\boldsymbol{P}_j^n}{\lambda_i^n-\lambda_j^n+2\beta_0}\boldsymbol{C}_2^{(1),n}\frac{1}{d_i^n+1}\\ &+ \boldsymbol{K}^{(0),n}\boldsymbol{P}_i^n\boldsymbol{C}_2^{(0),n}\left(\frac{\beta_1^2}{\beta_0^2}-\frac{\beta_2}{\beta_0}\frac{1}{d_i^n+1}\right)\frac{d_i^n}{2} - \boldsymbol{K}^{(0),n}\sum_j\frac{\boldsymbol{P}_i^n\hat{\boldsymbol{\gamma}}^{(1),n}\boldsymbol{P}_j^n}{\lambda_i^n-\lambda_j^n+2\beta_0}\boldsymbol{C}_2^{(0),n}\frac{\beta_1}{\beta_0}\frac{d_j^n}{d_i^n+1}\end{aligned}$$

$$- \boldsymbol{K}^{(0),n} \sum_j \frac{\boldsymbol{P}_i^n \hat{\boldsymbol{\gamma}}^{(1),n} \boldsymbol{P}_j^n}{\lambda_i^n - \lambda_j^n + 4\beta_0} \boldsymbol{C}_2^{(0),n} \frac{\beta_1}{\beta_0} \left(1 - \frac{d_j^n}{d_i^n + 1}\right) + \boldsymbol{K}^{(0),n} \sum_j \frac{\boldsymbol{P}_i^n \hat{\boldsymbol{\gamma}}^{(2),n} \boldsymbol{P}_j^n}{\lambda_i^n - \lambda_j^n + 4\beta_0} \boldsymbol{C}_2^{(0),n} \frac{1}{d_i^n + 1}$$
$$+ \boldsymbol{K}^{(0),n} \sum_{j,k} \frac{\boldsymbol{P}_i^n \hat{\boldsymbol{\gamma}}^{(1),n} \boldsymbol{P}_j^n \hat{\boldsymbol{\gamma}}^{(1),n} \boldsymbol{P}_k^n}{\lambda_j^n - \lambda_k^n + 2\beta_0} \left(\frac{1}{\lambda_i^n - \lambda_j^n + 2\beta_0} - \frac{1}{\lambda_i^n - \lambda_k^n + 4\beta_0}\right) \boldsymbol{C}_2^{(0),n} \frac{1}{d_i^n + 1}, \tag{3.37g}$$

$$\mathcal{G}^n = 2\beta_0 \left(C_{2,\gamma}^{(2),n} + \boldsymbol{A}^{(1),n} \cdot \boldsymbol{C}_2^{(1),n} + \boldsymbol{A}^{(2),n} \cdot \boldsymbol{C}_2^{(0),n}\right). \tag{3.37h}$$

The LO ($\alpha\alpha_s^{-1}$) term $\mathcal{L}_i^n$ was obtained by Witten [7]. The NLO (α) corrections $\mathcal{A}_i^n$, $\mathcal{B}_i^n$ and C^n without terms including $\boldsymbol{A}^{(1),n}$ were first derived by Bardeen and Buras [8] for the case of the *real* photon target (i.e., $P^2 = 0$). Later Uematsu and Walsh [12] analyzed the NLO (α) corrections for the case of the *virtual* photon target ($P^2 \gg \Lambda^2$) and the terms including $\boldsymbol{A}^{(1),n}$ were added to $\mathcal{A}_i^n$ and C^n. The coefficients $\mathcal{D}_i^n$, $\mathcal{E}_i^n$, $\mathcal{F}_i^n$ and $\mathcal{G}^n$ are the NNLO ($\alpha\alpha_s$) corrections and new.

These coefficients have, formally, singularities in their expressions Eqs. (3.37a)-(3.37h), however, Eq. (3.36) never diverge by these superficial poles. In fact, for $n = 2$, one of the eigenvalues, $\lambda_-^{n=2}$, in Eq. (3.28) vanishes and we have $d_-^{n=2} = 0$. This is due to the fact that the corresponding operator is the hadronic energy-momentum tensor and is, therefore, conserved with a null anomalous dimension [8]. The coefficients $\mathcal{A}_-^{n=2}$ and $\mathcal{E}_-^{n=2}$ have terms which are proportional to $1/d_-^{n=2}$ and thus diverge. However, we see from Eq. (3.36) that these coefficients are multiplied by a factor $[1-(\alpha_s(Q^2)/\alpha_s(P^2))^{d_-^{n=2}}]$ which vanishes. In the end, the coefficients $\mathcal{A}_-^{n=2}$ and $\mathcal{E}_-^{n=2}$ multiplied by this factor remain finite [12]. Moreover, we will extend this sum rules to real n (and complex n-plane) later. In that situation, for example, the factor $1/(\lambda_-^n - \lambda_+^n + 2\beta_0)$ in $\mathcal{A}_+^n$ diverge when $d_-^n - d_+^n + 1 \to 0$. However, such poles have corresponding counterparts, e.g.,

$$\mathcal{A}_+^n \left[1 - \left(\frac{\alpha_s(Q^2)}{\alpha_s(P^2)}\right)^{d_+^n}\right] \to -\boldsymbol{K}^{(0),n} \frac{\boldsymbol{P}_-^n \hat{\boldsymbol{\gamma}}^{(1),n} \boldsymbol{P}_+^n}{\lambda_-^n - \lambda_+^n + 2\beta_0} \boldsymbol{C}_2^{(0),n} \frac{1}{d_+^n} \left[1 - \left(\frac{\alpha_s(Q^2)}{\alpha_s(P^2)}\right)^{d_+^n}\right], \tag{3.38a}$$

$$\mathcal{B}_-^n \left[1 - \left(\frac{\alpha_s(Q^2)}{\alpha_s(P^2)}\right)^{d_-^n+1}\right] \to \boldsymbol{K}^{(0),n} \frac{\boldsymbol{P}_-^n \hat{\boldsymbol{\gamma}}^{(1),n} \boldsymbol{P}_+^n}{\lambda_-^n - \lambda_+^n + 2\beta_0} \boldsymbol{C}_2^{(0),n} \frac{1}{d_-^n + 1} \left[1 - \left(\frac{\alpha_s(Q^2)}{\alpha_s(P^2)}\right)^{d_-^n+1}\right]. \tag{3.38b}$$

These two terms exactly cancel if $d_-^n - d_+^n + 1 \to 0$. Consequently, one can see that Eq. (3.36) is analytic on the real axis for $n > 1$.

3.2 Necessary Quantities in the $\overline{\text{MS}}$ Scheme

All the quantities necessary to evaluate the NNLO ($\alpha\alpha_s$) corrections to the moment sum rules of $F_2^\gamma(x, Q^2, P^2)$ have been calculated and most of them are presented in the literature, except for the two-loop photon matrix elements of hadronic operators $A_\psi^{(2),n}$, $A_G^{(2),n}$ and $A_{NS}^{(2),n}$. Also for the three-loop anomalous dimensions $K_\psi^{(2),n}$, $K_G^{(2),n}$ and $K_{NS}^{(2),n}$, we only have approximate expressions in the forms of photon-quark and photon-gluon splitting functions (i.e., x-space).

If not otherwise mentioned, all the expressions listed in this section are the ones calculated in the modified minimal subtraction ($\overline{\text{MS}}$) scheme [19].

Quark-charge Factors and β-Function Parameters The following quark-charge factors are often used below:

$$\delta_S = \langle e^2 \rangle = \frac{1}{n_f} \sum_{i=1}^{n_f} e_i^2, \qquad \delta_{NS} = 1, \qquad \delta_\gamma = 3 n_f \langle e^4 \rangle = 3 \sum_{i=1}^{n_f} e_i^4. \tag{3.39}$$

The β-function parameters β_0, β_1 and β_2, which are defined by

$$\mu\frac{dg}{d\mu} = \beta(g) = -\frac{g^3}{16\pi^2}\beta_0 - \frac{g^5}{(16\pi^2)^2}\beta_1 - \frac{g^7}{(16\pi^2)^3}\beta_2 + O(g^9), \tag{3.40}$$

are given by [45, 46]

$$\beta_0 = \frac{11}{3}C_A - \frac{2}{3}n_f, \tag{3.41a}$$

$$\beta_1 = \frac{34}{3}C_A^2 - \frac{10}{3}C_A n_f - 2C_F n_f, \tag{3.41b}$$

$$\beta_2 = \frac{2857}{54}C_A^3 - \frac{1415}{54}C_A^2 n_f - \frac{205}{18}C_A C_F n_f + \frac{79}{54}C_A n_f^2 + C_F^2 n_f + \frac{11}{9}C_F n_f^2, \tag{3.41c}$$

with $C_A = 3$ and $C_F = 4/3$ in QCD.

Coefficient Functions As shown in Eqs. (3.35b) and (3.35c), we need the hadronic coefficient functions $C_{2,i}^n$ with $i = \psi, G$ and NS, and the photon coefficient function $C_{2,\gamma}^n$ up to the two-loop level.

At the tree-level, we have

$$C_{2,\psi}^{(0),n} = \delta_S, \qquad C_{2,G}^{(0),n} = 0, \qquad C_{2,NS}^{(0),n} = \delta_{NS}, \qquad C_{2,\gamma}^{(0),n} = 0. \tag{3.42}$$

The one-loop coefficient functions were calculated in the MS scheme in Refs. [19, 47]. The $\overline{\text{MS}}$ results are written in the form as

$$C_{2,\psi}^{(1),n} = \delta_S \overline{B}_\psi^n, \qquad C_{2,G}^{(1),n} = \delta_S \overline{B}_G^n, \qquad C_{2,NS}^{(1),n} = \delta_{NS} \overline{B}_{NS}^n, \qquad C_{2,\gamma}^{(1),n} = \delta_\gamma \overline{B}_\gamma^n, \tag{3.43}$$

where $\overline{B}_\psi^n = \overline{B}_{NS}^n$ and $\overline{B}_G^n$ are obtained, for example, from the MS scheme results for $B_\psi^n = B_{NS}^n$ and B_G^n given in Eqs. (4.10) and (4.11) of Ref. [19] by discarding the terms proportional to $\ln(4\pi - \gamma_E)$. $\overline{B}_\gamma^n$ is related to $\overline{B}_G^n$ by $\overline{B}_\gamma^n = (2/n_f)\overline{B}_G^n$.

The two-loop coefficient functions corresponding to the hadronic operators were calculated in the $\overline{\text{MS}}$ scheme in Ref. [48]. They were expressed in fractional momentum space as functions x. The results in Mellin space as functions of n are found, for example, in Ref. [49]:

$$C_{2,\psi}^{(2),n} = \delta_S \left[c_{2,q}^{(2),+\text{ns}}(n) + c_{2,q}^{(2),-\text{ns}}(n) + c_{2,q}^{(2),\text{ps}}(n)\right], \tag{3.44a}$$

$$C_{2,G}^{(2),n} = \delta_S c_{2,g}^{(2)}(n), \tag{3.44b}$$

$$C_{2,NS}^{(2),n} = \delta_{NS} \left[c_{2,q}^{(2),+\text{ns}}(n) + c_{2,q}^{(2),-\text{ns}}(n)\right], \tag{3.44c}$$

where $c_{2,q}^{(2),+\text{ns}}(n)$, $c_{2,q}^{(2),-\text{ns}}(n)$, $c_{2,q}^{(2),\text{ps}}(n)$ and $c_{2,g}^{(2)}(n)$ are given in Eqs. (197), (198), (201) and (202) in Appendix B of Ref.[49], respectively, with N being replaced by n. The two-loop photon coefficient function $C_{2,\gamma}^{(2),n}$ is expressed as

$$C_{2,\gamma}^{(2),n} = \delta_\gamma c_{2,\gamma}^{(2)}(n), \tag{3.44d}$$

where $c_{2,\gamma}^{(2)}(n)$ is obtained from $c_{2,g}^{(2)}(n)$ in Eq. (3.44b) by replacing $C_A \to 0$ and $n_f/2 \to 1$ [50].

Anomalous Dimensions The one-loop anomalous dimensions for the hadronic sector were calculated long time ago [51, 52]. The expressions of $\gamma_{NS}^{(0),n} = \gamma_{\psi\psi}^{(0),n}$, $\gamma_{\psi G}^{(0),n}$, $\gamma_{G\psi}^{(0),n}$ and $\gamma_{GG}^{(0),n}$ are given, for example, in Eqs.(4.1), (4.2), (4.3) and (4.4) of Ref. [8], respectively, with f being replaced by n_f. As for the one-loop

photonic anomalous dimension row vector $\boldsymbol{K}^{(0),n} = (\boldsymbol{K}_{\psi}^{(0),n}, \boldsymbol{K}_{G}^{(0),n}, \boldsymbol{K}_{NS}^{(0),n})$, we have $\boldsymbol{K}_{G}^{(0),n} = 0$ and $\boldsymbol{K}_{\psi}^{(0),n}$ and $\boldsymbol{K}_{NS}^{(0),n}$ are given, respectively, in Eqs. (4.5) and (4.6) of Ref. [8] with f being replaced by n_f again.

The two-loop anomalous dimensions for the hadronic sector were calculated in Ref. [47] and recalculated using a different method and a different gauge in Ref. [53]. The results by the two groups agreed with each other except in the part of $\gamma_{GG}^{(1),n}$ proportional to C_A^2, however, this discrepancy was solved later [54].

They are given by

$$\gamma_{NS}^{(1),n} = 2\gamma_{\rm ns}^{(1)+}(n), \tag{3.45a}$$
$$\gamma_{\psi\psi}^{(1),n} = 2\left[\gamma_{\rm ns}^{(1)+}(n) + \gamma_{\rm ps}^{(1)}(n)\right], \tag{3.45b}$$
$$\gamma_{\psi G}^{(1),n} = 2\gamma_{\rm qg}^{(1)}(n), \tag{3.45c}$$
$$\gamma_{G\psi}^{(1),n} = 2\gamma_{\rm gq}^{(1)}(n), \tag{3.45d}$$
$$\gamma_{GG}^{(1),n} = 2\gamma_{\rm gg}^{(1)}(n), \tag{3.45e}$$

where $\gamma_{\rm ns}^{(1)+}(n)$ is given in Eq. (3.5) of Ref. [55], and $\gamma_{\rm ps}^{(1)}(n)$, $\gamma_{\rm qg}^{(1)}(n)$, $\gamma_{\rm gq}^{(1)}(n)$ and $\gamma_{\rm gg}^{(1)}(n)$ are given, respectively, in Eqs. (3.6), (3.7), (3.8) and (3.9) of Ref.[56], with N being replaced by n. The factor of 2 in Eqs. (3.45) appears since, in Refs. [55] and [56], the anomalous dimension γ of the renormalized operator O is defined as $dO/d\ln(\mu^2) = -\gamma O$ instead of $dO/d\ln(\mu) = -\gamma O$.

The two-loop photonic anomalous dimensions $K_{\psi}^{(1),n}$, $K_{NS}^{(1),n}$ and $K_{G}^{(1),n}$ can be obtained from $\gamma_{\psi G}^{(1),n}$ and $\gamma_{GG}^{(1),n}$ by replacing color factors with relevant charge factors [8]. Moreover we need an additional operation for $K_{G}^{(1),n}$. They are given by

$$K_{\psi}^{(1),n} = -6n_f\langle e^2\rangle k_q^{(1)}(n), \tag{3.46a}$$
$$K_{G}^{(1),n} = -6n_f\langle e^2\rangle k_g^{(1)}(n), \tag{3.46b}$$
$$K_{NS}^{(1),n} = -6n_f\left(\langle e^4\rangle - \langle e^2\rangle^2\right) k_q^{(1)}(n), \tag{3.46c}$$

where $k_q^{(1)}(n)$ and $k_g^{(1)}(n)$ are obtained from $\gamma_{\rm qg}^{(1)}(n)$ and $(\gamma_{\rm gg}^{(1)}(n) - 2n_f C_F)$, with $\gamma_{\rm qg}^{(1)}(n)$ and $\gamma_{\rm qg}^{(1)}(n)$ in Eqs. (3.45), by replacing $n_f/2 \to 1$ and $C_A \to 0$. The term $2n_f C_F$ in $\gamma_{\rm gg}^{(1)}(n)$ must be subtracted since this term has originated as the gluon self-energy contribution and should be dropped for the photonic case [57, 58]. The factors $3n_f\langle e^2\rangle$ and $3n_f\left(\langle e^4\rangle - \langle e^2\rangle^2\right)$ in Eqs. (3.46) are the relevant charge factors, and the sign difference is due to the our convention for $\boldsymbol{K}^n$ in Eq. (3.34). The extra factor 2 is, again, originated in the difference in the definition of the anomalous dimensions.

The three-loop anomalous dimensions for the hadronic sector have been calculated recently in Refs. [55, 56]. They are expressed as

$$\gamma_{NS}^{(2),n} = 2\gamma_{\rm ns}^{(2)+}(n), \tag{3.47a}$$
$$\gamma_{\psi\psi}^{(2),n} = 2\left[\gamma_{\rm ns}^{(2)+}(n) + \gamma_{\rm ps}^{(2)}(n)\right], \tag{3.47b}$$
$$\gamma_{\psi G}^{(2),n} = 2\gamma_{\rm qg}^{(2)}(n), \tag{3.47c}$$
$$\gamma_{G\psi}^{(2),n} = 2\gamma_{\rm gq}^{(2)}(n), \tag{3.47d}$$
$$\gamma_{GG}^{(2),n} = 2\gamma_{\rm gg}^{(2)}(n), \tag{3.47e}$$

where $\gamma_{\rm ns}^{(2)+}(n)$ is given in Eq. (3.7) of Ref. [55], and $\gamma_{\rm ps}^{(2)}(n)$, $\gamma_{\rm qg}^{(2)}(n)$, $\gamma_{\rm gq}^{(2)}(n)$ and $\gamma_{\rm gg}^{(2)}(n)$ are given, respectively, in Eqs. (3.10), (3.11), (3.12) and (3.13) of Ref. [56], with N being replaced by n.

Concerning the three-loop anomalous dimensions $K_{\psi}^{(2),n}$, $K_{G}^{(2),n}$ and $K_{NS}^{(2),n}$, the exact expressions have not been in literature yet. Indeed, the lowest six even-integer Mellin moments, $n = 2, \cdots, 12$, of these anomalous dimensions were calculated and given in Ref. [50]. Quite recently, the authors of Ref. [50] have

Table 3.1: Numerical values of $k_{\rm ns}^{(2)}(n)$ and $k_g^{(2)}(n)$, and numerical values of the corresponding approximated expressions $k_{\rm ns}^{(2),\rm approx}(n)$ and $k_g^{(2),\rm approx}(n)$ for the lowest six even-integer values of n. The values for $k_{\rm ns}^{(2)}(n)$ and $k_g^{(2)}(n)$ are found in Eqs. (3.1) and (3.3) of Ref. [50] (Analytic expressions of them are given in Eqs. (A.1)-(A.12) of Ref. [50]). The values of $k_{\rm ns}^{(2),\rm approx}(n)$ and $k_g^{(2),\rm approx}(n)$ are obtained from the expressions given in Eqs. (B.2)-(B.5) in Appendix B.

n	$k_{\rm ns}^{(2)}(n)$	$k_{\rm ns}^{(2),\rm approx}(n)$	$k_g^{(2)}(n)$	$k_g^{(2),\rm approx}(n)$
2	- 86.9753+1.47051 n_f	- 86.9844+1.47104 n_f	31.4197 +5.15775 n_f	31.4155 +5.15803 n_f
4	-102.831 +1.47737 n_f	-102.848 +1.47787 n_f	23.9427 +1.10886 n_f	23.9419 +1.10888 n_f
6	-109.278 +1.65653 n_f	-109.299 +1.65699 n_f	15.6517 +0.695953 n_f	15.6507 +0.695944 n_f
8	-111.167 +1.69550 n_f	-111.192 +1.69592 n_f	10.9661 +0.498196 n_f	10.9651 +0.498178 n_f
10	-111.035 +1.67061 n_f	-111.062 +1.67099 n_f	8.16031+0.379060 n_f	8.15953+0.379038 n_f
12	-109.943 +1.61908 n_f	-109.972 +1.61943 n_f	6.34829+0.300274 n_f	6.34777+0.300250 n_f

presented compact parameterizations of the three-loop photon-non-singlet quark and photon-gluon splitting functions, $P_{\rm ns\gamma}^{(2)}(x)$ and $P_{\rm g\gamma}^{(2)}(x)$, instead of providing the exact analytic results [9]. It is remarked there that their parameterizations deviate from the lengthy full expressions by about 0.1% or less. They also gave in Ref. [9] the analytic expression of the three-loop photon-pure-singlet quark splitting function $P_{\rm ps\gamma}^{(2)}(x)$.

It is true that we can infer the analytic expressions for some parts of $K_\psi^{(2),n}$, $K_G^{(2),n}$ and $K_{NS}^{(2),n}$, from the known three-loop results of $\gamma_{\psi G}^{(2),n}$ and $\gamma_{GG}^{(2),n}$. For instance, the part of the expressions of $K_\psi^{(2),n}$ and $K_{NS}^{(2),n}$ which have the color factor C_F^2 are obtained from $\gamma_{\psi G}^{(2),n}$ by taking the terms which are proportional to the color factor $n_f C_F^2$. Also the terms of $K_G^{(2),n}$ with the color factors $n_f C_F$ and C_F^2 are related to the ones of $\gamma_{GG}^{(2),n}$ with the color factors $n_f^2 C_F$ and $n_f C_F^2$, respectively. But at present we do not have the exact analytic expressions of $K_\psi^{(2),n}$, $K_G^{(2),n}$ and $K_{NS}^{(2),n}$ as a whole.

Under these circumstances we are reconciled to use of approximate expressions for $K_\psi^{(2),n}$, $K_G^{(2),n}$ and $K_{NS}^{(2),n}$. They are obtained by taking the Mellin moments of the parameterizations for $P_{\rm ns\gamma}^{(2)}(x)$ and $P_{\rm g\gamma}^{(2)}(x)$, and of the exact result for $P_{\rm ps\gamma}^{(2)}(x)$, which are presented in Ref. [9]. Then we have

$$K_\psi^{(2),n} \approx -6 n_f \langle e^2 \rangle \left[k_{\rm ns}^{(2),\rm approx}(n) + k_{\rm ps}^{(2)}(n) \right], \tag{3.48a}$$

$$K_G^{(2),n} \approx -6 n_f \langle e^2 \rangle k_g^{(2),\rm approx}(n), \tag{3.48b}$$

$$K_{NS}^{(2),n} \approx -6 n_f \left(\langle e^4 \rangle - \langle e^2 \rangle^2 \right) k_{\rm ns}^{(2),\rm approx}(n), \tag{3.48c}$$

where the explicit expressions of $k_{\rm ns}^{(2),\rm approx}(n)$, $k_g^{(2),\rm approx}(n)$ and $k_{\rm ps}^{(2)}(n)$ are given in Eqs. (B.2)-(B.5) in Appendix B. As mentioned above, the lowest six even-integer Mellin moments, $n = 2, \cdots, 12$, of these anomalous dimensions were given in Ref. [50]. In Table 3.1, we give the approximated expressions $k_{\rm ns}^{(2),\rm approx}(n)$ and $k_g^{(2),\rm approx}(n)$ as well as the corresponding exact expressions $k_{\rm ns}^{(2)}(n)$ and $k_g^{(2)}(n)$ in numerical form for the lowest six even-integer values of n. We see the deviations of both $k_{\rm ns}^{(2),\rm approx}(n)$ from $k_{\rm ns}^{(2)}(n)$ and $k_g^{(2),\rm approx}(n)$ from $k_g^{(2)}(n)$ are far less than 0.1% for these values of n.

Photon Matrix Elements The two-loop operator matrix elements have been calculated up to the finite terms by Matiounine, Smith and van Neerven (MSvN) [59]. Using their results and changing the color-group factors, we can obtain the photon matrix elements of hadronic operators up to the two-loop level. First we clear up a subtle issue which appears in the calculation of the photon matrix elements of the hadronic operators. The one-loop gluon coefficient function $\overline{B}_G^n$ in Eq. (3.43) was calculated by two groups; the first

group is Bardeen, Buras, Duke and Muta (BBDM) [19], and second one is Floratos, Ross and Sachrajda (FRS) [47]. Both groups evaluated one-loop diagrams contributing to the forward virtual photon-gluon scattering as well as those contributing to the matrix element of the quark operator between gluon states, and they took a difference between the two to obtain $\overline{B}_G^n$. But actually BBDM calculated the gluon spin averaged contributions, i.e., multiplying $g_{\rho\tau}$ and contracting pairs of the Lorentz indices ρ and τ, whereas FRS picked up the parts which are proportional to $g_{\rho\tau}$. Thus the BBDM results on the contributions to the forward virtual photon-gluon scattering and the gluon matrix element of quark operator are different from those by FRS, however, the difference between the two contributions, i.e., $\overline{B}_G^n$, is the same as it should be.

We have defined the spin-averaged structure tensor $W_{\mu\nu}^{\gamma}$ as Eq. (3.1), taking a spin average of the target photon for the structure tensor $W_{\mu\nu\rho\tau}$. Therefore we should adopt the BBDM result rather than that of FRS. Then we get for the photon matrix elements of the hadronic operators at one-loop level,

$$A_{\psi}^{(1),n} = 3n_f\langle e^2\rangle a_q^{(1)}(n), \tag{3.49a}$$

$$A_{G}^{(1),n} = 0, \tag{3.49b}$$

$$A_{NS}^{(1),n} = 3n_f\left(\langle e^4\rangle - \langle e^2\rangle^2\right) a_q^{(1)}(n), \tag{3.49c}$$

where $a_q^{(1)}(n)$ is given in Eq. (B.5) in Appendix B. Actually, $a_q^{(1)}(n)$ is related to the BBDM result on the one-loop gluon matrix element of quark operator $A_{nG}^{(2)\psi}$ given in Eq. (6.2) of Ref. [19] as $A_{nG}^{(2)\psi} = (\alpha_s/4\pi)(n_f/2)a_q^{(1)}(n)$.

MSvN have presented in Appendix A of Ref. [59] full expressions for the two-loop corrected operator matrix elements which are unrenormalized and include external self-energy corrections. The expressions are given in parton momentum fraction (z) space. Taking the moments, the unrenormalized matrix elements of the (flavor-singlet) quark operators between gluon states are written in the form as (see Eq. (2.18) of Ref. [59]),

$$\hat{A}_{qg,\rho\tau}\left(n, \frac{-p^2}{\mu^2}, \frac{1}{\epsilon}\right) = \hat{A}_{qg}^{\rm PHYS}\left(n, \frac{-p^2}{\mu^2}, \frac{1}{\epsilon}\right) T_{\rho\tau}^{(1)} + \hat{A}_{qg}^{\rm EOM}\left(n, \frac{-p^2}{\mu^2}, \frac{1}{\epsilon}\right) T_{\rho\tau}^{(2)} + \hat{A}_{qg}^{\rm NGI}\left(n, \frac{-p^2}{\mu^2}, \frac{1}{\epsilon}\right) T_{\rho\tau}^{(3)}, \tag{3.50}$$

where

$$\hat{A}_{qg}^{k}\left(n, \frac{-p^2}{\mu^2}, \frac{1}{\epsilon}\right) = \int dz\, z^{n-1} \hat{A}_{qg}^{k}\left(z, \frac{-p^2}{\mu^2}, \frac{1}{\epsilon}\right), \qquad k = \text{PHYS, EOM, NGI}, \tag{3.51}$$

and the expressions of $\hat{A}_{qg}^{\rm PHYS}(n, -p^2/\mu^2, 1/\epsilon)$, $\hat{A}_{qg}^{\rm EOM}(n, -p^2/\mu^2, 1/\epsilon)$ and $\hat{A}_{qg}^{\rm NGI}(n, -p^2/\mu^2, 1/\epsilon)$ are given in Eqs. (A7), (A8) and (A9) of Ref. [59], respectively. For the explanation of the "PHYS", "EOM" and "NGI" parts, please refer to Ref.[59]. The tensors $T_{\rho\tau}^{(i)}$ ($i = 1, 2, 3$) are given by (see Eqs (2.19)-(2.21) of Ref. [59] and note that we have changed the Lorentz indices of gluon fields from $\mu\nu$ to $\rho\tau$),

$$T_{\rho\tau}^{(1)} = \left[g_{\rho\tau} - \frac{p_\rho\Delta_\tau + \Delta_\rho p_\tau}{\Delta\cdot p} + \frac{\Delta_\rho\Delta_\tau p^2}{(\Delta\cdot p)^2}\right](\Delta\cdot p)^n, \tag{3.52a}$$

$$T_{\rho\tau}^{(2)} = \left[\frac{p_\rho p_\tau}{p^2} - \frac{p_\rho\Delta_\tau + \Delta_\rho p_\tau}{\Delta\cdot p} + \frac{\Delta_\rho\Delta_\tau p^2}{(\Delta\cdot p)^2}\right](\Delta\cdot p)^n, \tag{3.52b}$$

$$T_{\rho\tau}^{(3)} = \left[-\frac{p_\rho\Delta_\tau + \Delta_\rho p_\tau}{2\Delta\cdot p} + \frac{\Delta_\rho\Delta_\tau p^2}{(\Delta\cdot p)^2}\right](\Delta\cdot p)^n, \tag{3.52c}$$

where Δ_μ is a lightlike vector ($\Delta^2 = 0$).

The expressions in Appendix A of Ref. [59] contains various polylogarithms such as $\mathrm{Li}_n(z)$ and $\mathrm{S}_{n,m}(z)$, but all of them can be translated into the harmonic polylogarithms [60]. The Mellin transform of the harmonic polylogarithms can be expressed in terms of the harmonic sums, and such method is implemented in the program package Harmpol written in Form [60, 61, 62].

The renormalization of $\hat{A}^k_{qg,\rho\tau}(n, -p^2/\mu^2, 1/\epsilon)$ proceeds as follows. First the coupling constant and gauge constant renormalization is performed. Then the remaining ultraviolet divergences are removed by multiplication of the operator renormalization constants. Up to the two-loop order, we get the finite expression at $\mu^2 = -p^2$ as following form:

$$\hat{A}_{qg,\rho\tau}\left(n, \frac{-p^2}{\mu^2}, \frac{1}{\epsilon}\right)\Big|_{\mu^2=-p^2} = \left[\frac{\alpha_s}{4\pi}a^{(1)}_{qg}(n) + \left(\frac{\alpha_s}{4\pi}\right)^2 a^{(2)}_{qg}(n)\right]T^{(1)}_{\rho\tau} + \left[\frac{\alpha_s}{4\pi}b^{(1)}_{qg}(n) + \left(\frac{\alpha_s}{4\pi}\right)^2 b^{(2)}_{qg}(n)\right]T^{(2)}_{\rho\tau} + \left(\frac{\alpha_s}{4\pi}\right)^2 a^{(2)}_{qA}(n)T^{(3)}_{\rho\tau}. \tag{3.53}$$

Here $a^{(2)}_{qA}(n)$ in Eq. (3.53) is made up of the terms proportional to $n_f C_A$ and is, therefore, irrelevant to the photon matrix element of the quark operator. Now multiplying $g^{\rho\tau}$ and contracting pairs of indices ρ and τ, we get

$$\frac{1}{2}g^{\rho\tau}\frac{1}{(\Delta\cdot p)^n}\hat{A}_{qg,\rho\tau}\left(n, \frac{-p^2}{\mu^2}, \frac{1}{\epsilon}\right)\Big|_{\mu^2=-p^2} = \frac{\alpha_s}{4\pi}\left[a^{(1)}_{qg}(n) - \frac{1}{2}b^{(1)}_{qg}(n)\right] + \left(\frac{\alpha_s}{4\pi}\right)^2\left[a^{(1)}_{qg}(n) - \frac{1}{2}b^{(1)}_{qg}(n) - \frac{1}{2}a^{(2)}_{qA}(n)\right]. \tag{3.54}$$

Indeed, the FRS result for the one-loop gluon matrix element of the quark operator corresponds $a^{(1)}_{qg}(n)$, while the BBDM result corresponds to the combination $[a^{(1)}_{qg}(n) - b^{(1)}_{qg}(n)/2]$, i.e., $a^{(1)}_q(n)$ in Eq. (B.5) is written as $(n_f)/2a^{(1)}_q(n) = [a^{(1)}_{qg}(n) - b^{(1)}_{qg}(n)/2]$.

The two-loop photon matrix elements of the quark operators are derived from the combination $[a^{(2)}_{qg}(n) - b^{(2)}_{qg}(n)/2]$ in Eq. (3.54) with the following replacements: $C_A \to 0$, $(n_f/2)^2 \to 0$ and $n_f C_F \to$ (relevant charge factor) $\times C_F$. The terms proportional to $(n_f/2)^2$ in $a^{(2)}_{qg}(n)$ and $b^{(2)}_{qg}(n)$ come from the external gluon self-energy corrections and must be discarded for the photon case. Then we have

$$A^{(2),n}_{\psi} = 3n_f\langle e^2\rangle a^{(2)}_q(n), \tag{3.55a}$$

$$A^{(2),n}_{NS} = 3n_f\left(\langle e^4\rangle - \langle e^2\rangle^2\right)a^{(2)}_q(n), \tag{3.55b}$$

where $a^{(2)}_q(n)$ is given in Eq. (B.6) in Appendix B.

Similarly the renormalized matrix elements of the gluon operators between gluon states at $\mu^2 = -p^2$ are written as (the unrenormalized version is given in Eq. (2.33) of Ref. [59])[♯1],

$$\hat{A}_{gg,\rho\tau}\left(n, \frac{-p^2}{\mu^2}, \frac{1}{\epsilon}\right)\Big|_{\mu^2=-p^2} = \left[\frac{\alpha_s}{4\pi}a^{(1)}_{gg}(n) + \left(\frac{\alpha_s}{4\pi}\right)^2 a^{(2)}_{gg}(n)\right]T^{(1)}_{\rho\tau} + \left[\frac{\alpha_s}{4\pi}b^{(1)}_{gg}(n) + \left(\frac{\alpha_s}{4\pi}\right)^2 b^{(2)}_{gg}(n)\right]T^{(2)}_{\rho\tau} + \left[\frac{\alpha_s}{4\pi}a^{(1)}_{gA}(n) + \left(\frac{\alpha_s}{4\pi}\right)^2 a^{(2)}_{gA}(n)\right]T^{(3)}_{\rho\tau}. \tag{3.56}$$

The one-loop results $a^{(1)}_{gg}(n)$, $b^{(1)}_{gg}(n)$ and $a^{(1)}_{gA}(n)$ are irrelevant to the photon matrix elements because they are proportional to the color factor C_A, or proportional to n_f but due to the external self-energy diagrams. Also the two-loop result $a^{(2)}_{gA}(n)$ is made up of the terms proportional to C_A^2 or $n_f C_A$ and is irrelevant. Then, to obtain $A^{(2),n}_G$, we take the combination $[a^{(2)}_{gg}(n) - b^{(2)}_{gg}(n)/2]$ and make replacements, $C_A \to 0$, $(n_f/2)^2 \to 0$ and $n_f C_F \to$ (relevant charge factor) $\times C_F$, with dropping the external gluon self-energy terms corresponding to $F^2 n_f C_F T_F \delta(1-z)(-55/3 + 16\zeta(3))$ in Eq. (A.12) of Ref. [59]. Finally we obtain for the photon matrix elements of the gluon operators,

$$A^{(2),n}_G = 3n_f\langle e^2\rangle a^{(2)}_G(n), \tag{3.57}$$

where $a^{(2)}_G(n)$ is given in Eq. (B.7) in Appendix B.

[♯1] Two terms $\gamma^{(0)}_{gg}b^{\epsilon,(1)}_{gg} + \gamma^{(0)}_{gq}b^{\epsilon,(1)}_{qg}$ are missing in the ϵ-independent terms of Eq. (2.35) of Ref. [59]. The both are needed in order to extract $b^{(2)}_{gg}(n)$ correctly.

Longitudinal Structure Function $F_L^\gamma(x, Q^2, P^2)$ So far, we have considered the structure function $F_2^\gamma(x, Q^2, P^2)$. We will now mention the moment sum rule of $F_L^\gamma(x, Q^2, P^2)$. From Eqs. (3.10), we can see that the difference between the moment sum rule of $F_2^\gamma(x, Q^2, P^2)$ and that of $F_L^\gamma(x, Q^2, P^2)$ is the coefficient functions. Therefore all we have to do is replacing $\boldsymbol{C}_2^{(k),n}$ and $C_{2,\gamma}^{(k),n}$ by $\boldsymbol{C}_L^{(k),n}$ and $C_{L,\gamma}^{(k),n}$ ($k = 0, 1, 2$), respectively, in the coefficients $\mathcal{L}_i^n$, $\mathcal{A}_i^n$, $\mathcal{B}_i^n$, $\mathcal{C}^n$, $\mathcal{D}_i^n$, $\mathcal{E}_i^n$, $\mathcal{F}_i^n$ and $\mathcal{G}^n$ in our formula Eq. (3.36), where $\boldsymbol{C}_L^{(k),n}$ and $C_{L,\gamma}^{(k),n}$ is given by (see also Eqs. (3.35b) and (3.35c))

$$\boldsymbol{C}_L^n(g) = \boldsymbol{C}_L^{(0),n} + \frac{g^2}{16\pi^2}\boldsymbol{C}_L^{(1),n} + \frac{g^4}{(16\pi^2)^2}\boldsymbol{C}_L^{(2),n} + O(g^6), \tag{3.58a}$$

$$C_{L,\gamma}^n(g,\alpha) = \frac{\alpha}{4\pi}\left[\boldsymbol{C}_{L,\gamma}^{(1),n} + \frac{g^2}{16\pi^2}\boldsymbol{C}_{L,\gamma}^{(2),n} + O(g^4)\right]. \tag{3.58b}$$

We note, however, that there is no contribution of the tree diagrams to the longitudinal coefficient functions and thus we have $\boldsymbol{C}_L^{(0),n} = \boldsymbol{0}$. Therefore, in the case of the longitudinal photon structure function $F_L^\gamma(x, Q^2, P^2)$, $O(1/\alpha_s)$ coefficient $\mathcal{L}_i$ Eq. (3.37a) vanishes when we replace $\boldsymbol{C}_2^{(0),n} \to \boldsymbol{C}_L^{(0),n} = \boldsymbol{0}$. and the its LO contribution is of order α.

Now, the moment sum rule of $F_L^\gamma(x, Q^2, P^2)$ up to the NLO ($O(\alpha\alpha_s)$) corrections is given as follows (See Eq. (3.36) for comparison):

$$\begin{aligned}
&\int_0^1 dx\, x^{n-2} F_L^\gamma(x, Q^2, P^2) \\
&\quad = \frac{\alpha}{4\pi}\frac{1}{2\beta_0}\Bigg\{\sum_i \mathcal{B}_{(L),i}^n\left[1 - \left(\frac{\alpha_s(Q^2)}{\alpha_s(P^2)}\right)^{d_i^n+1}\right] + C_{(L)}^n \\
&\qquad + \frac{\alpha_s(Q^2)}{4\pi}\left(\sum_i \mathcal{E}_{(L),i}^n\left[1 - \left(\frac{\alpha_s(Q^2)}{\alpha_s(P^2)}\right)^{d_i^n}\right] + \sum_i \mathcal{F}_{(L),i}^n\left[1 - \left(\frac{\alpha_s(Q^2)}{\alpha_s(P^2)}\right)^{d_i^n+1}\right] + \mathcal{G}_{(L)}^n\right) + O(\alpha_s^2)\Bigg\},
\end{aligned} \tag{3.59}$$

with $i = +, -, NS$, and the coefficients $\mathcal{B}_{(L),i}^n$, $C_{(L)}^n$, $\mathcal{E}_{(L),i}^n$, $\mathcal{F}_{(L),i}^n$ and $\mathcal{G}_{(L)}^n$ are (c.f., Eqs. (3.37))

$$\mathcal{B}_{(L),i}^n = \boldsymbol{K}^{(0),n}\boldsymbol{P}_i^n\boldsymbol{C}_L^{(1),n}\frac{1}{d_i^n+1}, \tag{3.60a}$$

$$C_{(L)}^n = 2\beta_0 C_{L,\gamma}^{(1),n}, \tag{3.60b}$$

$$\begin{aligned}
\mathcal{E}_{(L),i}^n = {}& \boldsymbol{K}^{(0),n}\boldsymbol{P}_i^n\boldsymbol{C}_L^{(1),n}\frac{\beta_1}{\beta_0}\frac{d_i^n-1}{d_i} - \boldsymbol{K}^{(0),n}\sum_j \frac{\boldsymbol{P}_j^n\hat{\boldsymbol{\gamma}}^{(1),n}\boldsymbol{P}_i^n}{\lambda_j^n - \lambda_i^n + 2\beta_0}\boldsymbol{C}_L^{(1),n}\frac{1}{d_i^n} + \boldsymbol{K}^{(1),n}\boldsymbol{P}_i^n\boldsymbol{C}_L^{(1),n}\frac{1}{d_i^n} \\
& - 2\beta_0\boldsymbol{A}^{(1),n}\boldsymbol{P}_i^n\boldsymbol{C}_L^{(1),n},
\end{aligned} \tag{3.60c}$$

$$\mathcal{F}_{(L),i}^n = \boldsymbol{K}^{(0),n}\boldsymbol{P}_i^n\boldsymbol{C}_L^{(2),n}\frac{1}{d_i^n+1} - \boldsymbol{K}^{(0),n}\boldsymbol{P}_i^n\boldsymbol{C}_L^{(1),n}\frac{\beta_1}{\beta_0}\frac{d_i^n}{d_i^n+1} + \boldsymbol{K}^{(0),n}\sum_j \frac{\boldsymbol{P}_i^n\hat{\boldsymbol{\gamma}}^{(1),n}\boldsymbol{P}_j^n}{\lambda_i^n - \lambda_j^n + 2\beta_0}\boldsymbol{C}_L^{(1),n}\frac{1}{d_i^n+1}, \tag{3.60d}$$

$$\mathcal{G}_{(L)}^n = 2\beta_0\left(C_{L,\gamma}^{(2),n} + \boldsymbol{A}^{(1),n}\cdot\boldsymbol{C}_L^{(1),n}\right). \tag{3.60e}$$

The coefficients $\mathcal{B}_{(L),i}^n$ and $C_{(L)}^n$ represents the LO terms [7, 8, 12], while the terms with $\mathcal{E}_{(L),i}^n$, $\mathcal{F}_{(L),i}^n$ and $\mathcal{G}_{(L)}^n$ the NLO ($\alpha\alpha_s$) contributions and new.

The one-loop longitudinal coefficient functions were well-known [19, 63, 64]. They are written in the form as

$$C_{L,\psi}^{(1),n} = \delta_S B_{\psi,L}^n, \qquad C_{L,G}^{(1),n} = \delta_S B_{G,L}^n, \qquad C_{L,NS}^{(1),n} = \delta_{NS} B_{NS,L}^n, \qquad C_{L,\gamma}^{(1),n} = \delta_\gamma B_{\gamma,L}^n, \tag{3.61}$$

Table 3.2: Numerical values of d_i^n $(i = +, -, NS)$ for $n = 2, 4, \cdots, 12$ in the case of $n_f = 3, 4$.

n	$n_f = 3$ d_+^n	d_-^n	d_{NS}^n	$n_f = 4$ d_+^n	d_-^n	d_{NS}^n
2	0.6173	0	0.3951	0.7467	0	0.4267
4	1.6376	0.7599	0.7753	1.8523	0.8170	0.8373
6	2.2029	0.9958	1.0004	2.4604	1.0743	1.0804
8	2.5873	1.1599	1.1620	2.8749	1.2521	1.2550
10	2.8816	1.2874	1.2885	3.1924	1.3900	1.3916
12	3.1209	1.3918	1.3926	3.4509	1.5030	1.5040

where $B_{\psi,L}^n = B_{NS,L}^n$, $B_{G,L}^n$ and $B_{\gamma,L}^n$ are given, for example, in Eqs. (6.2)-(6.4) of Ref .[8]. The two-loop longitudinal coefficient functions corresponding to the hadronic operators were calculated in the $\overline{\rm MS}$ scheme in [48][♯2]. The results in Mellin space as functions of n are found, for example, in Ref. [49]:

$$C_{L,\psi}^{(2),n} = \delta_S \left[c_{L,q}^{(2),\rm ns}(n) + c_{L,q}^{(2),\rm ps}(n) \right], \tag{3.62a}$$

$$C_{L,G}^{(2),n} = \delta_S c_{L,g}^{(2)}(n), \tag{3.62b}$$

$$C_{L,NS}^{(2),n} = \delta_{NS} c_{L,q}^{(2),\rm ns}(n), \tag{3.62c}$$

where $c_{L,q}^{(2),\rm ns}(n)$, $c_{L,q}^{(2),\rm ps}(n)$ and $c_{L,g}^{(2)}(n)$ are given in Eqs. (203), (204), and (205) in Appendix B of Ref. [49], respectively, with N being replaced by n. The two-loop photon longitudinal coefficient function $C_{L,\gamma}^{(2),n}$ is expressed as

$$C_{L,\gamma}^{(2),n} = \delta_\gamma c_{L,\gamma}^{(2)}(n), \tag{3.62d}$$

and $c_{L,\gamma}^{(2)}(n)$ is obtained from $c_{L,g}^{(2)}(n)$ in Eq. (3.62b) by replacing $C_A \to 0$ and $n_f/2 \to 1$.

3.3 Evaluation of the Moment Sum Rules

With all these necessary parameters listed in the previous section, we are now ready to analyze the moments of $F_2^\gamma(x, Q^2, P^2)$ up to the NNLO $(\alpha\alpha_s)$, and $F_L^\gamma(x, Q^2, P^2)$ up to the NLO $(\alpha\alpha_s)$. We first evaluate, for $F_2^\gamma(x, Q^2, P^2)$, the coefficients $\mathcal{L}_i^n$, $\mathcal{A}_i^n$, $\mathcal{B}_i^n$, C^n, $\mathcal{D}_i^n$, $\mathcal{E}_i^n$, $\mathcal{F}_i^n$ and $\mathcal{G}^n$, which are given in Eqs. (3.37), as well as d_i^n defined by Eq. (3.33), with $i = +, i, NS$, for $n = 2, 4, \cdots, 12$ in the cases of $n_f = 3$ and $n_f = 4$. The results are tabulated in Tables 3.2 (for d_i^n), 3.3 ($\mathcal{L}_i^n, \cdots, \mathcal{G}^n$ for $n_f = 3$) and 3.4 ($\mathcal{L}_i^n, \cdots, \mathcal{G}^n$ for $n_f = 4$).

In Table 1 of Ref. [12], the numerical values of the NLO coefficients $\mathcal{A}_i^n$, $\mathcal{B}_i^n$ with $i = +, -, NS$ and C^n were given for $n = 2, 4, \cdots, 20$ for $n_f = 4$. Our results $\mathcal{A}_i^n$, $\mathcal{B}_i^n$ and C^n in Table 3.4 are consistent with theirs except for the values of $\mathcal{A}_+^n$ and $\mathcal{A}_-^n$[♯3]. The discrepancy in the values of $\mathcal{A}_+^n$ and $\mathcal{A}_-^n$ arises from $(-6n_f\langle e^2\rangle \times 4C_F)$ in $K_G^{(1),n}$. See the discussion below Eqs. (3.46).

The numerical evaluation of the NNLO coefficients $\mathcal{D}_+^n$, $\mathcal{D}_-^n$ and $\mathcal{D}_{NS}^n$ in Tables 3.3 and 3.4 are performed by using the exact values of the three-loop anomalous dimensions $K_\psi^{(2),n}$, $K_G^{(2),n}$ and $K_{NS}^{(2),n}$ given in

[♯2]The earlier calculations [65, 66, 67, 68] were found partly incorrect. For quark coefficient functions $c_{L,q}^{(2),\rm ns}$ and $c_{L,q}^{(2),\rm ps}$ (see Eq. (3.62a) below), there is a complete agreement between Ref. [68] and Refs. [48, 69], and for gluon coefficient $c_{L,g}^{(2)}$ the result of Ref. [66] was corrected in Ref. [70].

[♯3]In Ref. [12], the expression in Ref. [47] is used for $\gamma_{GG}^{(1),n}$ which is contained in $\mathcal{A}_+^n$ and $\mathcal{A}_-^n$ as well as $\mathcal{B}_+^n$ and $\mathcal{B}_-^n$. Unfortunately, it is partly incorrect in the part proportional to C_A^2, but the difference is numerically small, as we can see in the difference between $\mathcal{B}_+^n$ and $\mathcal{B}_-^n$ in Table 3.4 and that in Table 1 of Ref. [12].

Table 3.3: Numerical values of $\mathcal{L}_i^n, \mathcal{A}_i^n, \mathcal{B}_i^n, \mathcal{D}_i^n, \mathcal{E}_i^n, \mathcal{F}_i^n$ $(i = +, -, NS)$, and C^n and $\mathcal{G}^n$ for $n = 2, 4, \cdots, 12$ in the case of $n_f = 3$. The calculation of $\mathcal{D}_i^n$ was performed by using the exact values of $K_i^{(2),n}$ in Ref. [50] (at upper levels) and also by using the approximated expressions of them given by Eqs. (3.48) (in parentheses at lower levels).

n	$\mathcal{L}_+^n$	$\mathcal{L}_-^n$	$\mathcal{L}_{NS}^n$	$\mathcal{A}_+^n$	$\mathcal{A}_-^n$	$\mathcal{A}_{NS}^n$	$\mathcal{B}_+^n$	$\mathcal{B}_-^n$	$\mathcal{B}_{NS}^n$	C^n
2	0.4690	0.4267	0.4248	-2.8403	—	-5.5940	1.7481	-1.8535	0.8290	-9.3333
4	0.004336	0.3639	0.1836	-0.5543	-2.6267	-1.3299	0.07353	3.3149	1.4607	-10.7467
6	0.0005428	0.2324	0.1164	0.06133	-1.8806	-0.9403	0.01652	2.9783	1.5349	-9.1088
8	0.0001493	0.1689	0.08451	0.009544	-1.6566	-0.8277	0.006245	2.9612	1.4906	-7.7504
10	0.00005803	0.1318	0.06591	0.002817	-1.5336	-0.7664	0.002993	2.8263	1.4169	-6.7116
12	0.00002748	0.1075	0.05375	0.001087	-1.4425	-0.7210	0.001652	2.6744	1.3390	-5.9074

n	$\mathcal{D}_+^n$	$\mathcal{D}_-^n$	$\mathcal{D}_{NS}^n$	$\mathcal{E}_+^n$	$\mathcal{E}_-^n$	$\mathcal{E}_{NS}^n$	$\mathcal{F}_+^n$	$\mathcal{F}_-^n$	$\mathcal{F}_{NS}^n$	$\mathcal{G}^n$
2	60.5098 (60.5014)	32.9286 (32.9251)	63.1965 (63.1909)	-10.5867	—	-10.9168	6.9729	-13.7973	3.7817	-251.3619
4	7.9871 (7.9873)	25.9791 (25.9222)	11.6147 (11.5840)	-9.3990	-23.9288	-10.5807	1.3106	48.8620	20.6599	-204.5836
6	0.01877 (0.01877)	-4007.0415 (-4011.3304)	24025.6303 (24050.8845)	1.8667	-24.0991	-12.4017	0.4596	56.4575	29.3881	-176.9466
8	0.03222 (0.03221)	165.7976 (165.9277)	82.2116 (82.2758)	0.3993	-29.0367	-14.5993	0.2217	67.5380	34.0579	-157.4181
10	-0.001732 (-0.001738)	109.3285 (109.4090)	54.5447 (54.5847)	0.1453	-32.8877	-16.4753	0.1249	73.0111	36.6197	-142.6108
12	-0.01825 (-0.01826)	86.8381 (86.9019)	43.3780 (43.4098)	0.06532	-35.8891	-17.9598	0.07764	75.9024	38.0024	-130.8717

Table 3.4: Numerical values of $\mathcal{L}_i^n, \mathcal{A}_i^n, \mathcal{B}_i^n, \mathcal{D}_i^n, \mathcal{E}_i^n, \mathcal{F}_i^n$ $(i = +, -, NS)$, and C^n and $\mathcal{G}^n$ for $n = 2, 4, \cdots, 12$ in the case of $n_f = 4$. The calculation of $\mathcal{D}_i^n$ was performed by using the exact values of $K_i^{(2),n}$ in Ref. [50] (at upper levels) and also by using the approximated expressions of them given by Eqs. (3.48) (in parentheses at lower levels).

n	$\mathcal{L}_+^n$	$\mathcal{L}_-^n$	$\mathcal{L}_{NS}^n$	$\mathcal{A}_+^n$	$\mathcal{A}_-^n$	$\mathcal{A}_{NS}^n$	$\mathcal{B}_+^n$	$\mathcal{B}_-^n$	$\mathcal{B}_{NS}^n$	C^n
2	0.8078	1.0582	0.6231	2.7608	—	-6.0944	3.8774	-8.5894	1.3076	-16.3237
4	0.009356	0.7327	0.2661	5.1244	-3.7321	-1.3858	0.1688	0.4820	2.1599	-18.7956
6	0.001235	0.4656	0.1679	0.09529	-2.9038	-1.0480	0.03909	6.0485	2.2395	-15.9311
8	0.0003465	0.3374	0.1215	0.01953	-2.7046	-0.9735	0.01495	5.9573	2.1613	-13.5552
10	0.0001362	0.2627	0.09461	0.006354	-2.5904	-0.9322	0.007216	5.6671	2.0468	-11.7384
12	0.00006497	0.2140	0.07704	0.002598	-2.4906	-0.8963	0.003999	5.3501	1.9293	-10.3319

n	$\mathcal{D}_+^n$	$\mathcal{D}_-^n$	$\mathcal{D}_{NS}^n$	$\mathcal{E}_+^n$	$\mathcal{E}_-^n$	$\mathcal{E}_{NS}^n$	$\mathcal{F}_+^n$	$\mathcal{F}_-^n$	$\mathcal{F}_{NS}^n$	$\mathcal{G}^n$
2	-84.4549 (-84.4748)	64.6182 (64.6102)	63.5804 (63.5722)	13.2519	—	-12.7900	7.0067	-68.4928	0.8275	-439.6247
4	-17.3048 (-17.3044)	-140.7574 (-140.9078)	-64.7231 (-64.7847)	92.4633	-2.4550	-11.2489	2.6666	-28.0786	24.5807	-357.8108
6	0.4163 (0.4163)	894.6070 (895.0955)	301.7867 (301.9492)	3.0154	-37.7241	-13.9828	1.0159	99.2476	37.1197	-309.4744
8	-0.04747 (-0.04749)	326.5791 (326.7480)	116.7791 (116.8392)	0.8428	-47.7463	-17.3117	0.5046	121.0094	43.9510	-275.3197
10	-0.2306 (-0.2306)	228.9242 (229.0460)	82.2373 (82.2809)	0.3366	-55.8735	-20.1683	0.2888	132.4677	47.7946	-249.4221
12	-0.7548 (-0.7548)	183.5002 (183.6024)	65.9952 (66.0319)	0.1600	-62.2711	-22.4456	0.1813	139.2236	49.9533	-228.8909

Table 3.5: Numerical values of $\mathcal{B}^n_{(L),i}$, $\mathcal{E}^n_{(L),i}$ and $\mathcal{F}^n_i$ ($i = +, -, NS$), and $\mathcal{C}^n_{(L)}$ and $\mathcal{G}^n_{(L)}$ for $n = 2, 4, \cdots, 12$ in the case of $n_f = 3$.

n	$\mathcal{B}^n_{(L),+}$	$\mathcal{B}^n_{(L),-}$	$\mathcal{B}^n_{(L),NS}$	$\mathcal{C}^n_{(L)}$	$\mathcal{E}^n_{(L),+}$	$\mathcal{E}^n_{(L),-}$	$\mathcal{E}^n_{(L),NS}$	$\mathcal{F}^n_{(L),+}$	$\mathcal{F}^n_{(L),-}$	$\mathcal{F}^n_{(L),NS}$	$\mathcal{G}^n_{(L)}$
2	-0.1042	2.2756	0.7552	16.0000	0.6312	—	-9.9448	-3.7360	43.0080	19.4570	-145.8462
4	-0.01985	0.4248	0.1958	6.4000	2.5372	-3.0666	-1.4185	-1.0919	13.1850	7.3012	-71.1680
6	-0.002791	0.1822	0.08867	3.4286	-0.3153	-1.4745	-0.7164	-0.2100	8.5456	4.0084	-41.6470
8	-0.0007395	0.1015	0.05008	2.1333	-0.04728	-0.9951	-0.4905	-0.06713	5.2598	2.5718	-27.4745
10	-0.0002690	0.06440	0.03196	1.4545	-0.01306	-0.7494	-0.3716	-0.02783	3.6483	1.8031	-19.5670
12	-0.0001186	0.04432	0.02205	1.0549	-0.004690	-0.5948	-0.2958	-0.01355	2.6990	1.3400	-14.6901

Table 3.6: Numerical values of $\mathcal{B}^n_{(L),i}$, $\mathcal{E}^n_{(L),i}$ and $\mathcal{F}^n_i$ ($i = +, -, NS$), and $\mathcal{C}^n_{(L)}$ and $\mathcal{G}^n_{(L)}$ for $n = 2, 4, \cdots, 12$ in the case of $n_f = 4$.

n	$\mathcal{B}^n_{(L),+}$	$\mathcal{B}^n_{(L),-}$	$\mathcal{B}^n_{(L),NS}$	$\mathcal{C}^n_{(L)}$	$\mathcal{E}^n_{(L),+}$	$\mathcal{E}^n_{(L),-}$	$\mathcal{E}^n_{(L),NS}$	$\mathcal{F}^n_{(L),+}$	$\mathcal{F}^n_{(L),-}$	$\mathcal{F}^n_{(L),NS}$	$\mathcal{G}^n_{(L)}$
2	-0.7180	5.6437	1.1076	27.9835	-2.4540	—	-10.8345	-25.1262	102.7244	25.8712	-255.0808
4	-0.04757	0.8719	0.2838	11.1934	-26.0571	-4.4410	-1.4782	-2.6019	55.6466	9.7196	-124.4708
6	-0.006807	0.3677	0.1279	5.9965	-0.5251	-2.2930	-0.7985	-0.5074	15.8890	5.3484	-72.8394
8	-0.001817	0.2034	0.07202	3.7311	-0.1024	-1.6306	-0.5769	-0.1634	9.8180	3.4379	-48.0521
10	-0.0006639	0.1287	0.04587	2.5440	-0.03097	-1.2686	-0.4520	-0.06805	6.8065	2.4139	-34.2221
12	-0.0002936	0.08836	0.03161	1.8451	-0.01174	-1.0284	-0.3677	-0.03325	5.0356	1.7960	-25.6925

Ref. [50] for $n = 2, 4, \cdots, 12$ (at upper levels) and also by using the approximated expressions of them given by Eqs. (3.48) (in parentheses at lower levels). The coefficients $\mathcal{A}^n_-$ and $\mathcal{E}^n_-$ cannot be evaluated at $n = 2$ because they become singular there. We will come back later to consider this singularity in more detail.

The coefficients $\mathcal{D}^-_+$ and $\mathcal{D}^n_{NS}$ in Tables 3.3 and 3.4 take exceptionally large values at $n = 6$. This is due to the fact that $\mathcal{D}^-_+$ and $\mathcal{D}^n_{NS}$ have the terms with the denominator $1/(d^n_- - 1)$ and $1/(d^n_{NS} - 1)$, respectively, in their expressions Eq. (3.37e). As we can see in Table 3.2, d^n_- and d^n_{NS} happen to be very close to one at $n = 6$ both for $n_f = 3$ and $n_f = 4$. We see, however, from Eq. (3.36) that $\mathcal{D}^-_+$ and $\mathcal{D}^n_{NS}$ in the moment sum rule are multiplied, respectively, by the factor $\left[1 - (\alpha_s(Q^2)/\alpha_s(P^2))^{d^n_- - 1}\right]$ and $\left[1 - (\alpha_s(Q^2)/\alpha_s(P^2))^{d^n_{NS} - 1}\right]$, which are very small if d^n_- and d^n_{NS} are close to one. Therefore the contributions of the parts with $\mathcal{D}^-_+$ and $\mathcal{D}^n_{NS}$ to the 6-th moment of $F^\gamma_2(x, Q^2, P^2)$ do not outstand from the others.

For $F^\gamma_L(x, Q^2, P^2)$, we also evaluate $\mathcal{B}^n_{(L),i}$, $\mathcal{C}^n_{(L)}$, $\mathcal{E}^n_{(L),i}$, $\mathcal{F}^n_{(L),i}$ and $\mathcal{G}^n_{(L)}$ given in Eqs. (3.60) and tabulate them in Tables 3.5 (for $n_f = 3$) and 3.6 (for $n_f = 4$). The coefficient $\mathcal{E}^n_{(L),-}$ also become singular at $n = 2$.

Sum Rule for the Second Moment The second moment sum rule for the structure function F^γ_2,

$$\int_0^1 dx\, F^\gamma_2(x, Q^2, P^2), \tag{3.63}$$

can be studied by taking the limit $n \to 2$ in Eq. (3.36). At $n = 2$, one of the eigenvalues of $\boldsymbol{\gamma}^{n=2}(g)$, the anomalous dimension matrix in the hadronic sector given in Eq. (3.15), vanishes, due to the conservation of the hadronic energy-momentum tensor. Thus we have a zero eigenvalue $\lambda^{n=2}_- = 0$ for the one-loop anomalous dimension matrix $\boldsymbol{\gamma}^{(0),n=2}(g)$, and therefore we get $d^{n=2}_- = \lambda^{n=2}_-/(2\beta_0) = 0$. Among the coefficients which appeared in Eq. (3.36), $\mathcal{A}^n_-$ and $\mathcal{E}^n_-$ would develop singularities at $n = 2$, because they contain terms with the factor $1/d^n_-$. However, as we can see from Eq. (3.36), both $\mathcal{A}^n_-$ and $\mathcal{E}^n_-$ are multiplied by a factor

Table 3.7: The ratios of the NLO (α) and the NNLO ($\alpha\alpha_s$) corrections to the LO ($\alpha\alpha_s^{-1}$) for the second moment of $F_2^\gamma(x, Q^2, P^2)$ in several cases of Q^2 and P^2. For QCD running coupling constant α_s, we have used the formula given in Eq. (3.67) with $\Lambda = 200\,\mathrm{MeV}$.

	Q^2 / GeV^2	P^2 / GeV^2	$\alpha_s(Q^2)$	$\alpha_s(P^2)$	NLO / LO	NNLO / LO	NNLO / (LO + NLO)
$n_f = 3$	30	1	0.1696	0.3253	-0.2063	-0.07910	-0.09966
	100	1	0.1461	0.3253	-0.1649	-0.05576	-0.06676
	100	3	0.1461	0.2487	-0.1949	-0.06339	-0.07874
$n_f = 4$	30	1	0.1853	0.3546	-0.1950	-0.07996	-0.09934
	100	1	0.1595	0.3546	-0.1541	-0.05506	-0.06509
	100	3	0.1595	0.2717	-0.1855	-0.06503	-0.07984

$\left[1 - (\alpha_s(Q^2)/\alpha_s(P^2))^{d_i^n}\right]$, which also vanishes at $n = 2$. Therefore, recalling that $(1/\epsilon)(1 - x^\epsilon) = -\ln(x)$ in the limit of $\epsilon \to 0$, we find that the $\mathcal{A}_-^n$ and $\mathcal{E}_-^n$ parts of Eq. (3.36) give finite contributions as

$$\lim_{n\to 2} \mathcal{A}_-^n \left[1 - \left(\frac{\alpha_s(Q^2)}{\alpha_s(P^2)}\right)^{d_-^n}\right] = -\overline{\mathcal{A}}_-^{n=2} \ln \frac{\alpha_s(Q^2)}{\alpha_s(P^2)}, \tag{3.64a}$$

$$\lim_{n\to 2} \mathcal{E}_-^n \left[1 - \left(\frac{\alpha_s(Q^2)}{\alpha_s(P^2)}\right)^{d_-^n}\right] = -\overline{\mathcal{E}}_-^{n=2} \ln \frac{\alpha_s(Q^2)}{\alpha_s(P^2)}. \tag{3.64b}$$

where $\overline{\mathcal{A}}_-^{n=2}$ and $\overline{\mathcal{E}}_-^{n=2}$ are given by

$$\overline{\mathcal{A}}_-^{n=2} = \left[-\boldsymbol{K}^{(0),n} \sum_j \frac{\boldsymbol{P}_j^n \hat{\boldsymbol{\gamma}}^{(1),n} \boldsymbol{P}_-^n}{\lambda_j^n + 2\beta_0} \boldsymbol{C}_2^{(0),n} - \boldsymbol{K}^{(0),n} \boldsymbol{P}_-^n \boldsymbol{C}_2^{(0),n} \frac{\beta_1}{\beta_0} + \boldsymbol{K}^{(1),n} \boldsymbol{P}_-^n \boldsymbol{C}_2^{(0),n} \right]\Bigg|_{n=2}, \tag{3.65a}$$

$$\begin{aligned} \overline{\mathcal{E}}_-^{n=2} = \Bigg[& -\boldsymbol{K}^{(0),n} \boldsymbol{P}_-^n \boldsymbol{C}_2^{(1),n} \frac{\beta_1}{\beta_0} - \boldsymbol{K}^{(0),n} \sum_j \frac{\boldsymbol{P}_j^n \hat{\boldsymbol{\gamma}}^{(1),n} \boldsymbol{P}_-^n}{\lambda_j^n + 2\beta_0} \boldsymbol{C}_2^{(1),n} + \boldsymbol{K}^{(1),n} \boldsymbol{P}_-^n \boldsymbol{C}_2^{(1),n} \\ & - \boldsymbol{K}^{(0),n} \sum_j \frac{\boldsymbol{P}_-^n \hat{\boldsymbol{\gamma}}^{(1),n} \boldsymbol{P}_j^n}{-\lambda_j^n + 2\beta_0} \boldsymbol{C}_2^{(0),n} \frac{\beta_1}{\beta_0} - \boldsymbol{K}^{(0),n} \sum_{j,k} \frac{\boldsymbol{P}_j^n \hat{\boldsymbol{\gamma}}^{(1),n} \boldsymbol{P}_-^n \hat{\boldsymbol{\gamma}}^{(1),n} \boldsymbol{P}_k^n}{(-\lambda_k^n + 2\beta_0)(\lambda_j^n + 2\beta_0)} \boldsymbol{C}_2^{(0),n} \\ & + \boldsymbol{K}^{(1),n} \sum_j \frac{\boldsymbol{P}_-^n \hat{\boldsymbol{\gamma}}^{(1),n} \boldsymbol{P}_j^n}{-\lambda_j^n + 2\beta_0} \boldsymbol{C}_2^{(0),n} \Bigg]\Bigg|_{n=2}. \end{aligned} \tag{3.65b}$$

The numerical values of $\overline{\mathcal{A}}_-^{n=2}$ and $\overline{\mathcal{E}}_-^{n=2}$ are

$$\text{for } n_f = 3, \qquad \overline{\mathcal{A}}_-^{n=2} = -1.3274, \qquad \overline{\mathcal{E}}_-^{n=2} = 5.7664, \tag{3.66a}$$

$$\text{for } n_f = 4, \qquad \overline{\mathcal{A}}_-^{n=2} = -2.2857, \qquad \overline{\mathcal{E}}_-^{n=2} = 18.5530. \tag{3.66b}$$

To estimate the impacts of the NLO (α) and NNLO ($\alpha\alpha_s$) corrections compared to the LO ($\alpha\alpha_s^{-1}$) term in the second moment sum rule for $F_2^\gamma(x, Q^2, P^2)$, we now evaluate them numerically in several cases of Q^2 and P^2. For the QCD running coupling constant $\alpha_s(Q^2)$, hereafter we use the following formula which takes into account the β function up to the three-loop level (See Eq. (9.5) in Ref. [71]),

$$\frac{\alpha_s(Q^2)}{4\pi} = \frac{1}{\beta_0 L} - \frac{1}{(\beta_0 L)^2} \frac{\beta_1}{\beta_0} \ln L + \frac{1}{(\beta_0 L)^3} \left(\frac{\beta_1}{\beta_0}\right)^2 \left[\left(\ln L - \frac{1}{2}\right)^2 + \frac{\beta_0 \beta_2}{\beta_1^2} - \frac{5}{4} \right] + \mathcal{O}\left(\frac{1}{L^4}\right), \tag{3.67}$$

Table 3.8: The ratios of the NLO ($\alpha\alpha_s$) corrections to the LO (α) for the second moment of $F_L^\gamma(x, Q^2, P^2)$ in several cases of Q^2 and P^2. For QCD running coupling constant α_s, we have used the formula given in Eq. (3.67) with $\Lambda = 200\,\mathrm{MeV}$.

	Q^2 / GeV^2	P^2 / GeV^2	$\alpha_s(Q^2)$	$\alpha_s(P^2)$	NLO / LO
$n_f = 3$	30	1	0.1696	0.3253	-0.09483
	100	1	0.1461	0.3253	-0.07881
	100	3	0.1461	0.2487	-0.08450
$n_f = 4$	30	1	0.1853	0.3546	-0.1046
	100	1	0.1595	0.3546	-0.08671
	100	3	0.1595	0.2717	-0.09316

where $L = \ln(Q^2/\Lambda^2)$ and β_0, β_1 and β_2 are given in Eqs. (3.41). Here we take, for instance, $(Q^2, P^2) = (30\,\mathrm{GeV}^2, 1\,\mathrm{GeV}^2)$, $(100\,\mathrm{GeV}^2, 1\,\mathrm{GeV}^2)$ and $(100\,\mathrm{GeV}^2, 3\,\mathrm{GeV}^2)$, with $\Lambda = 200\,\mathrm{MeV}$. These parameters are considered to satisfy the condition $\Lambda^2 \ll P^2 \ll Q^2$. The results are given in Table 3.7. For the kinematical region of Q^2 and P^2 which we have studied, the NNLO corrections are found to be rather large. When $P^2 = 1\,\mathrm{GeV}^2$ and $Q^2 = 30\text{-}100\,\mathrm{GeV}^2$, or $P^2 = 3\,\mathrm{GeV}^2$ and $Q^2 = 100\,\mathrm{GeV}^2$, and n_f is three or four, the NNLO corrections are 7%-10% of the sum of the LO and NLO contributions. We already know that the NLO contribution takes negative values [12]. We find that the NNLO corrections also give negative contributions to the sum rule. In fact, we will see in the next chapter that the NNLO corrections reduce $F_2^\gamma(x, Q^2, P^2)$ at large x.

The analysis for the second moment sum rule for $F_L^\gamma(x, Q^2, P^2)$,

$$\int_0^1 dx\, F_L^\gamma(x, Q^2, P^2), \tag{3.68}$$

can be studied in the same way. For $n = 2$, the $\mathcal{E}^n_{(L),-}$ part of Eq. (3.59) becomes

$$\lim_{n\to 2} \mathcal{E}^n_{(L),-} \left[1 - \left(\frac{\alpha_s(Q^2)}{\alpha_s(P^2)} \right)^{d^n_-} \right] = -\bar{\mathcal{E}}^{n=2}_{(L),-} \ln \frac{\alpha_s(Q^2)}{\alpha_s(P^2)}. \tag{3.69}$$

where $\bar{\mathcal{E}}^{n=2}_{(L),-}$ is given by

$$\bar{\mathcal{E}}^{n=2}_{(L),-} = \left[-\boldsymbol{K}^{(0),n} \boldsymbol{P}^n_- \boldsymbol{C}_2^{(1),n} \frac{\beta_1}{\beta_0} - \boldsymbol{K}^{(0),n} \sum_j \frac{\boldsymbol{P}^n_j \hat{\boldsymbol{\gamma}}^{(1),n} \boldsymbol{P}^n_-}{\lambda^n_j + 2\beta_0} \boldsymbol{C}_2^{(1),n} + \boldsymbol{K}^{(1),n} \boldsymbol{P}^n_- \boldsymbol{C}_2^{(1),n} \right] \Bigg|_{n=2}. \tag{3.70}$$

The numerical values of $\bar{\mathcal{E}}^{n=2}_{(L),-}$ is

$$\text{for } n_f = 3, \qquad \bar{\mathcal{E}}^{n=2}_{(L),-} = -7.0795, \tag{3.71a}$$

$$\text{for } n_f = 4, \qquad \bar{\mathcal{E}}^{n=2}_{(L),-} = -12.1905. \tag{3.71b}$$

We list in Table 3.8 the NLO contributions to the second moment sum rule for $F_L^\gamma(x, Q^2, P^2)$, with the parameters same as Table 3.7. We can see that the NLO corrections give negative contribution to the sum rule.

Chapter 4

Numerical Analysis

In the previous chapter, we obtained the moment sum rules for the spin-averaged virtual photon structure functions $F_2^\gamma(x, Q^2, P^2)$ up to the NNLO and $F_L^\gamma(x, Q^2, P^2)$ up to the NLO, corresponding to the order $\alpha\alpha_s$. Now, our main concern is x-dependence of the structure functions rather than the moments of them. This will be achieved by numerically inverting these sum rules, but this operation requires complete n-dependence of the sum rules over the complex n-plane. The moment sum rules Eqs. (3.36) and (3.59) are valid only for even n, however, all (complex) moments for n are uniquely fixed by analytic continuation from these even n results.

In this chapter, we will first discuss how the continuation can be done, and then execute the inversion to obtain the structure functions.

4.1 Numerical Evaluation of Sum Rules

Harmonic Sums As we can see from Eqs. (3.36) and (3.37) (or Eqs. (3.59) and (3.60) for $F_L^\gamma(x, Q^2, P^2)$), the n-th moment sum rules are written in terms of coefficient functions, anomalous dimensions and photon matrix elements. These ingredients, which are necessary to evaluate the $\alpha\alpha_s$ corrections to the sum rules, are often expressed in terms of the rational functions of n and the various harmonic sums [61]. The single harmonic sums are defined by

$$S_k(n) = \sum_{j=1}^{n} \frac{1}{j^k}, \qquad S_{-k}(n) = \sum_{j=1}^{n} \frac{(-1)^j}{j^k}, \tag{4.1}$$

where $k = 1, 2, \cdots$. The higher multiple sums are defined recursively:

$$S_{k,\vec{m}}(n) = \sum_{j=1}^{n} \frac{1}{j^k} S_{\vec{m}}(j), \qquad S_{-k,\vec{m}}(n) = \sum_{j=1}^{n} \frac{(-1)^j}{j^k} S_{\vec{m}}(j). \tag{4.2}$$

To invert the (even) n-moment sum rules so that we get the structure functions as functions of x, we need to obtain the representation of these sums analytically continued from their values on the (even) integer n.

There are several proposals for the numerical continuation [72, 73], however, we use here a naïve method; we use the asymptotic series expansions of the sums together with the translation relations of them. As a simple example, first we consider $S_1(n)$. The asymptotic series expansion of $S_1(n)$ is well-known, and we can expand it up to arbitrary order:

$$S_1(n) = \ln(n) + \gamma_E + \frac{1}{2n} - \frac{1}{12n^2} + \frac{1}{120n^4} + \cdots. \tag{4.3}$$

This form has simple analytic properties, and reproduces values at integers quite well for large n. On the other hand, $S_1(n)$ satisfies the following translation relation:

$$S_1(n) = S_1(n+1) - \frac{1}{n+1}. \tag{4.4}$$

This relation is valid not only for integer n, but also for complex n. Therefore, our algorithm to evaluate $S_1(n)$ at arbitrary n is as follows[♯1]:

- For $|n| \geq n_0$, where n_0 is some real constant at which the asymptotic series expansion well converge within an accuracy we need, we use the asymptotic expansion Eq. (4.3) to evaluate $S_1(n)$.
- For $|n| < n_0$, we use the translation relation Eq. (4.4) and shift $n \to n+1$ recursively in order to reach $S_1(n)$ with $|n| \geq n_0$.

Indeed, a similar method has been used to evaluate the digamma function $\psi(n) = S_1(n) - \gamma_E - 1/n$ as well as other polygammas, e.g., [74].

Now, it seems quite natural to evaluate the multiple harmonic sums in a parallel manner. Consider the evaluation of a more complicated harmonic sum $S_{1,1,-2,1}(n)$ as an example. $S_{1,1,-2,1}(n)$ can be straightforwardly expanded from *even*[♯2]values as

$$\begin{aligned} S^{\text{even}}_{1,1,-2,1}(n) = {} & c_{0,2}\ln^2(n) + c_{0,1}\ln(n) + c_{0,0} + \frac{c_{1,1}\ln(n)}{n} + \frac{c_{1,0}}{n} \\ & + \frac{c_{2,1}\ln(n)}{n^2} + \frac{c_{2,0}}{n^2} + \frac{c_{3,0}}{n^3} + \frac{c_{4,1}\ln(n)}{n^4} + \frac{c_{4,0}}{n^4} + \frac{c_{5,1}\ln(n)}{n^5} + \frac{c_{5,0}}{n^5} + \cdots, \end{aligned} \tag{4.5}$$

where

$$\begin{aligned} c_{0,2} &= c_{1,1} = -\frac{5}{16}\zeta(3) = -0.37564278\cdots, \\ c_{0,1} &= -\frac{5}{8}\gamma_E\zeta(3) - \frac{3}{40}\zeta^2(2) = -0.63658940\cdots, \\ c_{0,0} &= -\frac{3}{40}\gamma_E\zeta^2(2) - \frac{5}{16}\gamma_E^2\zeta(3) - \ln(2)\,\mathrm{Li}_4\left(\frac{1}{2}\right) - \frac{7}{16}\ln^2(2)\zeta(3) + \frac{1}{6}\ln^3(2)\zeta(2) \\ &\quad - \frac{1}{30}\ln^5(2) + \frac{1}{8}\zeta(2)\zeta(3) + \frac{1}{8}\zeta(5) - \mathrm{Li}_5\left(\frac{1}{2}\right) = -0.89930722\cdots, \\ c_{1,0} &= -\frac{5}{16}\gamma_E\zeta(3) - \frac{3}{80}\zeta^2(2) + \frac{5}{16}\zeta(3) = 0.057348080\cdots, \\ c_{2,1} &= \frac{5}{96}\zeta(3) = 0.062607130\cdots, \\ c_{2,0} &= \frac{5}{96}\gamma_E\zeta(3) + \frac{1}{160}\zeta^2(2) - \frac{15}{64}\zeta(3) = -0.22868296\cdots, \\ c_{3,0} &= \frac{5}{64}\zeta(3) = 0.093910695\cdots, \\ c_{4,1} &= \frac{1}{8} - \frac{1}{192}\zeta(3) = 0.11873928\cdots, \\ c_{4,0} &= -\frac{1}{192}\gamma_E\zeta(3) + \frac{1}{8}\gamma_E - \frac{1}{1600}\zeta^2(2) - \frac{5}{2304}\zeta(3) = 0.064238415\cdots, \\ c_{5,1} &= -\frac{9}{16} = -0.5625, \\ c_{5,0} &= \frac{1}{4} - \frac{9}{16}\gamma_E - \frac{5}{384}\zeta(3) = -0.090335594\cdots. \end{aligned} \tag{4.6}$$

The translation relation for $S^{\text{even}}_{1,1,-2,1}(n)$, which we need to shift n, is given by

$$S^{\text{even}}_{1,1,-2,1}(n) = S^{\text{even}}_{1,1,-2,1}(n+2) - \left(\frac{1}{n+1} + \frac{1}{n+2}\right) S^{\text{even}}_{1,-2,1}(n+2) + \frac{1}{(n+1)(n+2)} S^{\text{even}}_{-2,1}(n+2). \tag{4.7}$$

[♯1] In fact, at n near the negative real axis, the expansion Eq. (4.3) do not work well even if $|n| > n_0$. Therefore, to be exact, if n is in the region $\mathrm{Re}(n) < n_0 \wedge |\mathrm{Im}(n)| < n_0$, we shift n by using Eq. (4.4) until $\mathrm{Re}(n) \geq n_0$. More details are given in Appendix C.

[♯2] Since the moment sum rules of $F_2^\gamma(x, Q^2, P^2)$ and $F_L^\gamma(x, Q^2, P^2)$ are valid for even n values due to the crossing symmetry of them, the analytic continuation should be performed from even n. Therefore whenever $(-1)^n$ appears, it should be replaced by $(+1)$.

Note that the right-hand side of Eq. (4.7) is written in terms of $S^{\rm even}_{1,1,-2,1}(n)$ itself and lower harmonic sums $S^{\rm even}_{1,-2,1}(n)$ and $S^{\rm even}_{-2,1}(n)$ with larger argument $n+2$. Then $S^{\rm even}_{1,-2,1}(n)$ and $S^{\rm even}_{-2,1}(n)$ can be evaluated in a similar fashion, therefore we can shift the argument of $S^{\rm even}_{1,1,-2,1}(n)$ as $n \to n+2$. Using Eq. (4.5) with Eq. (4.7), as in the case of $S_1(n)$, we can evaluate $S^{\rm even}_{1,1,-2,1}(n)$ on the whole complex plane.

In practice, taking $n_0 = 16$, we need to expand $S_1(n)$ and $S^{\rm even}_{1,1,-2,1}(n)$ up to the order $1/n^{10}$ and $1/n^{18}$, respectively, in order the ensure the double precision accuracy (15 significant figures) with a truncation error at $n = n_0$. See Appendix C for more details on the evaluation of the harmonic sums.

Numerical Evaluation of Sum Rules Since we can now make analytic continuation of the harmonic sums from their even values, we can evaluate the n-th moments of the virtual photon structure functions Eqs. (3.36) and. (3.59) with the arbitrary n. In Fig. 4.1, we plot the moments of the spin-averaged virtual photon structure function $F_2^\gamma(x, Q^2, P^2)$,

$$M_2^\gamma(n, Q^2, P^2) = \int_0^1 dx\, x^{n-2} F_2^\gamma(x, Q^2, P^2), \tag{4.8}$$

which is explicitly given in Eq. (3.36), predicted by perturbative QCD for the case of $n_f = 4$, $Q^2 = 30\text{GeV}^2$ and $P^2 = 1\text{GeV}^2$, on the real axis. For the QCD running coupling constant $\alpha_s(Q^2)$, we use the Eq. (3.67) with the QCD scale parameter $\Lambda = 200\,\text{MeV}$. Here we plot three curves, the LO (the order of $\alpha\alpha_s^{-1}$), NLO (including α corrections) and NNLO (including up to $\alpha\alpha_s$ corrections) QCD results. We can see that the moments of $F_2^\gamma(x, Q^2, P^2)$ can be obtained as a smooth function of n for $n > 1$, as expected. We can also see that the NNLO corrections surely reduce the moments of $F_2^\gamma(x, Q^2, P^2)$, as we have caught a glimpse of it in the previous section.

We also plot, in Fig. 4.2, the LO (α) and NLO ($\alpha\alpha_s$) results of the moments of the longitudinal virtual photon structure function $F_L^\gamma(x, Q^2, P^2)$,

$$M_L^\gamma(n, Q^2, P^2) = \int_0^1 dx\, x^{n-2} F_L^\gamma(x, Q^2, P^2), \tag{4.9}$$

which is explicitly given in Eq. (3.59), for the case of $n_f = 4$, $Q^2 = 30\text{GeV}^2$ and $P^2 = 1\text{GeV}^2$ with $\Lambda = 200\,\text{MeV}$.

4.2 Numerical Inversion

We now numerically perform the inverse Mellin transform of Eq. (4.8) to obtain $F_2^\gamma(x, Q^2, P^2)$ as a function of x. $F_L^\gamma(x, Q^2, P^2)$ can be obtained as a function of x from Eq. (4.9) in the same way. By inverting the moments Eq. (4.8) we get

$$\frac{F_2^\gamma(x, Q^2, P^2)}{x} = \frac{1}{2\pi i} \int_{c-i\infty}^{c+i\infty} dn\, x^{-n} M_2^\gamma(n, Q^2, P^2), \tag{4.10}$$

where c is a real constant being larger than a real constant c_0 which has to be such that the integral $M_2^\gamma(n = c, Q^2, P^2)$ Eq. (4.8) is absolutely convergent; In our case $c_0 = 1$ from the discussion in the previous section.

Integration Contour In practice, it is known that for the good convergence of the numerical integration, one would be better off changing the contour in the complex n-plane from C_0 to C_1 shown as Fig. 4.3 (e.g., [74]) :

$$\frac{F_2^\gamma(x, Q^2, P^2)}{x} = \frac{1}{2\pi i} \left[\int_{c+\infty\times e^{-i\phi}}^{c} + \int_{c}^{c+\infty\times e^{+i\phi}} \right] dn\, x^{-n} M_2^\gamma(n, Q^2, P^2), \tag{4.11}$$

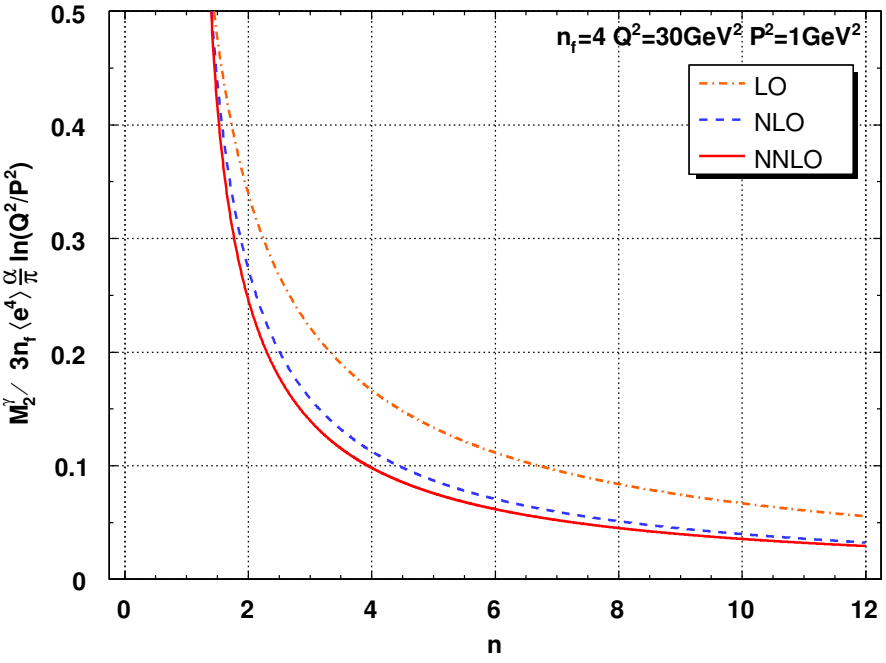

Figure 4.1: Moments of the spin-averaged virtual photon structure function $F_2^\gamma(x, Q^2, P^2)$ in units of $[3n_f\langle e^4\rangle\alpha/\pi \ln(Q^2/P^2)]$ for $Q^2 = 30\,\mathrm{GeV}^2$ and $P^2 = 1\,\mathrm{GeV}^2$ with $n_f = 4$ and the QCD scale parameter $\Lambda = 200\,\mathrm{MeV}$. We plot the QCD leading order (LO), the next-to-leading order (NLO) and the next-to-next-to-leading order (NNLO) results.

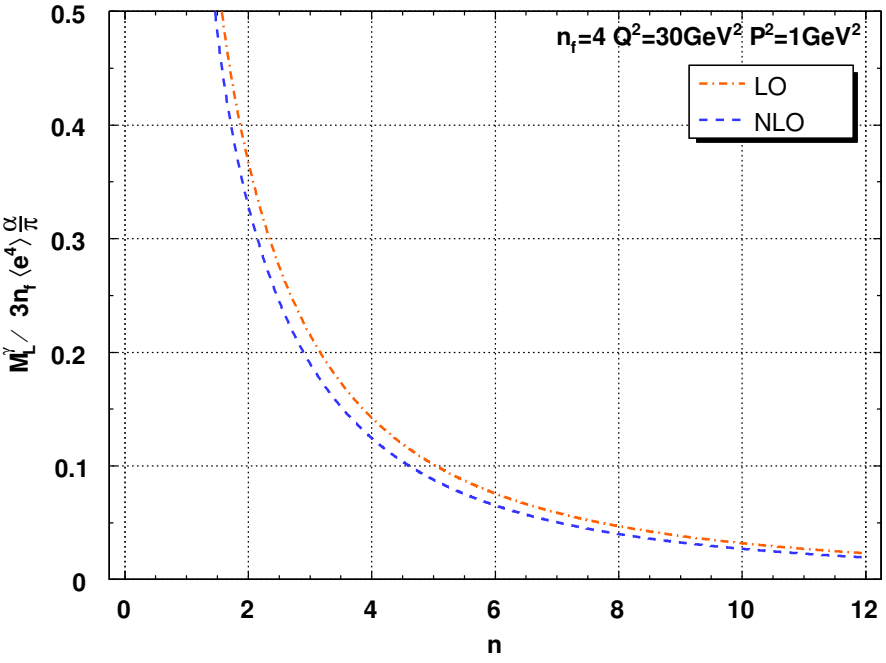

Figure 4.2: Moments of the longitudinal virtual photon structure function $F_L^\gamma(x, Q^2, P^2)$ in units of $(3n_f\langle e^4\rangle\alpha/\pi)$ for $Q^2 = 30\,\mathrm{GeV}^2$ and $P^2 = 1\,\mathrm{GeV}^2$ with $n_f = 4$ and $\Lambda = 200\,\mathrm{MeV}$. We plot the QCD leading order (LO) and the next-to-leading order (NLO) results.

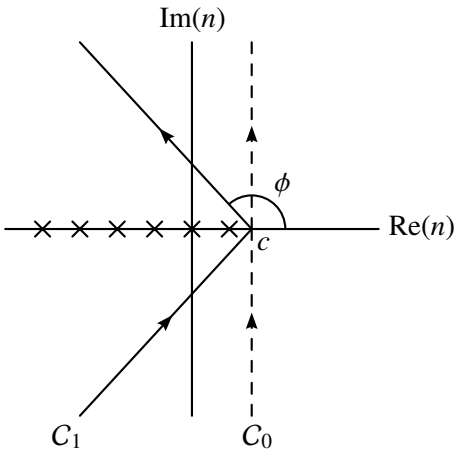

Figure 4.3: The contour of the integral for the inverse Mellin transform.

This deformation of the integration contour is legal if $M_2^\gamma(n, Q^2, P^2)$ has no singularities in the region enclosed by $C_0 - C_1$ and in our case this is true since all singularities lie on the real axis $n = 1, 0, -1, -2, \cdots$. Furthermore, it is beneficial to rewrite Eq. (4.11) as an integration over a real variable:

$$\frac{F_2^\gamma(x, Q^2, P^2)}{x} = \frac{1}{2\pi i}\int_0^\infty dz \left[e^{i\phi}x^{-n}M_2^\gamma(n, Q^2, P^2) - e^{-i\phi}x^{-n^*}M_2^\gamma(n^*, Q^2, P^2)\right], \tag{4.12}$$

where $n = c + ze^{i\phi}$. Using $[M_2^\gamma(n, Q^2, P^2)]^* = M_2^\gamma(n^*, Q^2, P^2)$, we finally obtain[♯3]

$$\frac{F_2^\gamma(x, Q^2, P^2)}{x} = \frac{1}{\pi}\int_0^\infty dz\ \mathrm{Im}\left[e^{i\phi}x^{-n}M_2^\gamma(n, Q^2, P^2)\right]. \tag{4.13}$$

Formally, the value of this integral does not depend $c > c_0$ and $\pi/2 \le \phi < \pi$, however, it is suitable to choose $\phi > \pi/2$ rather than $\phi = \pi/2$ because it gives an exponential dumping like

$$x^{-n} \sim \exp\left[z\cos\phi\ln\left(\frac{1}{x}\right)\right], \qquad z \to \infty. \tag{4.14}$$

Numerical Inversion of Moments of F_2^γ and F_L^γ In Fig. 4.4 we plot the virtual photon structure function $F_2^\gamma(x, Q^2, P^2)$ predicted by perturbative QCD for the case of $Q^2 = 30\mathrm{GeV}^2$ and $P^2 = 1\mathrm{GeV}^2$ with $n_f = 4$. Here we plot three curves, the LO (the order of $\alpha\alpha_s^{-1}$), NLO (including α corrections) and NNLO (including up to $\alpha\alpha_s$ corrections) QCD results. It is noted that here we have used the QCD running coupling constant $\alpha_s(Q^2)$, governed by the formula Eq. (3.67) which is valid up to three-loop level, even for the LO and NLO analyses, and we have taken $\Lambda = 200\,\mathrm{MeV}$. The LO and NLO QCD results for the same values of Q^2, P^2 and n_f were already given in Fig. 6 of Ref. [12]. But in their analyses, the formula for $\alpha_s(Q^2)$, which is valid in the one-loop level, was used to obtain the LO curve, while for the NLO curve, the formula which is

[♯3] Replacing $z \to sz$ ($s > 0$) and identifying $se^{i\phi} = -\epsilon + i$ with real constant ϵ (s should be adequately chosen), we can rewrite Eq. (4.13) as

$$\begin{aligned}\frac{F_2^\gamma(x, Q^2, P^2)}{x} &= \frac{1}{\pi}\int_0^\infty dz\ \mathrm{Im}[(-\epsilon + i)x^{-n}M_2^\gamma(n, Q^2, P^2)], \qquad n = c - \epsilon z + iz,\\ &= \frac{1}{\pi}\int_0^\infty dz\Big\{\mathrm{Re}[x^{-n}M_2^\gamma(n, Q^2, P^2)] - \epsilon\,\mathrm{Im}[x^{-n}M_2^\gamma(n, Q^2, P^2)]\Big\}.\end{aligned}$$

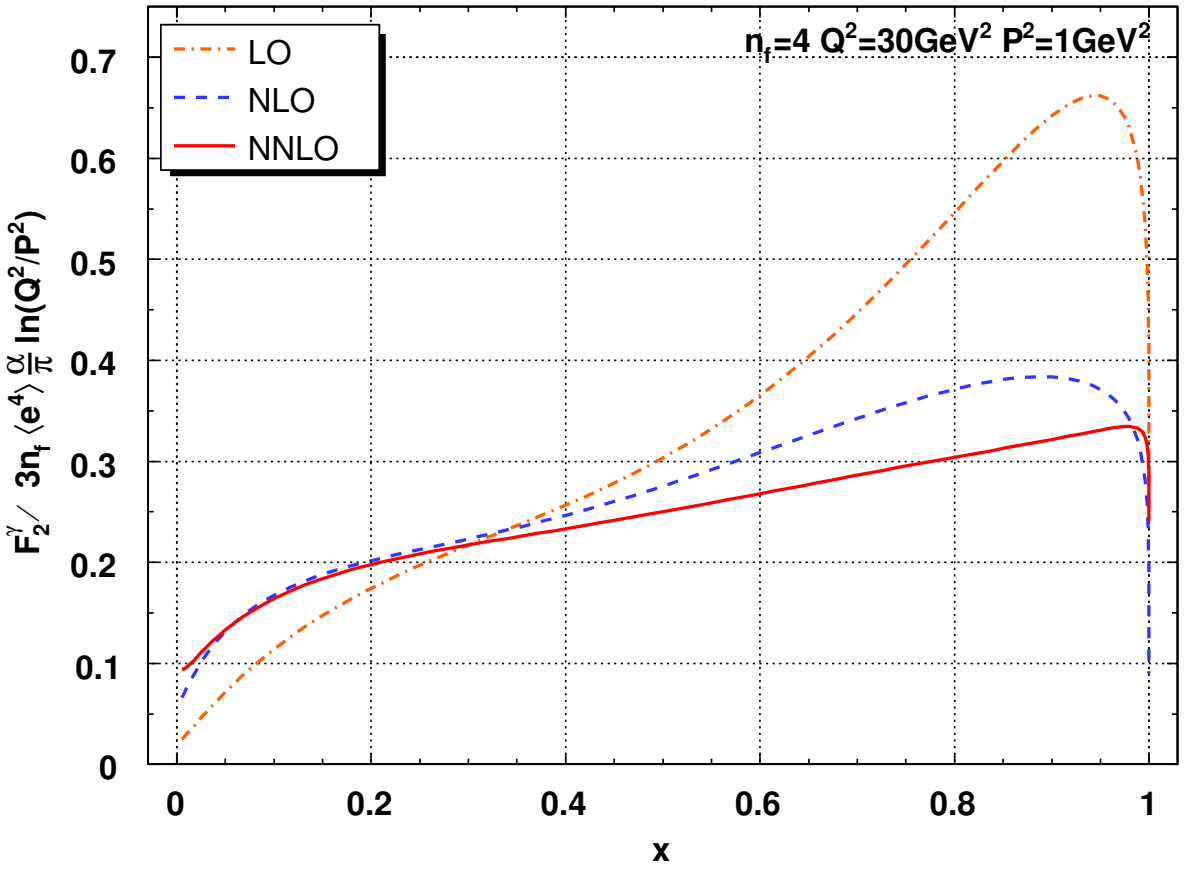

Figure 4.4: Virtual photon structure function $F_2^\gamma(x, Q^2, P^2)$ in units of $[3n_f\langle e^4\rangle\alpha/\pi \ln(Q^2/P^2)]$ for $Q^2 = 30\,\mathrm{GeV}^2$ and $P^2 = 1\,\mathrm{GeV}^2$ with $n_f = 4$ and the QCD scale parameter $\Lambda = 200\,\mathrm{MeV}$. We plot the QCD leading order (LO), the next-to-leading order (NLO) and the next-to-next-to-leading order (NNLO) results.

valid up to the two-loop level was used. Moreover they set the QCD scale parameter $\Lambda = 100\,\mathrm{MeV}$ in both cases. The LO result in Fig. 4.4 has a similar shape as the corresponding one in Fig. 6 of Ref. [12], but is different in magnitude; the former is slightly larger than the latter for almost the whole x. This is due to the fact that the one-loop-level formula for $\alpha_s(Q^2)$ (and $\alpha_s(P^2)$) with $\Lambda = 100\,\mathrm{MeV}$ was used for the LO result in Ref. [12] while we applied the three-loop-level formula even for the LO result with $\Lambda = 200\,\mathrm{MeV}$. On the other hand, the NLO curve in Fig. 4.4 is rather similar to the corresponding one in Fig. 6 of Ref. [12], in shape and magnitude.

Now we can find in Fig. 4.4 that there exist notable NNLO corrections at large x. The corrections are negative for almost the whole x and thus the NNLO curve comes below the NLO curve. This is expected from the n-space analysis above.

We have also studied the QCD corrections to $F_2^\gamma(x, Q^2, P^2)$ with difference Q^2 and P^2 with same $n_f = 4$. In Fig. 4.5, we plot the case for (a) $Q^2 = 100\,\mathrm{GeV}^2$ and $P^2 = 1\,\mathrm{GeV}^2$ (b) $Q^2 = 100\,\mathrm{GeV}^2$ and $P^2 = 3\,\mathrm{GeV}^2$. In both cases, the NNLO corrections reduce $F_2^\gamma(x, Q^2, P^2)$, especially at large x. We have not seen any sizable change for the structure function normalized by $[3n_f\langle e^4\rangle\alpha/\pi \ln(Q^2/P^2)]$ for these different values of Q^2 and P^2. We have examined the $n_f = 3$ and $n_f = 5$ case as well in Fig. 4.5. It is observed that the normalized structure function is insensitive to the number of active flavors.

In Fig. 4.6 we plot the longitudinal virtual photon structure function $F_L^\gamma(x, Q^2, P^2)$ predicted by pertur-

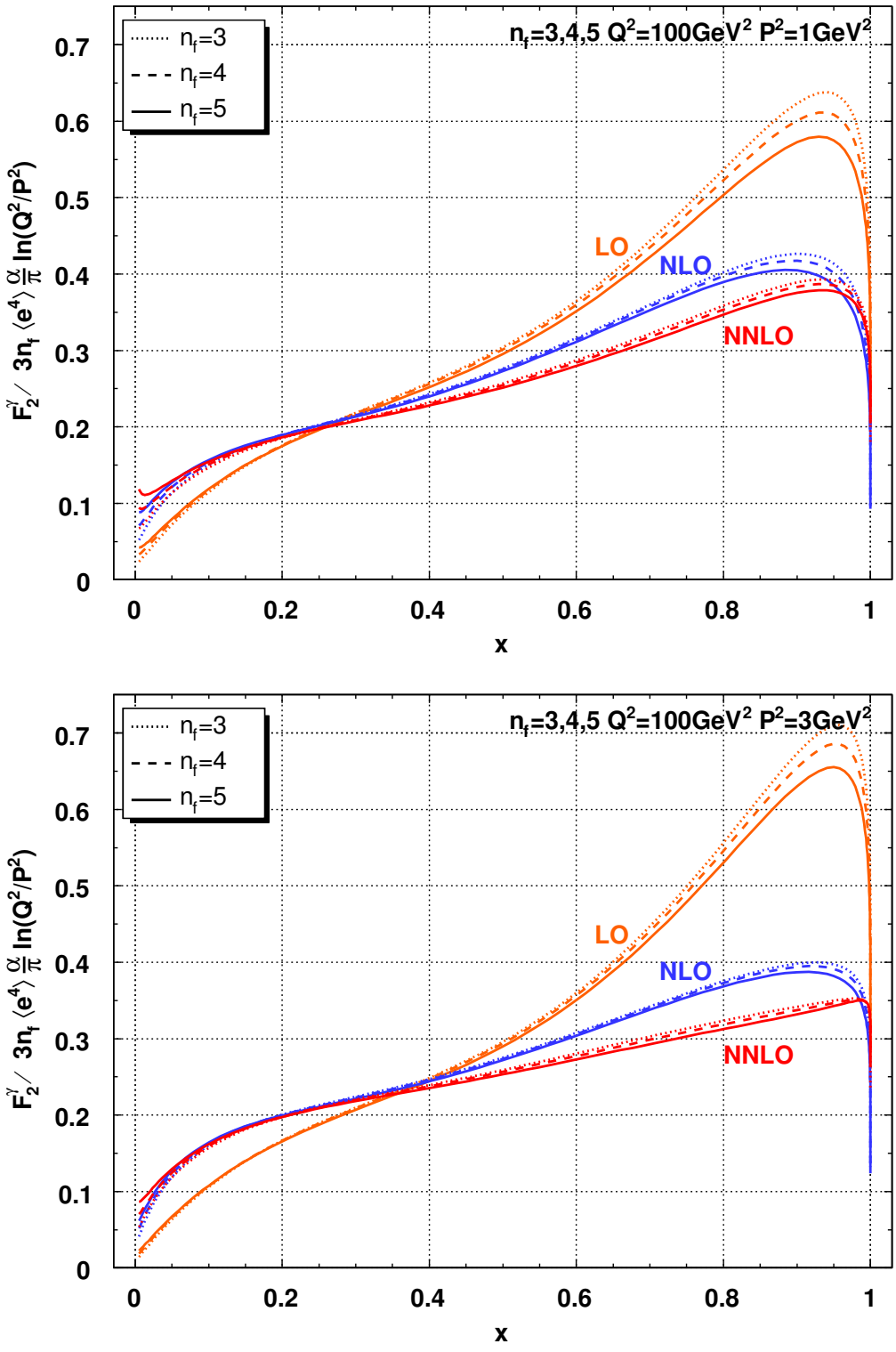

Figure 4.5: Virtual photon structure function $F_2^\gamma(x, Q^2, P^2)$ in units of $[3n_f\langle e^4\rangle\alpha/\pi \ln(Q^2/P^2)]$ for (a) $Q^2 = 100\,\mathrm{GeV}^2$ and $P^2 = 1\,\mathrm{GeV}^2$ (b) $Q^2 = 100\,\mathrm{GeV}^2$ and $P^2 = 3\,\mathrm{GeV}^2$ with $n_f = 3, 4, 5$ and $\Lambda = 200\,\mathrm{MeV}$. We plot the QCD leading order (LO), the next-to-leading order (NLO) and the next-to-next-to-leading order (NNLO) results.

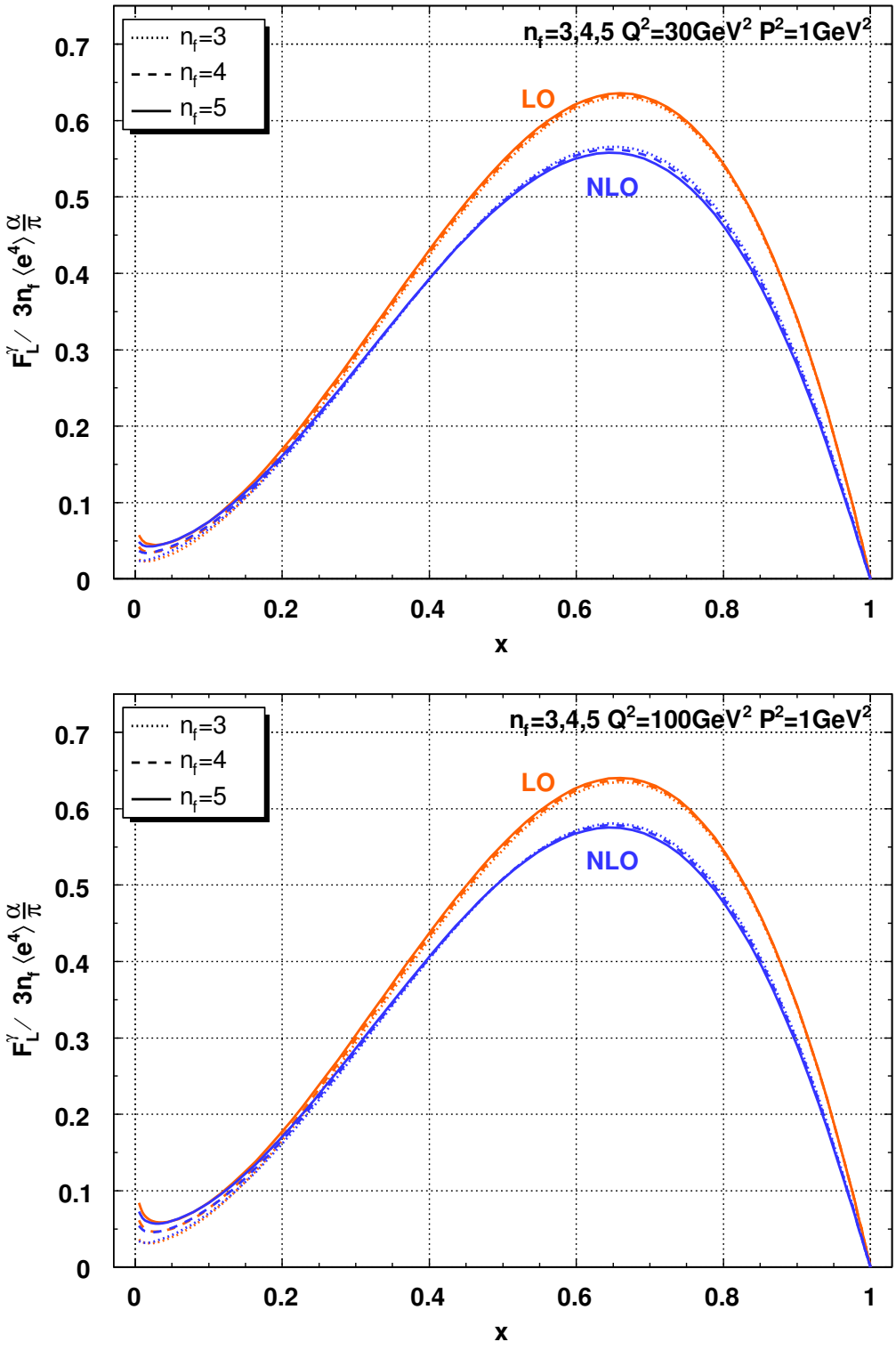

Figure 4.6: Longitudinal virtual photon structure function $F_L^\gamma(x, Q^2, P^2)$ in units of $(3n_f\langle e^4\rangle\alpha/\pi)$ for (a) $Q^2 = 30\,\mathrm{GeV}^2$ and $P^2 = 1\,\mathrm{GeV}^2$ (b) $Q^2 = 100\,\mathrm{GeV}^2$ and $P^2 = 1\,\mathrm{GeV}^2$ with $n_f = 3, 4, 5$ and $\Lambda = 200\,\mathrm{MeV}$. We plot the QCD leading order (LO) and the next-to-leading order (NLO) results.

bative QCD for the case of $Q^2 = 30\text{GeV}^2$ and $P^2 = 1\text{GeV}^2$ with $n_f = 3, 4, 5$ and $\Lambda = 200\,\text{GeV}^2$. Here we plot three set of two curves, the LO (the order of α) and NLO (including $\alpha\alpha_s$ corrections) QCD results for $n_f = 3, 4, 5$. We can find from Fig. 4.6 that there exist non-negligible NLO corrections and these corrections are negative, and the normalized structure function is insensitive to the number of active flavors.

Box-diagram Contributions In Ref. [12] on the analysis of $F_2^\gamma(x, Q^2, P^2)$ up to the NLO, Uematsu and Walsh pointed out that in the limit

$$\ln \frac{Q^2}{P^2} \ll \ln \frac{P^2}{\Lambda^2}, \tag{4.15}$$

the moments of $F_2^\gamma(x, Q^2, P^2)$ approach the ones of the box-diagram contribution. Actually, taking the limit Eq. (4.15), the NLO QCD result of the moments of $F_2^\gamma(x, Q^2, P^2)$ reduces to the box-diagram result of that. So let us take same limit Eq. (4.15) for the NNLO formula of $F_2^\gamma(x, Q^2, P^2)$ given in Eq. (3.36). Since the limit Eq. (4.15) means $\ln(Q^2/\Lambda^2) \approx \ln(P^2/\Lambda^2)$, we define

$$\frac{\alpha_s(Q^2)}{\alpha_s(P^2)} \equiv 1 + \kappa, \tag{4.16}$$

where $|\kappa| \ll 1$. Then we find in the limit Eq. (4.16),

$$\begin{aligned}\int_0^1 dx\, x^{n-2} F_2^\gamma(x, Q^2, P^2) = \frac{\alpha}{4\pi}\frac{1}{2\beta_0}\Bigg\{ &\frac{4\pi}{\alpha_s(Q^2)}\sum_i \mathcal{L}_i^n\left[-(d_i^n+1)\kappa - \frac{(d_i^n+1)d_i^n}{2}\kappa^2\right] \\ &+ \sum_i \mathcal{A}_i^n\left(-d_i^n\kappa\right) + \sum_i \mathcal{B}_i^n\left[-(d_i^n+1)\kappa\right] + C^n \\ &+ \frac{\alpha_s(Q^2)}{4\pi}\mathcal{G}^n + O(\alpha_s^2, \alpha_s\kappa, \kappa^2)\Bigg\},\end{aligned} \tag{4.17}$$

with $i = +, -, NS$. Then using the expressions of $\mathcal{L}_i^n$, $\mathcal{A}_i^n$ and $\mathcal{B}_i^n$ given in Eqs. (3.37a)-(3.37c) and a relation

$$-\frac{4\pi}{\alpha_s(Q^2)}\kappa = \beta_0 \ln\frac{Q^2}{P^2} - \frac{\beta_1}{\beta_0}\kappa + O(\kappa^2), \tag{4.18}$$

we obtain

$$\begin{aligned}&\int_0^1 dx\, x^{n-2} F_2^\gamma(x, Q^2, P^2) \\ &\quad= \frac{\alpha}{4\pi}\frac{1}{2\beta_0}\Bigg\{\tilde{\mathcal{L}}^n\left(2\beta_0 \ln\frac{Q^2}{P^2}\right) + C^n \\ &\qquad + \frac{\alpha_s(Q^2)}{4\pi}\left[\frac{1}{2\beta_0}\tilde{\mathcal{A}}^n\left(2\beta_0\ln\frac{Q^2}{P^2}\right)^2 + \tilde{\mathcal{B}}^n\left(2\beta_0\ln\frac{Q^2}{P^2}\right) + \mathcal{G}^n\right] + O(\alpha_s^2, \alpha_s\kappa, \kappa^2)\Bigg\},\end{aligned} \tag{4.19}$$

where

$$\tilde{\mathcal{L}}^n = \frac{1}{2}\boldsymbol{K}^{(0),n}\cdot\boldsymbol{C}_2^{(0),n}, \tag{4.20a}$$

$$\tilde{\mathcal{A}}^n = -\frac{1}{8}\boldsymbol{K}^{(0),n}\hat{\boldsymbol{\gamma}}^{(0),n}\boldsymbol{C}_2^{(0),n}, \tag{4.20b}$$

$$\tilde{\mathcal{B}}^n = \frac{1}{2}\left(\boldsymbol{K}^{(1),n}\cdot\boldsymbol{C}_2^{(0),n} + \boldsymbol{K}^{(0),n}\cdot\boldsymbol{C}_2^{(1),n} - \boldsymbol{A}^{(1),n}\hat{\boldsymbol{\gamma}}^{(0),n}\boldsymbol{C}_2^{(0),n}\right), \tag{4.20c}$$

and C^n and $\mathcal{G}^n$ are given in Eqs. (3.37d) and (3.37h), respectively. It is noted that all β_0 in the expression of the right-hand side in Eq. (4.19) are canceled, and these terms are proportional to the charge factor $n_f\langle e^4\rangle$ and $\alpha_s C_F n_f\langle e^4\rangle$. These facts suggest that the right-hand side is the moments of the box-diagram contribution including corrections of one-gluon exchange, i.e., α_s corrections. Note that inverting the some coefficients in Eq. (4.19),

$$\int_0^1 dx\, x^{n-2}\tilde{\mathcal{L}}(x) = \tilde{\mathcal{L}}^n, \tag{4.21a}$$

$$\int_0^1 dx\, x^{n-2}C(x) = C^n, \tag{4.21b}$$

$$\int_0^1 dx\, x^{n-2}\tilde{\mathcal{A}}(x) = \tilde{\mathcal{A}}^n, \tag{4.21c}$$

$$\int_0^1 dx\, x^{n-2}\tilde{\mathcal{B}}(x) = \tilde{\mathcal{B}}^n, \tag{4.21d}$$

can be easily done:

$$\tilde{\mathcal{L}}(x) = 12n_f\langle e^4\rangle x(1-2x+2x^2), \tag{4.22a}$$

$$C(x) = -48\beta_0 n_f\langle e^4\rangle x[(1-2x+2x^2)\ln(x)+1-3x+3x^2], \tag{4.22b}$$

$$\tilde{\mathcal{A}}(x) = -6C_F n_f\langle e^4\rangle x[2(1-2x+4x^2)\ln(x)-4(1-2x+2x^2)\ln(1-x)+1-4x], \tag{4.22c}$$

$$\begin{aligned}\tilde{\mathcal{B}}(x) = 12C_F n_f\langle e^4\rangle x[&(1-2x+4x^2)\ln^2(x)+2(1-2x+2x^2)\ln^2(1-x)\\ &-4(1-2x+2x^2)\ln(x)\ln(1-x)+(3-4x+8x^2)\ln(x)+8x(1-x)\ln(1-x)\\ &+14-29x+20x^2-4(1-2x+2x^2)\zeta(2)],\end{aligned} \tag{4.22d}$$

but the inverse Mellin transform of $\mathcal{G}^n$ is rather complicated and contains untrivial polylogarithms up to weight 3.

The box-diagram contribution for $F_L^\gamma(x,Q^2,P^2)$ is quite similarly obtained such as Eq. (4.19),

$$\int_0^1 dx\, x^{n-2}F_L^\gamma(x,Q^2,P^2) = \frac{\alpha}{4\pi}\frac{1}{2\beta_0}\left\{C_{(L)}^n + \frac{\alpha_s(Q^2)}{4\pi}\left[\tilde{\mathcal{B}}_{(L)}^n\left(2\beta_0\ln\frac{Q^2}{P^2}\right)+\mathcal{G}_{(L)}^n\right]+O(\alpha_s^2,\alpha_s\kappa,\kappa^2)\right\}, \tag{4.23}$$

where

$$\tilde{\mathcal{B}}_{(L)}^n = \frac{1}{2}\boldsymbol{K}^{(0),n}\cdot\boldsymbol{C}_L^{(1),n}, \tag{4.24}$$

and $C_{(L)}^n$ and $\mathcal{G}_{(L)}^n$ are given in Eqs. (3.60b) and (3.60e), respectively. By inverting

$$\int_0^1 dx\, x^{n-2}C_{(L)}(x) = C_{(L)}^n, \tag{4.25a}$$

$$\int_0^1 dx\, x^{n-2}\tilde{\mathcal{B}}_{(L)}(x) = \tilde{\mathcal{B}}_{(L)}^n, \tag{4.25b}$$

$$\int_0^1 dx\, x^{n-2}\mathcal{G}_{(L)}(x) = \mathcal{G}_{(L)}^n, \tag{4.25c}$$

we can obtain

$$C_{(L)}(x) = 96\beta_0 n_f \langle e^4 \rangle x^2 (1-x), \tag{4.26a}$$

$$\tilde{\mathcal{B}}_{(L)}(x) = 48 C_F n_f \langle e^4 \rangle x [2x \ln(x) + (1-x)(1+2x)], \tag{4.26b}$$

$$\begin{aligned} \mathcal{G}_{(L)}(x) = \frac{32}{5}\beta_0 C_F n_f \langle e^4 \rangle \Bigg[& -x^2(35+12x^2)\ln^2(x) + 4\left(\frac{1}{x} - 5x^2 + 6x^4\right)\ln(x)\ln(1-x) \\ & + 4\left(\frac{1}{x} - 5x^2 + 6x^4\right)\mathrm{Li}_2(-x) - (4 + 28x + 63x^2 - 66x^3)\ln(x) \\ & + 30x^2(1-x)\ln(1-x) + 2(2 - 23x + 3x^2 + 18x^3) - 4x^2(5-6x^2)\zeta(2)\Bigg]. \end{aligned} \tag{4.26c}$$

Note that $C_{(L)}(x)$, $\tilde{\mathcal{B}}_{(L)}(x)$ and $\mathcal{G}_{(L)}(x)$ vanish both at $x = 0$ and $x = 1$.

In Fig. 4.7, we plot the $F_2^\gamma(x, Q^2, P^2)$ obtained by inverting Eq. (4.19), the leading-logarithm box-diagram contributions (only $\tilde{\mathcal{L}}^n$ term), the box-diagram contributions including non leading-logarithm terms ($\tilde{\mathcal{L}}^n$ and C^n terms) and the (conjectured) box-diagram contributions including corrections of one-gluon exchange, as well as original QCD predictions. We also plot, in Fig. 4.8, the $F_L^\gamma(x, Q^2, P^2)$ obtained by inverting Eq. (4.23), the leading box-diagram contributions (only $C_{(L)}^n$ term) and the (conjectured) box-diagram contributions including corrections of one-gluon exchange, as well as original QCD predictions. We can see that QCD predictions show the same tendency of the box-diagram contributions in this kinematic region.

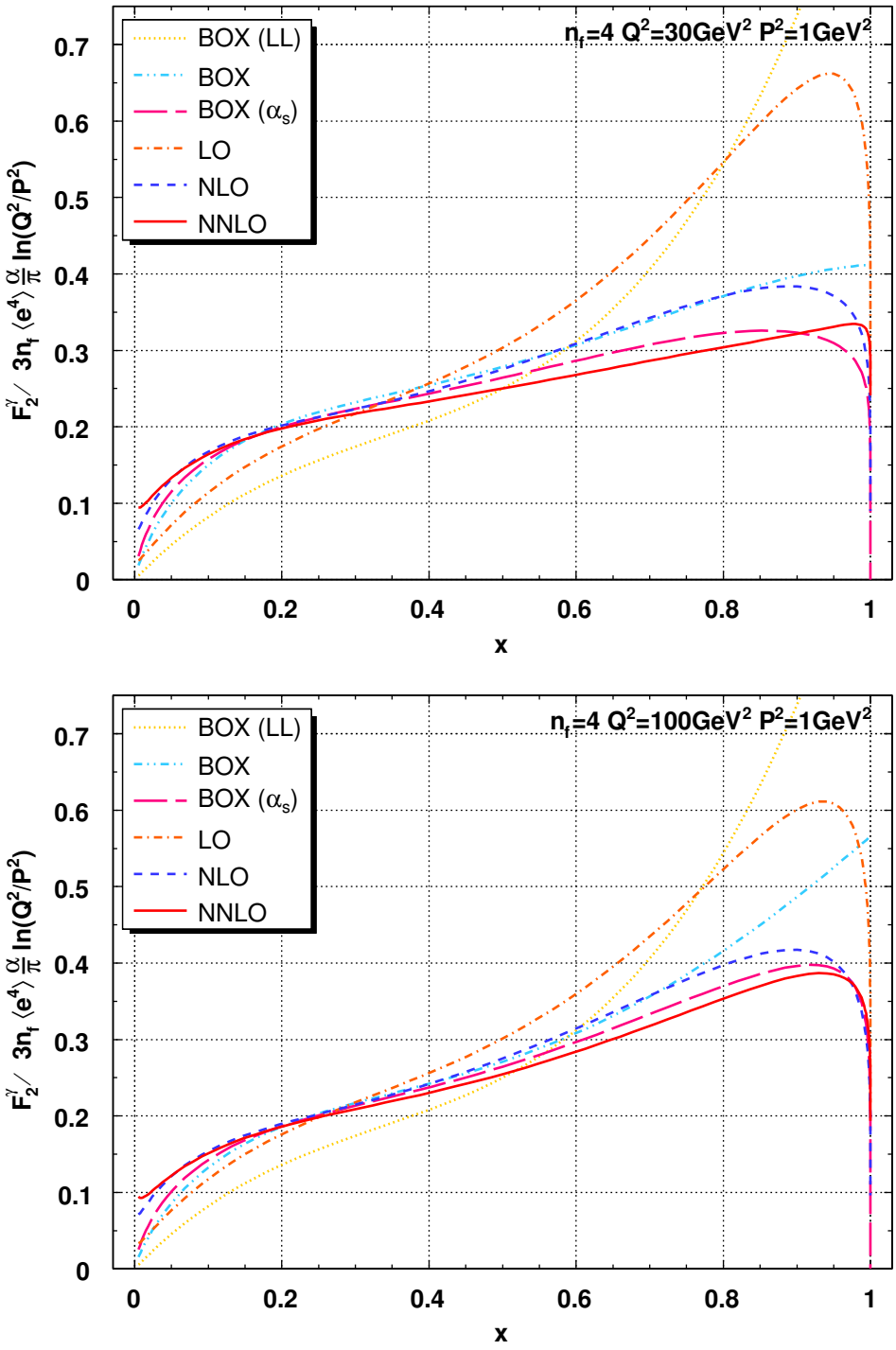

Figure 4.7: QCD corrections and the box-diagram contributions for the virtual photon structure function $F_2^\gamma(x, Q^2, P^2)$ in units of $[3n_f\langle e^4\rangle\alpha/\pi \ln(Q^2/P^2)]$ for (a) $Q^2 = 30\,\mathrm{GeV}^2$ and $P^2 = 1\,\mathrm{GeV}^2$ (b) $Q^2 = 100\,\mathrm{GeV}^2$ and $P^2 = 1\,\mathrm{GeV}^2$ with $n_f = 4$ and $\Lambda = 200\,\mathrm{MeV}$. We plot the leading-logarithm box-diagram contributions (BOX (LL)), the box-diagram contributions including non leading-logarithm terms (BOX), the box-diagram contributions including corrections of one-gluon exchange which are speculated from Eq. (4.19) (BOX (α_s)), the QCD leading order (LO), the next-to-leading order (NLO) and the next-to-next-to-leading order (NNLO) results.

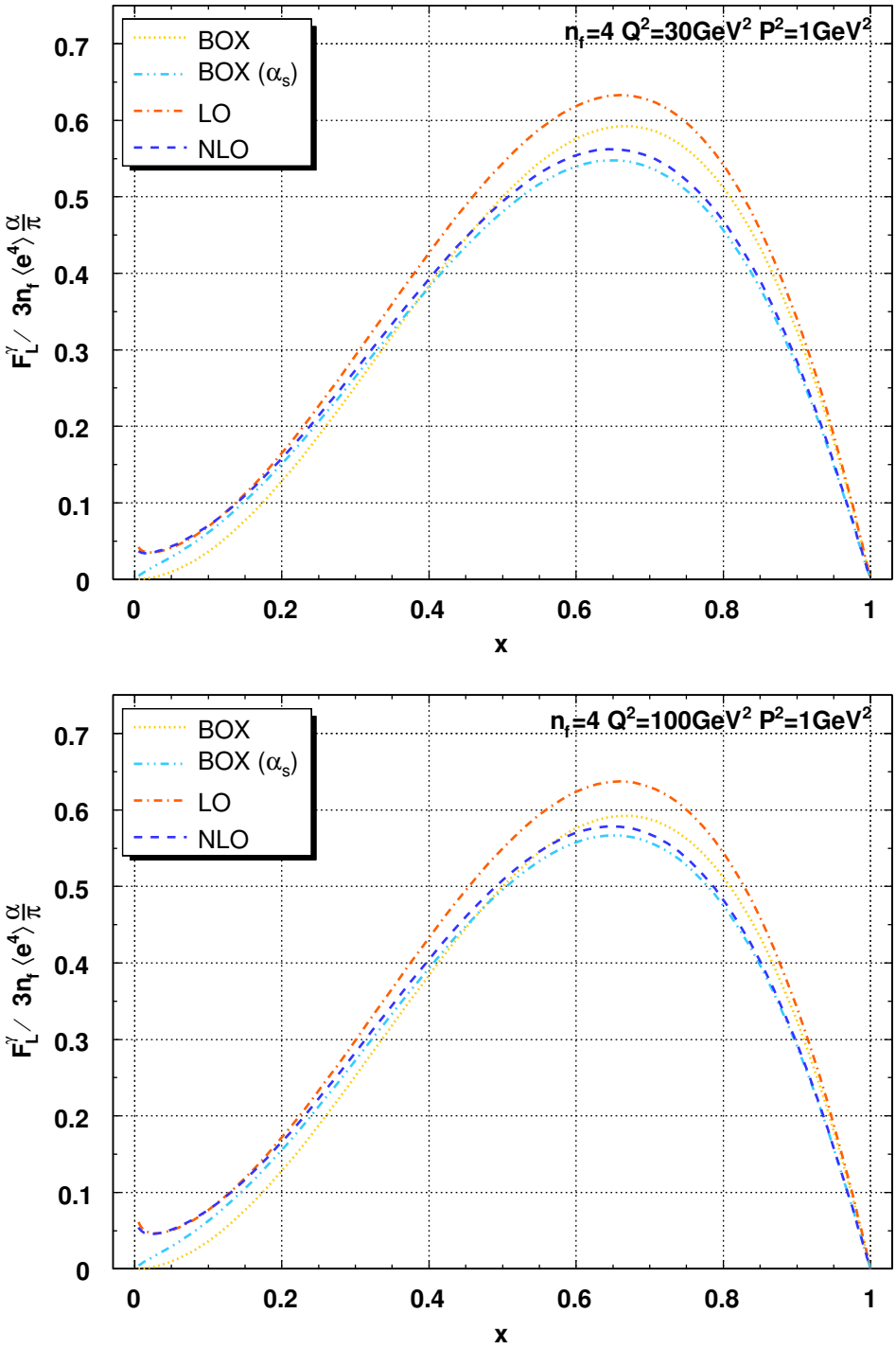

Figure 4.8: QCD corrections and the box-diagram contributions for the virtual photon structure function $F_L^\gamma(x, Q^2, P^2)$ in units of $(3n_f\langle e^4\rangle\alpha/\pi)$ for (a) $Q^2 = 30\,\mathrm{GeV}^2$ and $P^2 = 1\,\mathrm{GeV}^2$ (b) $Q^2 = 100\,\mathrm{GeV}^2$ and $P^2 = 1\,\mathrm{GeV}^2$ with $n_f = 4$ and $\Lambda = 200\,\mathrm{MeV}$. We plot the box-diagram contributions (BOX), the box-diagram contributions including corrections of one-gluon exchange which are speculated from Eq. (4.23) (BOX (α_s)), the QCD leading order (LO) and the next-to-leading order (NLO) results.

Chapter 5

Summary

In this thesis, we have investigated the unpolarized (spin-averaged) virtual photon structure functions $F_2^\gamma(x, Q^2, P^2)$, which is expected to be measured in the future e^+e^- collider experiments such as ILC, for the kinematical region $\Lambda^2 \ll P^2 \ll Q^2$ in massless QCD. In this kinematic region, contrary to real photon case, the asymptotic freedom nature of QCD allows us to calculate structure functions in all orders by perturbation.

Using the framework of the OPE supplemented by the RG method, we obtained the definite predictions for the moments of $F_2^\gamma(x, Q^2, P^2)$ up to the NNLO (the order $\alpha\alpha_s$). The inverse Mellin transform of the moments was numerically performed to express the structure function $F_2^\gamma(x, Q^2, P^2)$ as a function of x. We found that the NNLO corrections are negative for almost the whole x, and not negligible especially at large x.

We also examined the longitudinal structure function $F_L^\gamma(x, Q^2, P^2)$ up to the NLO (the order $\alpha\alpha_s$). We found that the NLO corrections to $F_L^\gamma(x, Q^2, P^2)$ have negative contributions for almost the whole x.

Although we have ignored in our kinematical region, we should also consider the power corrections of the form $(P^2/Q^2)^k$, which are arising from the target mass effects as well as from higher twist effects. Furthermore it was conjectured in Eqs. (4.19) and (4.23) that these expressions coincide with the box-diagrams contributions including corrections of one-gluon exchange, but we postpone confirmation of this conjecture to a future study.

Acknowledgments

First of all, I would like to express my gratitude to my supervisor, Prof. Ken Sasaki for invaluable suggestions, comments, instructions. He introduced me to the field of Particle Physics and Phenomenology, and I have learned from him how to approach essentials of physics. I am grateful to Prof. Tuneo Uematsu, who was a collaborator of this work, for fruitful discussions and his kindness. I am much obliged to Dr. Kazumasa Ohkuma for his thoughtful advice and encouragement. Special thanks to all my friends and other people close to me for making my nine years in Yokohama so enjoyable.

Finally, I would like to greatly acknowledge all my family, and particularly my parents, for their continuous and generous support.

Appendix A

Explicit Form of $\boldsymbol{M}^n$ and $\boldsymbol{X}^n$

Here we present the explicit form of the integrals needed for evaluating $\boldsymbol{M}^n(Q^2/P^2, \bar{g}(P^2))$ in Eq. (3.21a) and $\boldsymbol{X}^n(Q^2/P^2, \bar{g}(P^2))$ in Eq. (3.21b) up to NNLO. First, using Eq. (3.26) with Eq. (3.32), the T-ordered exponential in $\boldsymbol{M}^n(Q^2/P^2, \bar{g}(P^2))$ is expanded such as

$$
\begin{aligned}
&T\exp\left[\int_{g_2}^{g_1} dg \frac{\hat{\boldsymbol{\gamma}}^n(g)}{\beta(g)}\right] \\
&\quad= \sum_i \boldsymbol{P}_i^n \left(\frac{g_2^2}{g_1^2}\right)^{d_i^n} \left[1 + d_i^n \frac{\beta_1}{\beta_0}\frac{g_1^2 - g_2^2}{16\pi^2} - \frac{d_i^n}{2}\left(\frac{\beta_1^2}{\beta_0^2} - \frac{\beta_2}{\beta_0}\right)\frac{g_1^4 - g_2^4}{(16\pi^2)^2} + \frac{1}{2}(d_i^n)^2 \frac{\beta_1^2}{\beta_0^2}\left(\frac{g_1^2 - g_2^2}{16\pi^2}\right)^2\right] \\
&\qquad - \frac{1}{16\pi^2}\sum_{i,j} \boldsymbol{P}_i^n \hat{\boldsymbol{\gamma}}^{(1),n} \boldsymbol{P}_j^n \left\{ \frac{1}{\lambda_i^n - \lambda_j^n + 2\beta_0}\left(1 + \frac{\beta_1}{\beta_0}\frac{d_i^n g_1^2 - d_j^n g_2^2}{16\pi^2}\right)\left[g_1^2\left(\frac{g_2^2}{g_1^2}\right)^{d_j^n} - g_2^2\left(\frac{g_2^2}{g_1^2}\right)^{d_i^n}\right] \right. \\
&\qquad\qquad \left. - \frac{1}{16\pi^2}\frac{1}{\lambda_i^n - \lambda_j^n + 4\beta_0}\frac{\beta_1}{\beta_0}(1 + d_i^n - d_j^n)\left[g_1^4\left(\frac{g_2^2}{g_1^2}\right)^{d_j^n} - g_2^4\left(\frac{g_2^2}{g_1^2}\right)^{d_i^n}\right]\right\} \\
&\qquad - \frac{1}{(16\pi^2)^2}\sum_{i,j} \frac{\boldsymbol{P}_i^n \hat{\boldsymbol{\gamma}}^{(2),n} \boldsymbol{P}_j^n}{\lambda_i^n - \lambda_j^n + 4\beta_0}\left[g_1^4\left(\frac{g_2^2}{g_1^2}\right)^{d_j^n} - g_2^4\left(\frac{g_2^2}{g_1^2}\right)^{d_i^n}\right] \\
&\qquad + \frac{1}{(16\pi^2)^2}\sum_{i,j,k} \boldsymbol{P}_i^n \hat{\boldsymbol{\gamma}}^{(1),n} \boldsymbol{P}_j^n \hat{\boldsymbol{\gamma}}^{(1),n} \boldsymbol{P}_k^n \frac{1}{\lambda_j^n - \lambda_k^n + 2\beta_0} \\
&\qquad\quad \times \left\{ \frac{1}{\lambda_i^n - \lambda_k^n + 4\beta_0}\left[g_1^4\left(\frac{g_2^2}{g_1^2}\right)^{d_k^n} - g_2^4\left(\frac{g_2^2}{g_1^2}\right)^{d_i^n}\right] - \frac{1}{\lambda_i^n - \lambda_j^n + 2\beta_0}\left[g_1^2 g_2^2\left(\frac{g_2^2}{g_1^2}\right)^{d_j^n} - g_2^4\left(\frac{g_2^2}{g_1^2}\right)^{d_i^n}\right]\right\}.
\end{aligned}
\tag{A.1}
$$

Next, using the previous result Eq. (A.1), one can evaluate the integral in $\boldsymbol{X}^n(Q^2/P^2, \bar{g}(P^2))$ as

$$
\begin{aligned}
&\int_{g_2}^{g_1} dg \frac{\boldsymbol{K}^n(g,\alpha)}{\beta(g)} T\exp\left[\int_{g_2}^{g} dg' \frac{\hat{\boldsymbol{\gamma}}^n(g')}{\beta(g')}\right] \Big/ \left(\frac{\alpha}{4\pi}\frac{1}{2\beta_0}\right) \\
&\quad= \left(\frac{g_2^2}{16\pi^2}\right)^{-1} \sum_i \left[\boldsymbol{K}^{(0),n}\boldsymbol{P}_i^n \frac{1}{1 + d_i^n}\right]\left[1 - \left(\frac{g_2^2}{g_1^2}\right)^{d_i^n + 1}\right] \\
&\qquad + \sum_i \left[-\boldsymbol{K}^{(0),n}\boldsymbol{P}_i^n \frac{\beta_1}{\beta_0}\frac{1 - d_i^n}{d_i^n} - \boldsymbol{K}^{(0),n}\sum_j \frac{\boldsymbol{P}_j^n \hat{\boldsymbol{\gamma}}^{(1),n} \boldsymbol{P}_i^n}{\lambda_j^n - \lambda_i^n + 2\beta_0}\frac{1}{d_i^n} + \boldsymbol{K}^{(1),n}\boldsymbol{P}_i^n \frac{1}{d_i^n}\right]\left[1 - \left(\frac{g_2^2}{g_1^2}\right)^{d_i^n}\right] \\
&\qquad + \sum_i \left[-\boldsymbol{K}^{(0),n}\boldsymbol{P}_i^n \frac{\beta_1}{\beta_0}\frac{d_i^n}{1 + d_i^n} + \boldsymbol{K}^{(0),n}\sum_j \frac{\boldsymbol{P}_i^n \hat{\boldsymbol{\gamma}}^{(1),n} \boldsymbol{P}_j^n}{\lambda_i^n - \lambda_j^n + 2\beta_0}\frac{1}{1 + d_i^n}\right]\left[1 - \left(\frac{g_2^2}{g_1^2}\right)^{d_i^n + 1}\right] \\
&\qquad + \frac{g_2^2}{16\pi^2}\sum_i \left[-\boldsymbol{K}^{(0),n}\boldsymbol{P}_i^n \left(\frac{\beta_1^2}{\beta_0^2} - \frac{\beta_2}{\beta_0}\frac{1}{1 - d_i^n}\right)\left(1 - \frac{d_i^n}{2}\right) - \boldsymbol{K}^{(0),n}\sum_j \frac{\boldsymbol{P}_j^n \hat{\boldsymbol{\gamma}}^{(1),n} \boldsymbol{P}_i^n}{\lambda_j^n - \lambda_i^n + 2\beta_0}\frac{\beta_1}{\beta_0}\frac{1 - d_j^n}{1 - d_i^n}\right.
\end{aligned}
$$

$$
\begin{aligned}
&- \boldsymbol{K}^{(0),n} \sum_j \frac{\boldsymbol{P}_j^n \hat{\boldsymbol{\gamma}}^{(1),n} \boldsymbol{P}_i^n}{\lambda_j^n - \lambda_i^n + 4\beta_0} \frac{\beta_1}{\beta_0} \left(1 + \frac{d_j^n}{1 - d_i^n}\right) + \boldsymbol{K}^{(0),n} \sum_j \frac{\boldsymbol{P}_j^n \hat{\boldsymbol{\gamma}}^{(2),n} \boldsymbol{P}_i^n}{\lambda_j^n - \lambda_i^n + 4\beta_0} \frac{1}{1 - d_i^n} \\
&- \boldsymbol{K}^{(0),n} \sum_{j,k} \frac{\boldsymbol{P}_k^n \hat{\boldsymbol{\gamma}}^{(1),n} \boldsymbol{P}_j^n \hat{\boldsymbol{\gamma}}^{(1),n} \boldsymbol{P}_i^n}{(\lambda_j^n - \lambda_i^n + 2\beta_0)(\lambda_k^n - \lambda_i^n + 4\beta_0)} \frac{1}{1 - d_i^n} + \boldsymbol{K}^{(1),n} \boldsymbol{P}_i^n \frac{\beta_1}{\beta_0} \\
&+ \boldsymbol{K}^{(1),n} \sum_j \frac{\boldsymbol{P}_j^n \hat{\boldsymbol{\gamma}}^{(1),n} \boldsymbol{P}_i^n}{\lambda_j^n - \lambda_i^n + 2\beta_0} \frac{1}{1 - d_i^n} - \boldsymbol{K}^{(2),n} \boldsymbol{P}_i^n \frac{1}{1 - d_i^n} \Bigg] \left[1 - \left(\frac{g_2^2}{g_1^2}\right)^{d_i^n - 1}\right] \\
+ \frac{g_2^2}{16\pi^2} \sum_i \Bigg[&\boldsymbol{K}^{(0),n} \boldsymbol{P}_i^n \frac{\beta_1^2}{\beta_0^2} (1 - d_i^n) - \boldsymbol{K}^{(0),n} \sum_j \frac{\boldsymbol{P}_i^n \hat{\boldsymbol{\gamma}}^{(1),n} \boldsymbol{P}_j^n}{\lambda_i^n - \lambda_j^n + 2\beta_0} \frac{\beta_1}{\beta_0} \frac{1 - d_i^n}{d_i^n} \\
&+ \boldsymbol{K}^{(0),n} \sum_j \frac{\boldsymbol{P}_j^n \hat{\boldsymbol{\gamma}}^{(1),n} \boldsymbol{P}_i^n}{\lambda_j^n - \lambda_i^n + 2\beta_0} \frac{\beta_1}{\beta_0} - \boldsymbol{K}^{(0),n} \sum_{j,k} \frac{\boldsymbol{P}_j^n \hat{\boldsymbol{\gamma}}^{(1),n} \boldsymbol{P}_i^n \hat{\boldsymbol{\gamma}}^{(1),n} \boldsymbol{P}_k^n}{(\lambda_i^n - \lambda_k^n + 2\beta_0)(\lambda_j^n - \lambda_i^n + 2\beta_0)} \frac{1}{d_i^n} \\
&- \boldsymbol{K}^{(1),n} \boldsymbol{P}_i^n \frac{\beta_1}{\beta_0} + \boldsymbol{K}^{(1),n} \sum_j \frac{\boldsymbol{P}_i^n \hat{\boldsymbol{\gamma}}^{(1),n} \boldsymbol{P}_j^n}{\lambda_i^n - \lambda_j^n + 2\beta_0} \frac{1}{d_i^n} \Bigg] \left[1 - \left(\frac{g_2^2}{g_1^2}\right)^{d_i^n}\right] \\
+ \frac{g_2^2}{16\pi^2} \sum_i \Bigg[&\boldsymbol{K}^{(0),n} \boldsymbol{P}_i^n \left(\frac{\beta_1^2}{\beta_0^2} - \frac{\beta_2}{\beta_0} \frac{1}{1 + d_i^n}\right) \frac{d_i^n}{2} - \boldsymbol{K}^{(0),n} \sum_j \frac{\boldsymbol{P}_i^n \hat{\boldsymbol{\gamma}}^{(1),n} \boldsymbol{P}_j^n}{\lambda_i^n - \lambda_j^n + 2\beta_0} \frac{\beta_1}{\beta_0} \frac{d_j^n}{1 + d_i^n} \\
&- \boldsymbol{K}^{(0),n} \sum_j \frac{\boldsymbol{P}_i^n \hat{\boldsymbol{\gamma}}^{(1),n} \boldsymbol{P}_j^n}{\lambda_i^n - \lambda_j^n + 4\beta_0} \frac{\beta_1}{\beta_0} \left(1 - \frac{d_j^n}{1 + d_i^n}\right) \\
&+ \boldsymbol{K}^{(0),n} \sum_j \frac{\boldsymbol{P}_i^n \hat{\boldsymbol{\gamma}}^{(2),n} \boldsymbol{P}_j^n}{\lambda_i^n - \lambda_j^n + 4\beta_0} \frac{1}{1 + d_i^n} \\
&+ \boldsymbol{K}^{(0),n} \sum_{j,k} \frac{\boldsymbol{P}_i^n \hat{\boldsymbol{\gamma}}^{(1),n} \boldsymbol{P}_j^n \hat{\boldsymbol{\gamma}}^{(1),n} \boldsymbol{P}_k^n}{\lambda_j^n - \lambda_k^n + 2\beta_0} \\
&\qquad \times \left(\frac{1}{\lambda_i^n - \lambda_j^n + 2\beta_0} - \frac{1}{\lambda_i^n - \lambda_k^n + 4\beta_0}\right) \frac{1}{1 + d_i^n} \Bigg] \left[1 - \left(\frac{g_2^2}{g_1^2}\right)^{d_i^n + 1}\right].
\end{aligned}
\tag{A.2}
$$

Appendix B

Explicit Expressions of Necessary Quantities in the $\overline{\rm MS}$ Scheme

We give the explicit expressions of some quantities whcih are necessary to evaluate the moment sum rules but have not been in literature explicitly — the three-loop photon-hadron mixing anomalous dimensions $k_{\rm ns}^{(2),\rm approx}(n)$, $k_g^{(2),\rm approx}(n)$ and $k_{\rm ps}^{(2)}(n)$ which have appeared in Eqs. (3.48), and the photon matrix elements up to the two-loop level, $a_q^{(1)}(n)$, $a_q^{(2)}(n)$ and $a_g^{(2)}(n)$ which have appeared in Eqs. (3.49), (3.55) and (3.57), respectively — for even n in the $\overline{\rm MS}$ scheme. They are expressed in terms of rational functions of n and the harmonic sums [61]

$$S_m(n) = \sum_{j=1}^{n} \frac{1}{j^m}, \qquad S_{-m}(n) = \sum_{j=1}^{n} \frac{(-1)^j}{j^m}, \qquad S_{m_1,m_2}(n) = \sum_{j=1}^{n} \frac{1}{j^{m_1}} S_{m_2}(j). \tag{B.1}$$

Futhermore, they contains values of the Riemann ζ-functions.

Three-loop Photon-Hadron Mixing Anomalous Dimensions Here we present the approximated three-loop photon-hadron mixing anomalous dimensions $k_{\rm ns}^{(2),\rm approx}(n)$ and $k_g^{(2),\rm approx}(n)$, and the exact result $k_{\rm ps}^{(2)}(n)$, which are appeared in Eqs. (3.48). They are obtained by taking the Mellin moments of the parameterizations for the $P_{{\rm ns}\gamma}^{(2)}(x)$ and $P_{{\rm g}\gamma}^{(2)}(x)$, and of the exact result for $P_{{\rm ps}\gamma}^{(2)}(x)$, which are given in Eqs. (6)-(8) of Ref. [9].

First, $k_{\rm ns}^{(2),\rm approx}(n)$ is expressed as

$$\begin{aligned}
k_{\rm ns}^{(2),\rm approx}(n) \;\equiv\; & -\int_0^1 dx\, x^{n-1}\Big(\text{the r.h.s. of Eq. (6) in Ref. [9]}\Big) \\
=\; & -\frac{128 S_1(n)^4}{27n} + \frac{62.5244 S_1(n)^3}{n} - \frac{50.08 S_1(n)^3}{n+1} - \frac{256 S_2(n) S_1(n)^2}{9n} \\
& - \frac{175.3 S_1(n)^2}{n} - \frac{195.4 S_1(n)^2}{n^2} - \frac{150.24 S_1(n)^2}{(n+1)^2} - \frac{203.227 S_2(n) S_1(n)}{n} \\
& - \frac{150.24 S_2(n) S_1(n)}{n+1} - \frac{1024 S_3(n) S_1(n)}{27n} - \frac{128 S_2(n)^2}{9n} + \frac{785.14 S_1(n)}{n} \\
& - \frac{325.4 S_1(n)}{n^3} - \frac{300.48 S_1(n)}{(n+1)^3} - \frac{175.3 S_2(n)}{n} - \frac{520.8 S_2(n)}{n^2} - \frac{150.24 S_2(n)}{(n+1)^2} \\
& - \frac{591.151 S_3(n)}{n} - \frac{100.16 S_3(n)}{n+1} - \frac{256 S_4(n)}{9n} - \frac{492.087}{n} + \frac{1262}{n+1} - \frac{449.2}{n+2} \\
& + \frac{1445}{n+3} + \frac{1279.86}{n^2} + \frac{1169}{(n+1)^2} - \frac{403.2}{n^3} + \frac{160}{n^4} - \frac{300.48}{(n+1)^4} - \frac{512}{9n^5} \\
+\; & n_f \Bigg[-\frac{32 S_1(n)^3}{27n} - \frac{258.142 S_1(n)^2}{n} + \frac{270 S_1(n)^2}{n+1} + \frac{269.4 S_1(n)^2}{n^2} \\
& + \frac{535.244 S_2(n) S_1(n)}{n} - \frac{905.06 S_1(n)}{n} + \frac{540 S_1(n)}{(n+1)^2} + \frac{17.046 S_1(n)}{n^3}
\end{aligned}$$

$$
\begin{aligned}
&-\frac{258.142S_2(n)}{n}+\frac{270S_2(n)}{n+1}+\frac{286.446S_2(n)}{n^2}+\frac{553.476S_3(n)}{n}\\
&-\frac{628.124}{n}-\frac{114.4}{n+1}+\frac{24.86}{n+2}+\frac{53.39}{n+3}-\frac{49.5895}{n^2}-\frac{26.63}{(n+1)^2}\\
&+\frac{21.984}{n^3}+\frac{540}{(n+1)^3}-\frac{64}{9n^4}\Bigg]. \qquad \text{(B.2)}
\end{aligned}
$$

Secondly, $k_g^{(2),\mathrm{approx}}(n)$ is expressed as

$$
\begin{aligned}
k_g^{(2),\mathrm{approx}}(n) \;\equiv\; & -\int_0^1 dx\, x^{n-1}\Big(\text{the r.h.s. of Eq. (7) in Ref. [9]}\Big)\\
=\;& \frac{32S_1(n)^3}{27n}-\frac{32S_1(n)^3}{27(n+1)}+\frac{79.13S_1(n)^2}{n}-\frac{79.13S_1(n)^2}{n+1}-\frac{433.2S_1(n)^2}{n^2}\\
&+\frac{429.644S_1(n)^2}{(n+1)^2}-\frac{862.844S_2(n)S_1(n)}{n}+\frac{862.844S_2(n)S_1(n)}{n+1}\\
&+\frac{1512.39S_1(n)}{n}-\frac{1512.39S_1(n)}{n+1}+\frac{549.5S_1(n)}{n^2}-\frac{707.76S_1(n)}{(n+1)^2}-\frac{2460S_1(n)}{n^3}\\
&+\frac{4185.69S_1(n)}{(n+1)^3}+\frac{628.63S_2(n)}{n}-\frac{628.63S_2(n)}{n+1}-\frac{2893.2S_2(n)}{n^2}\\
&+\frac{3756.04S_2(n)}{(n+1)^2}-\frac{3324.03S_3(n)}{n}+\frac{3324.03S_3(n)}{n+1}\\
&+\frac{73.1409}{n-1}-\frac{1673.57}{n}+\frac{3180.43}{n+1}-\frac{1420}{n+2}+\frac{406.7}{n+3}-\frac{566.7}{n+4}+\frac{128}{3(n-1)^2}\\
&+\frac{6400}{3n^2}-\frac{3688.39}{(n+1)^2}-\frac{2247.4}{n^3}+\frac{990.14}{(n+1)^3}+\frac{1600}{3n^4}+\frac{9438.76}{(n+1)^4}-\frac{3584}{9n^5}\\
&+\frac{3584}{9(n+1)^5}+\Big(\frac{2460}{n}-\frac{2460}{n+1}\Big)\zeta(3)+\Big(\frac{2460}{n^2}-\frac{2460}{(n+1)^2}\Big)\zeta(2)\\
&+n_f\Bigg[\frac{32S_1(n)^2}{9n}-\frac{32S_1(n)^2}{9(n+1)}-\frac{9.133S_1(n)^2}{n^2}+\frac{9.133S_1(n)^2}{(n+1)^2}-\frac{18.266S_2(n)S_1(n)}{n}\\
&\quad+\frac{18.266S_2(n)S_1(n)}{n+1}+\frac{46.4264S_1(n)}{n}-\frac{46.4264S_1(n)}{n+1}+\frac{16.18S_1(n)}{n^2}\\
&\quad-\frac{23.2911S_1(n)}{(n+1)^2}-\frac{76.66S_1(n)}{n^3}+\frac{113.192S_1(n)}{(n+1)^3}+\frac{19.7356S_2(n)}{n}\\
&\quad-\frac{19.7356S_2(n)}{n+1}-\frac{85.793S_2(n)}{n^2}+\frac{104.059S_2(n)}{(n+1)^2}-\frac{94.926S_3(n)}{n}\\
&\quad+\frac{94.926S_3(n)}{n+1}+\frac{40.5597}{n-1}-\frac{21.1683}{n}+\frac{17.0286}{n+1}-\frac{93.37}{n+2}+\frac{101.05}{n+3}-\frac{44.1}{n+4}\\
&\quad+\frac{115.341}{n^2}-\frac{161.767}{(n+1)^2}-\frac{52.82}{n^3}+\frac{13.3489}{(n+1)^3}-\frac{128}{9n^4}+\frac{299}{(n+1)^4}\Bigg]. \qquad \text{(B.3)}
\end{aligned}
$$

Finally, $k_{\mathrm{ps}}^{(2)}(n)$ is expressed as

$$
\begin{aligned}
k_{\mathrm{ps}}^{(2)}(n) \;\equiv\; & -\int_0^1 dx\, x^{n-1}\Big(\text{the r.h.s. of Eq. (8) in Ref. [9]}\Big)\\
=\;& n_f C_F\Bigg[-\frac{2464}{81(n-1)}+\frac{432}{n}+\frac{72}{n+1}-\frac{38360}{81(n+2)}-\frac{344}{n^2}-\frac{368}{(n+1)^2}\\
&\quad-\frac{3584}{27(n+1)^2}+\frac{288}{n^3}+\frac{208}{(n+1)^3}+\frac{448}{9(n+2)^3}-\frac{96}{n^4}+\frac{96}{(n+1)^4}\\
&\quad+\frac{256}{3(n+2)^4}+\frac{64}{n^5}-\frac{128}{(n+1)^5}\Bigg]. \qquad \text{(B.4)}
\end{aligned}
$$

Note that $k_{\rm ps}^{(2)}(n)$ is an exact result.

Photon Matrix Elements up to Two-loop Level Here we present the photon matrix elements up to the two-loop level $a_q^{(1)}(n)$, $a_q^{(2)}(n)$ and $a_g^{(2)}(n)$ which are appeared in Eqs. (3.49), (3.55) and (3.57), respectively. Then are obtained by taking the Mellin moments of the unnormalized photon matrix elements in Eqs. (A7)-(A9), and (A12)-(A14) of Ref. [59], and executing correct renormalizations, and picking up the relevant terms with changing color factors.

First, $a_q^{(1)}(n)$ is expressed as

$$a_q^{(1)}(n) = 4\left[-\frac{1}{n} + \frac{1}{n^2} - \frac{4}{(n+1)^2} + \frac{4}{(n+2)^2} + \left(\frac{1}{n} - \frac{2}{n+1} + \frac{2}{n+2}\right)S_1(n)\right]. \tag{B.5}$$

Secondly, $a_q^{(2)}(n)$ is expressed as

$$\begin{aligned}
a_q^{(2)}(n) \;=\; & C_F\Big\{\Big(\frac{1}{n} - \frac{2}{n+1} + \frac{2}{n+2}\Big)\Big(-\frac{4}{3}S_1(n)^3 - 4S_2(n)S_1(n) + \frac{64}{3}S_3(n) \\
& \qquad -16S_{2,1}(n) - 48\zeta(3)\Big) \\
& +S_1(n)^2\Big(\frac{6}{n} - \frac{8}{n+1} + \frac{16}{n+2} - \frac{16}{n^2} + \frac{40}{(n+1)^2} - \frac{32}{(n+2)^2}\Big) \\
& +S_1(n)\Big(\frac{4}{n} - \frac{80}{n+1} + \frac{56}{n+2} + \frac{16}{n^2} - \frac{48}{(n+1)^2} + \frac{64}{(n+2)^2} \\
& \qquad -\frac{32}{n^3} + \frac{176}{(n+1)^3} - \frac{128}{(n+2)^3}\Big) \\
& +S_2(n)\Big(\frac{6}{n} + \frac{8}{n+1} - \frac{16}{n^2} + \frac{40}{(n+1)^2} - \frac{32}{(n+2)^2}\Big) \\
& +\frac{38}{n} - \frac{70}{n+1} + \frac{56}{n+2} + \frac{56}{n^2} - \frac{198}{(n+1)^2} + \frac{144}{(n+2)^2} - \frac{22}{n^3} \\
& -\frac{40}{(n+1)^3} + \frac{128}{(n+2)^3} + \frac{20}{n^4} + \frac{88}{(n+1)^4}\Big\}.
\end{aligned} \tag{B.6}$$

Finally, $a_g^{(2)}(n)$ is expressed as

$$\begin{aligned}
a_g^{(2)}(n) \;=\; & C_F\Big\{\Big(S_1(n)^2 + S_2(n)\Big)\Big(\frac{16}{3(n-1)} + \frac{4}{n} - \frac{4}{n+1} - \frac{16}{3(n+2)} - \frac{8}{n^2} - \frac{8}{(n+1)^2}\Big) \\
& +S_1(n)\Big(-\frac{32}{9(n-1)} - \frac{32}{n} + \frac{32}{n+1} + \frac{32}{9(n+2)} + \frac{32}{n^2} + \frac{8}{(n+1)^2} \\
& \qquad -\frac{64}{3(n+2)^2} - \frac{32}{n^3} - \frac{48}{(n+1)^3}\Big) \\
& +S_{-2}(n)\Big(\frac{32}{3(n-1)} - \frac{32}{n} + \frac{32}{n+1} - \frac{32}{3(n+2)}\Big) \\
& +\frac{872}{27(n-1)} - \frac{80}{n} + \frac{16}{n+1} + \frac{856}{27(n+2)} - \frac{40}{n^2} + \frac{104}{(n+1)^2} + \frac{64}{9(n+2)^2} + \frac{44}{n^3} \\
& +\frac{28}{(n+1)^3} - \frac{128}{3(n+2)^3} - \frac{40}{n^4} - \frac{88}{(n+1)^4}\Big\}.
\end{aligned} \tag{B.7}$$

Appendix C

Harmonic sums and their asymptotic series expansions

C.1 Primary Definition and Basic Properties

The harmonic sums [61] are recursively defined by

$$S_{k,\vec{m}}(n) = \sum_{j=1}^{n} \frac{[\mathrm{sgn}(k)]^j}{j^{|k|}} S_{\vec{m}}(j), \qquad S(n) = 1, \qquad n = 0, 1, 2, \cdots \in \mathbb{N}. \tag{C.1}$$

The all indices of the sum, which consist of the leading (left-most) index k and the vector of the remaining indices $\vec{m}$, can take non-zero integers. $\mathrm{sgn}(k)$ represents the the sign of k, i.e., $(+1)$ for $k > 0$ and (-1) for $k < 0$. $S(n)$ indicates the sum with no index. The depth of a harmonic sum is defined as the number of its indices, and the weight of that is defined as the sum of the absolute values of its indices. For example,

$$S_{1,-3,2}(n) = \sum_{i=1}^{n} \frac{1}{i} \sum_{j=1}^{i} \frac{(-1)^j}{j^3} \sum_{k=1}^{j} \frac{1}{k^2}, \tag{C.2}$$

is one of the harmonic sums with its depth 3 and its weight 6. Note that, in this convention, the negative index indicates the alternating series. The following sums may be found in the old literature:

$$S'_k\left(\frac{n}{2}\right) \equiv \sum_{j=1}^{n/2} \frac{1}{j^k} = 2^{k-1}[S_k(n) + S_{-k}(n)], \qquad \text{for even } n, \qquad k = 1, 2, \cdots, \tag{C.3}$$

$$\tilde{S}(n) \equiv \sum_{j=1}^{n} \frac{(-1)^j}{j^2} \sum_{l=1}^{j} \frac{1}{l} = S_{-2,1}(n). \tag{C.4}$$

The definitions of the harmonic sums Eq. (C.1) implies that they satisfy the following translation relations:

$$S_{k,\vec{m}}(n) = S_{k,\vec{m}}(n+1) - \frac{[\mathrm{sgn}(k)]^{n+1}}{(n+1)^{|k|}} S_{\vec{m}}(n+1). \tag{C.5}$$

The set of the harmonic sums is not fully independent. For example, from the relation

$$\sum_{\substack{n \geq j_1 \geq 1 \\ n \geq j_2 \geq 1}} = \sum_{n \geq j_1 \geq j_2 \geq 1} + \sum_{n \geq j_2 \geq j_1 \geq 1} - \sum_{n \geq j_1 = j_2 \geq 1}, \tag{C.6}$$

one can obtain

$$\begin{aligned} S_{k_1,\vec{m}_1}(n) S_{k_2,\vec{m}_2}(n) = &\sum_{j=1}^{n} \frac{[\mathrm{sgn}(k_1)]^j}{j^{|k_1|}} S_{\vec{m}_1}(j) S_{k_2,\vec{m}_2}(j) + \sum_{j=1}^{n} \frac{[\mathrm{sgn}(k_2)]^j}{j^{|k_2|}} S_{k_1,\vec{m}_1}(j) S_{\vec{m}_2}(j) \\ &- \sum_{j=1}^{n} \frac{[\mathrm{sgn}(k_1)\,\mathrm{sgn}(k_2)]^j}{j^{|k_1|+|k_2|}} S_{\vec{m}_1}(j) S_{\vec{m}_2}(j). \end{aligned} \tag{C.7}$$

Using Eq. (C.7) recursively until one of the two sums has no more indices, one can reduce products of the harmonic sums with an identical argument to the single higher harmonic sums, e.g.,

$$S_{k_1}(n)S_{k_2}(n) = S_{k_1,k_2}(n) + S_{k_2,k_1}(n) - S_{k_1\wedge k_2}(n), \tag{C.8a}$$

$$S_{k_1}(n)S_{k_2,k_3}(n) = S_{k_1,k_2,k_3}(n) + S_{k_2,k_1,k_3}(n) + S_{k_2,k_3,k_1}(n) - S_{k_1\wedge k_2,k_3}(n) - S_{k_2,k_1\wedge k_3}(n), \tag{C.8b}$$

$$\begin{aligned} S_{k_1}(n)S_{k_2,k_3,k_4}(n) = {} & S_{k_1,k_2,k_3,k_4}(n) + S_{k_2,k_1,k_3,k_4}(n) + S_{k_2,k_3,k_1,k_4}(n) + S_{k_2,k_3,k_4,k_1}(n) \\ & - S_{k_1\wedge k_2,k_3,k_4}(n) - S_{k_2,k_1\wedge k_3,k_4}(n) - S_{k_2,k_3,k_1\wedge k_4}(n), \end{aligned} \tag{C.8c}$$

$$\vdots \qquad\qquad \vdots$$

where the pseudo addition operator $\wedge$ is defined by

$$k_1 \wedge k_2 \equiv \mathrm{sgn}(k_1)\,\mathrm{sgn}(k_2)(|k_1| + |k_2|) = \mathrm{sgn}(k_2)k_1 + \mathrm{sgn}(k_1)k_2. \tag{C.9}$$

The harmonic sums whose left-most index equals to one are logarithmically divergent when the argument goes infinity $n \to \infty$. The product identities Eq. (C.7) or Eqs. (C.8) can be used to single out the $S_1(n)$ as the divergent part from such sums. For example,

$$S_{1,1,2}(n) = \frac{1}{2}S_1^2(n)S_2(n) + S_1(n)S_3(n) - S_1(n)S_{2,1}(n) + \frac{1}{2}S_4(n) - S_{3,1}(n) + S_{2,1,1}(n). \tag{C.10}$$

The manipulations of these kind are implemented in the program package Summer written in Form [61, 62].

The Mellin transform of the harmonic polylogarithm, which is introduced in Ref. [60], can be written in terms of the harmonic sums, and the inverse Mellin transform of the harmonic sum is obtained in terms of the harmonic polylogarithms, reversely. These methods are also implemented in the program package Harmpol written in Form [60, 61, 62]. More relations of the harmonic sums can be found in Refs. [61, 73, 75].

C.2 Analytic Continuation

We here consider the analytic continuation of the harmonic sums over the complex plane as a start point of the asymptotic expansion of these sums. It is well-known that the single harmonic sums can be analytically continued in terms of polygamma functions $\psi^{(n)}(z)$ (e.g., [73-b]):

$$S_k(n) = \frac{(-1)^{k-1}}{(k-1)!}\psi^{(k-1)}(n+1) + \begin{cases} \gamma_E, & k = 1, \\ \zeta(k), & k \geq 2, \end{cases} \tag{C.11a}$$

$$S_{-k}(n) = (-1)^n\frac{(-1)^{k-1}}{(k-1)!}\beta^{(k-1)}(n+1) - \eta(k), \qquad k \geq 1, \tag{C.11b}$$

where

$$\psi^{(n)}(z) = \frac{d^{n+1}}{dz^{n+1}}\ln\Gamma(z), \qquad \beta^{(n)}(z) = \frac{1}{2^{n+1}}\left[\psi^{(n)}\left(\frac{z+1}{2}\right) - \psi^{(n)}\left(\frac{z}{2}\right)\right], \tag{C.12}$$

and the Euler-Mascheroni constant γ_E, the Riemann zeta function $\zeta(k)$ and the Dirichlet eta function $\eta(k)$ are given by[♯1]

$$\gamma_E = \lim_{n\to\infty}[S_1(n) - \ln(n)], \tag{C.13}$$

$$\zeta(k) = S_k(\infty) = \sum_{j=1}^{\infty}\frac{1}{j^k}, \qquad k > 1, \tag{C.14}$$

$$\eta(k) = -S_{-k}(\infty) = \sum_{j=1}^{\infty}\frac{(-1)^{j-1}}{j^k} = \left(1 - \frac{1}{2^{k-1}}\right)\zeta(k), \qquad k \geq 1. \tag{C.15}$$

[♯1] Taking the limit of $\eta(k)$ as $k \to 1$ one obtain $\eta(1) = \ln(2)$.

Moreover, the higher harmonic sums can be expressed in terms of Mellin transforms (i.e., integral representations being analytic with respect to n) of basic functions as well as polygamma functions [73].

Here we use, however, another method for the continuation of the harmonic sums, from the aspect of the unified description for all harmonic sums. Eq. (C.1) can be rewritten as the following form:

$$S_{k,\vec{m}}(n) = S_{k,\vec{m}}(\infty) - [\mathrm{sgn}(k)]^n \sum_{j=1}^{\infty} \frac{[\mathrm{sgn}(k)]^j}{(n+j)^{|k|}} S_{\vec{m}}(n+j), \qquad S(n) = 1, \qquad k \leq -1 \quad \text{or} \quad 1 < k. \tag{C.16}$$

In this form, n is no more the upper limit of the sum as in the case of Eq. (C.1), and Eq. (C.16) is defined not only for integer n but also for any real and/or complex n values [72] (see also Appendix of Ref. [76]). The values of the harmonic sums at infinity, which are related to the Euler-Zagier sums [77, 78], are already investigated in detail and these values up to the weight 9 are tabulated in the Summer package [61, 62]. An untrivial aspect of the continuation of the harmonic sums by Eq. (C.16) is how the harmonic sums whose leading index equals to one, which are logarithmically divergent as $n \to \infty$, are treated[♯2].

To avoid the logarithmic divergences along with the sums with leading 1's, we need some regularization for these sums. The most simple one is to take the sum up to a rather large integer N, e.g.,

$$S_1(n) = \lim_{N\to\infty} \left[S_1(N) - \sum_{j=1}^{N-n} \frac{1}{n+j} \right]. \tag{C.17}$$

However, in our purpose, we propose that it is more convenient to use the following regularization:

$$S_1(n) = \lim_{\epsilon\to 0} \left[S_{1+\epsilon}(\infty) - \sum_{j=1}^{\infty} \frac{1}{(n+j)^{1+\epsilon}} \right], \tag{C.18}$$

where ϵ is an infinitesimal positive number. Note that

$$S_{1+\epsilon}(\infty) = \zeta(1+\epsilon) = \frac{1}{\epsilon} + \gamma_E + O(\epsilon), \tag{C.19}$$

and the $1/\epsilon$ pole corresponds to a logarithmic divergence in Eq. (C.17), $S_1(N) \sim \ln(N) + \gamma_E$. Hereafter, we use the later one for the regularization. For higher harmonic sums, we will replace $1 \to 1 + \epsilon$ all at once.

[♯2] One of the possible solutions for this issue is to avoid Eq. (C.16) for the continuation of the harmonic sums whose left-most index equals to one. For example, $S_{1,1,2}(n)$ can be rewritten as in Eq. (C.10). $S_{2,1}(n)$ and $S_{3,1}(n)$ in the right-hand side can be defined by Eq. (C.16) if $S_1(n)$ is defined, and $S_{2,1,1}(n)$ can be defined by using $S_{1,1}(n) = 1/2[S_1^2(n) + S_2(n)]$. Then, the analytic continuations of the single harmonic sums are given by Eqs. (C.11), and therefore $S_{1,1,2}(n)$ can be defined by Eq. (C.10) over the complex plane. Actually, in Ref. [79], the asymptotic series expansions of the harmonic sums are obtained (their definition for the harmonic sums are slightly different from ours and they only consider positive indices), without introducing any regularization, by using these relations for the sums with leading 1's and by using, in terms of our expressions,

$$\sum_{j=1}^{\infty} \frac{\ln^m(n+j)}{(n+j)^k} \sim \sum_{r=0}^{\infty} \frac{B_r}{r!} \left(-\frac{\partial}{\partial k}\right)^m \frac{(k)_{r-1}}{n^{k+r-1}}, \qquad k > 1,$$

$$\sum_{j=1}^{\infty} \frac{(-1)^j \ln^m(n+j)}{(n+j)^k} \sim \sum_{r=1}^{\infty} (2^r - 1) \frac{B_r}{r!} \left(-\frac{\partial}{\partial k}\right)^m \frac{(k)_{r-1}}{n^{k+r-1}}, \qquad k \geq 1,$$

as well as Eqs. (C.25).

For example,

$$
\begin{aligned}
S_{1,1,-2,1}(n) &= \lim_{\epsilon\to 0} S_{1+\epsilon,1+\epsilon,-2,1+\epsilon}(n) \\
&= \lim_{\epsilon\to 0}\Bigg\{ S_{1+\epsilon,1+\epsilon,-2,1+\epsilon}(\infty) - \sum_{j_1=1}^{\infty} \frac{1}{(n+j_1)^{1+\epsilon}} \Bigg[S_{1+\epsilon,-2,1+\epsilon}(\infty) - \sum_{j_2=1}^{\infty} \frac{1}{(n+j_1+j_2)^{1+\epsilon}} \Bigg\{ S_{-2,1+\epsilon}(\infty) \\
&\qquad - (-1)^n (-1)^{j_1+j_2} \sum_{j_3=1}^{\infty} \frac{(-1)^{j_3}}{(n+j_1+j_2+j_3)^2} \Bigg[S_{1+\epsilon}(\infty) - \sum_{j_4=1}^{\infty} \frac{1}{(n+j_1+j_2+j_3+j_4)^{1+\epsilon}} \Bigg] \Bigg\} \Bigg] \Bigg\}
\end{aligned}
\tag{C.20}
$$

The translation relation Eq. (C.5) is valid for the harmonic sums defined over the complex plane by Eq. (C.16) (with the regularization by introducing ϵ, if needed). In actual application, for the sums which have negative indices, $(-1)^n$ should be replaced $(+1)$ or (-1), depending on which one needs to start analytic continuation from even or odd values. In general, one can formally write

$$
S_{\vec{m}}(n) = S^{(0)}_{\vec{m}}(n) + (-1)^n S^{(1)}_{\vec{m}}(n) + (-1)^{2n} S^{(2)}_{\vec{m}}(n) + (-1)^{3n} S^{(3)}_{\vec{m}}(n) + \cdots , \tag{C.21}
$$

and then analytic continuations of this function in the complex domain from even or odd values are given by

$$
S^{\text{even}}_{\vec{m}}(n) = S^{(0)}_{\vec{m}}(n) + S^{(1)}_{\vec{m}}(n) + S^{(2)}_{\vec{m}}(n) + S^{(3)}_{\vec{m}}(n) + \cdots , \tag{C.22a}
$$

$$
S^{\text{odd}}_{\vec{m}}(n) = S^{(0)}_{\vec{m}}(n) - S^{(1)}_{\vec{m}}(n) + S^{(2)}_{\vec{m}}(n) - S^{(3)}_{\vec{m}}(n) + \cdots . \tag{C.22b}
$$

The translation relation Eq. (C.5), which is valid for the harmonic sum Eq. (C.21), is translated for the sums defined by Eqs. (C.22) as follows:

$$
S^{\text{even}}_{k,\vec{m}}(n) = S^{\text{odd}}_{k,\vec{m}}(n+1) - \frac{\text{sgn}(k)}{(n+1)^{|k|}} S^{\text{odd}}_{\vec{m}}(n+1), \tag{C.23a}
$$

$$
S^{\text{odd}}_{k,\vec{m}}(n) = S^{\text{even}}_{k,\vec{m}}(n+1) - \frac{1}{(n+1)^{|k|}} S^{\text{even}}_{\vec{m}}(n+1). \tag{C.23b}
$$

Or it is more convenient to use

$$
S^{\text{even}}_{k_1,k_2,\vec{m}}(n) = S^{\text{even}}_{k_1,k_2,\vec{m}}(n+2) - \left[\frac{1}{(n+2)^{|k_1|}} + \frac{\text{sgn}(k_1)}{(n+1)^{|k_1|}} \right] S^{\text{even}}_{k_2,\vec{m}}(n+2) + \frac{\text{sgn}(k_1)}{(n+1)^{|k_1|}} \frac{1}{(n+2)^{|k_2|}} S^{\text{even}}_{\vec{m}}(n+2), \tag{C.24a}
$$

$$
S^{\text{odd}}_{k_1,k_2,\vec{m}}(n) = S^{\text{odd}}_{k_1,k_2,\vec{m}}(n+2) - \left[\frac{\text{sgn}(k_1)}{(n+2)^{|k_1|}} + \frac{1}{(n+1)^{|k_1|}} \right] S^{\text{odd}}_{k_2,\vec{m}}(n+2) + \frac{1}{(n+1)^{|k_1|}} \frac{\text{sgn}(k_2)}{(n+2)^{|k_2|}} S^{\text{odd}}_{\vec{m}}(n+2). \tag{C.24b}
$$

C.3 Asymptotic Series Expansion

Using the Euler-Maclaurin summation formula, one can easily obtain the following series expansions, which are valid in the sense of the asymptotic expansion for $n \to \infty$:

$$
\sum_{j=1}^{\infty} \frac{1}{(n+j)^k} \sim \sum_{r=0}^{\infty} \frac{B_r}{r!} \frac{(k)_{r-1}}{n^{k+r-1}}, \qquad k > 1, \tag{C.25a}
$$

$$
\sum_{j=1}^{\infty} \frac{(-1)^j}{(n+j)^k} \sim \sum_{r=1}^{\infty} (2^r - 1) \frac{B_r}{r!} \frac{(k)_{r-1}}{n^{k+r-1}}, \qquad k \geq 1, \tag{C.25b}
$$

where

$$(x)_n = \frac{\Gamma(x+n)}{\Gamma(x)}, \tag{C.26}$$

is the Pochhammer symbol and B_r are the Bernoulli numbers defined by

$$\frac{x}{e^x - 1} = \sum_{r=0}^{\infty} \frac{B_r}{r!} x^r, \tag{C.27}$$

i.e., $B_0 = 1, B_1 = -1/2, B_2 = 1/6, B_3 = 0, B_4 = -1/30, B_5 = 0, B_6 = 1/42, \cdots$. With the aid of Eqs. (C.25), as a corollary, we can get the following asymptotic expansions of the single harmonic sums:

$$S_k(n) \sim S_k(\infty) - \sum_{r=0}^{\infty} \frac{B_r}{r!} \frac{(k)_{r-1}}{n^{k+r-1}}, \qquad k > 1, \tag{C.28a}$$

$$S_{-k}(n) \sim S_{-k}(\infty) - (-1)^n \sum_{r=1}^{\infty} (2^r - 1) \frac{B_r}{r!} \frac{(k)_{r-1}}{n^{k+r-1}}, \qquad k \geq 1. \tag{C.28b}$$

The regularization Eq. (C.18) allows us to simply obtain the expansion of $S_1(n)$ in a similar way. Noting that the $1/\epsilon$ poles appear in $S_{1+\epsilon}(\infty)$ and $(1+\epsilon)_{-1}$:

$$S_{1+\epsilon}(\infty) = \zeta(1+\epsilon) = \frac{1}{\epsilon} + \gamma_E + O(\epsilon), \qquad (1+\epsilon)_{-1} = \frac{1}{\epsilon}, \tag{C.29}$$

then we get[#3]

$$\begin{aligned} S_1(n) &\sim S_{1+\epsilon}(\infty) - \frac{(1+\epsilon)_{-1}}{n^\epsilon} - \sum_{r=1}^{\infty} \frac{B_r}{r!} \frac{(1+\epsilon)_{r-1}}{n^{r+\epsilon}} \\ &= \ln(n) + \gamma_E - \sum_{r=1}^{\infty} \frac{B_r}{r} \frac{1}{n^r}, \qquad \epsilon \to 0. \end{aligned} \tag{C.30}$$

The asymptotic expansions of the higher harmonic sums defined by Eq. (C.16) are obtained by repeated use of Eqs. (C.25). For the harmonic sums whose indices contain 1's, one can regularize the logarithmic divergences by replacing $1 \to 1 + \epsilon$ all at once. After use of Eqs. (C.25), we expand the obtained expression with respect to ϵ. Then the $1/\epsilon$ poles appear only in $S_{1+\epsilon}(\infty)$ and $(1 + m\epsilon)_{-1}$. As an example, consider the expansion of $S_{1+\epsilon,1+\epsilon,-2,1+\epsilon}(n)$:

$$\begin{aligned} &S_{1+\epsilon,1+\epsilon,-2,1+\epsilon}(n) \\ &= S_{1+\epsilon,1+\epsilon,-2,1+\epsilon}(\infty) - \sum_{j_1=1}^{\infty} \frac{1}{(n+j_1)^{1+\epsilon}} S_{1+\epsilon,-2,1+\epsilon}(\infty) \\ &\quad + \sum_{j_1=1}^{\infty} \frac{1}{(n+j_1)^{1+\epsilon}} \sum_{j_2=1}^{\infty} \frac{1}{(n+j_1+j_2)^{1+\epsilon}} S_{-2,1+\epsilon}(\infty) \\ &\quad - (-1)^n \sum_{j_1=1}^{\infty} \frac{(-1)^{j_1}}{(n+j_1)^{1+\epsilon}} \sum_{j_2=1}^{\infty} \frac{(-1)^{j_2}}{(n+j_1+j_2)^{1+\epsilon}} \sum_{j_3=1}^{\infty} \frac{(-1)^{j_3}}{(n+j_1+j_2+j_3)^2} S_{1+\epsilon}(\infty) \\ &\quad + (-1)^n \sum_{j_1=1}^{\infty} \frac{(-1)^{j_1}}{(n+j_1)^{1+\epsilon}} \sum_{j_2=1}^{\infty} \frac{(-1)^{j_2}}{(n+j_1+j_2)^{1+\epsilon}} \sum_{j_3=1}^{\infty} \frac{(-1)^{j_3}}{(n+j_1+j_2+j_3)^2} \sum_{j_4=1}^{\infty} \frac{1}{(n+j_1+j_2+j_3+j_4)^{1+\epsilon}} \end{aligned}$$

[#3] Of course one can obtain this result by applying the Euler-Maclaurin summation formula to the second term in Eq. (C.17) and by making use of $S_1(N) \sim \ln(N) + \gamma_E$.

$$
\begin{aligned}
&\sim S_{1+\epsilon,1+\epsilon,-2,1+\epsilon}(\infty) - \left[\frac{(1+\epsilon)_{-1}}{n^{\epsilon}} + \sum_{r=1}^{\infty}\frac{B_r}{r!}\frac{(1+\epsilon)_{r-1}}{n^{r+\epsilon}}\right] S_{1+\epsilon,-2,1+\epsilon}(\infty) \\
&\quad + \left\{(1+\epsilon)_{-1}\left[\frac{(1+2\epsilon)_{-1}}{n^{2\epsilon}} + \sum_{r=1}^{\infty}\frac{B_r}{r!}\frac{(1+2\epsilon)_{r-1}}{n^{r+2\epsilon}}\right] + \sum_{r_1=1}^{\infty}\frac{B_{r_1}}{r_1!}(1+\epsilon)_{r_1-1}\sum_{r_2=0}^{\infty}\frac{B_{r_2}}{r_2!}\frac{(1+r_1+2\epsilon)_{r_2-1}}{n^{r_1+r_2+2\epsilon}}\right\} \\
&\qquad \times S_{-2,1+\epsilon}(\infty) \\
&\quad - (-1)^n \sum_{r_1=1}^{\infty}(2^{r_1}-1)\frac{B_{r_1}}{r_1!}(2)_{r_1-1}\sum_{r_2=1}^{\infty}(2^{r_2}-1)\frac{B_{r_2}}{r_2!}(2+r_1+\epsilon)_{r_2-1}\sum_{r_3=1}^{\infty}(2^{r_3}-1)\frac{B_{r_3}}{r_3!}\frac{(2+r_1+r_2+2\epsilon)_{r_3-1}}{n^{1+r_1+r_2+r_3+2\epsilon}} \\
&\qquad \times S_{1+\epsilon}(\infty) \\
&\quad + (-1)^n\Bigg\{(1+\epsilon)_{-1}\sum_{r_1=1}^{\infty}(2^{r_1}-1)\frac{B_{r_1}}{r_1!}(2+\epsilon)_{r_1-1}\sum_{r_2=1}^{\infty}(2^{r_2}-1)\frac{B_{r_2}}{r_2!}(2+r_1+2\epsilon)_{r_2-1} \\
&\qquad\qquad \times \sum_{r_3=1}^{\infty}(2^{r_3}-1)\frac{B_{r_3}}{r_3!}\frac{(2+r_1+r_2+3\epsilon)_{r_3-1}}{n^{1+r_1+r_2+r_3+3\epsilon}} \\
&\qquad + \sum_{r_1=1}^{\infty}\frac{B_{r_1}}{r_1!}(1+\epsilon)_{r_1-1}\sum_{r_2=1}^{\infty}(2^{r_2}-1)\frac{B_{r_2}}{r_2!}(2+r_1+\epsilon)_{r_2-1}\sum_{r_3=1}^{\infty}(2^{r_3}-1)\frac{B_{r_3}}{r_3!}(2+r_1+r_2+2\epsilon)_{r_3-1} \\
&\qquad\qquad \times \sum_{r_4=1}^{\infty}(2^{r_4}-1)\frac{B_{r_4}}{r_4!}\frac{(2+r_1+r_2+r_3+3\epsilon)_{r_4-1}}{n^{1+r_1+r_2+r_3+r_4+3\epsilon}}\Bigg\}. \qquad \text{(C.31)}
\end{aligned}
$$

Here the singularities of the values of the harmonic sums at infinity can be extracted in terms of $S_{1+\epsilon}(\infty)$:

$$
\begin{aligned}
S_{1+\epsilon,1+\epsilon,-2,1+\epsilon}(\infty) = {}& \frac{1}{2}S_{1+\epsilon}^2(\infty)S_{-2,1+\epsilon}(\infty) + S_{1+\epsilon}(\infty)S_{-2,2+2\epsilon}(\infty) + S_{1+\epsilon}(\infty)S_{-3-\epsilon,1+\epsilon}(\infty) \\
& - 2S_{1+\epsilon}(\infty)S_{-2,1+\epsilon,1+\epsilon}(\infty) + \frac{1}{2}S_{-2,3+3\epsilon}(\infty) + \frac{1}{2}S_{-4-2\epsilon,1+\epsilon}(\infty) + S_{-3-\epsilon,2+2\epsilon}(\infty) \\
& - \frac{3}{2}S_{-2,1+\epsilon,2+2\epsilon}(\infty) - \frac{3}{2}S_{-2,2+2\epsilon,1+\epsilon}(\infty) - 2S_{-3-\epsilon,1+\epsilon,1+\epsilon}(\infty) + \frac{1}{2}S_{2+2\epsilon,-2,1+\epsilon}(\infty) \\
& + 3S_{-2,1+\epsilon,1+\epsilon,1+\epsilon}(\infty), \qquad \text{(C.32a)}
\end{aligned}
$$

$$
S_{1+\epsilon,-2,1+\epsilon}(\infty) = S_{1+\epsilon}(\infty)S_{-2,1+\epsilon}(\infty) + S_{-2,2+2\epsilon}(\infty) + S_{-3-\epsilon,1+\epsilon}(\infty) - 2S_{-2,1+\epsilon,1+\epsilon}(\infty). \qquad \text{(C.32b)}
$$

They are expanded such as[♯4]

$$
S_{1+\epsilon}(\infty) = \frac{1}{\epsilon} + \gamma_E + O(\epsilon), \qquad S_{-2,1+\epsilon}(\infty) = S_{-2,1}(\infty) + O(\epsilon). \qquad \text{(C.33)}
$$

The Pochhammer symbols $(a+m\epsilon)_{r-1}$ $(a \geq 2)$ can be simply expanded by using

$$
\frac{d}{dx}(x)_n = (x)_n[\psi(x+n) - \psi(x)], \qquad \text{(C.34)}
$$

$$
\psi^{(p)}(x+n) - \psi^{(p)}(x) = (-1)^p p![S_{p+1}(x+n-1) - S_{p+1}(x-1)]. \qquad \text{(C.35)}
$$

[♯4] Formally they should be expanded up to higher order such as

$$
\begin{aligned}
S_{1+\epsilon}(\infty) &= \frac{1}{\epsilon} + \gamma_E - \epsilon\gamma_1 + \frac{\epsilon^2}{2!}\gamma_2 - \frac{\epsilon^3}{3!}\gamma_3 + \cdots, \\
S_{-2,1+\epsilon}(\infty) &= S_{-2,1}(\infty) + \left.\frac{dS_{-2,1+\epsilon}(\infty)}{d\epsilon}\right|_{\epsilon=0}\epsilon + \left.\frac{d^2S_{-2,1+\epsilon}(\infty)}{d\epsilon^2}\right|_{\epsilon=0}\frac{\epsilon^2}{2!} + \left.\frac{d^3S_{-2,1+\epsilon}(\infty)}{d\epsilon^3}\right|_{\epsilon=0}\frac{\epsilon^3}{3!} + \cdots.
\end{aligned}
$$

However, these higher order terms are finally canceled with the cancellation of the $1/\epsilon^m$ poles, and never appear in the final expression after taking the limit $\epsilon \to 0$.

Putting it all together and taking the limit $\epsilon \to 0$, one can obtain

$$
\begin{aligned}
&S_{1,1,-2,1}(n) \\
&\quad \sim \frac{1}{2}S_{-2,1}(\infty)L^2(n) + [S_{-3,1}(\infty) + S_{-2,2}(\infty) - 2S_{-2,1,1}(\infty)]L(n) + \frac{1}{2}S_{-4,1}(\infty) + S_{-3,2}(\infty) + \frac{1}{2}S_{-2,3}(\infty) \\
&\qquad - 2S_{-3,1,1}(\infty) - \frac{3}{2}S_{-2,1,2}(\infty) - \frac{3}{2}S_{-2,2,1}(\infty) + \frac{1}{2}S_{2,-2,1}(\infty) + 3S_{-2,1,1,1}(\infty) \\
&\qquad + \frac{1}{2}S_{-2,1}(\infty)\frac{L(n)}{n} + \left[-\frac{1}{2}S_{-2,1}(\infty) + \frac{1}{2}S_{-3,1}(\infty) + \frac{1}{2}S_{-2,2}(\infty) - S_{-2,1,1}(\infty)\right]\frac{1}{n} \\
&\qquad - \frac{1}{12}S_{-2,1}(\infty)\frac{L(n)}{n^2} + \left[\frac{3}{8}S_{-2,1}(\infty) - \frac{1}{12}S_{-3,1}(\infty) - \frac{1}{12}S_{-2,2}(\infty) + \frac{1}{6}S_{-2,1,1}(\infty)\right]\frac{1}{n^2} - \frac{1}{8}S_{-2,1}(\infty)\frac{1}{n^3} \\
&\qquad + \left[\frac{1}{120}S_{-2,1}(\infty) + \frac{(-1)^n}{8}\right]\frac{L(n)}{n^4} + \left[\frac{1}{288}S_{-2,1}(\infty) + \frac{1}{120}S_{-3,1}(\infty) + \frac{1}{120}S_{-2,2}(\infty) - \frac{1}{60}S_{-2,1,1}(\infty)\right]\frac{1}{n^4} \\
&\qquad - (-1)^n\frac{9}{16}\frac{L(n)}{n^5} + \left[\frac{1}{48}S_{-2,1}(\infty) + \frac{(-1)^n}{4}\right]\frac{1}{n^5} + \cdots,
\end{aligned}
$$

where

$$L(n) = \ln(n) + \gamma_E. \tag{C.36}$$

C.4 Numerical Evaluation of the Harmonic Sums over the Complex Plane

Now, we consider how to evaluate the harmonic sums numerically in the complex domain. The simplest method is evaluate the infinite sum in Eq. (C.16) recursively (the single harmonic sums are translated into polygammas), e.g., [72] (See also [80]). In most cases, however, as easily expected the numerical convergence is very slow.

Another approach to obtain the appropriate representations of the harmonic sums for the complex argument is to express them in terms of the Mellin transforms of several basic functions as well as polygamma functions [73]. The integrand of the Mellin transform is numerically expanded by using the minimax approximation method and then the Mellin transform is given in a semi-analytical way (See also Appendix of Ref. [74]). In Ref. [73-c], they found the appropriate representations for the individual basic functions, the building blocks of the three-loop anomalous dimensions, which corresponds to weight 5. Their numerical representations are fast and precise enough, and thus they are satisfiable in our application at this time. However, if one wants to obtain the representations up to more higher weight functions, then the newer basic functions appear, and one have to consider each newer basic functions (for example, the massless three-loop Wilson coefficients [81] are expressed in n-space in terms of the harmonic sums up to weight 6). Moreover, the reconstruction of the harmonic sums from the Mellin transforms of the basic functions is rather complicated.

This is why other methods for the numerical evaluation of the harmonic sums over the complex n-plane are welcome. Here we make use of the asymptotic series expansions of the harmonic sums at large n together with the translation relations of them, which are discussed in the previous section, for the numerical evaluation. In fact, for evaluating polygamma functions, which are related with single harmonic sums by Eqs. (C.11), the asymptotic expansions and translation relations of them are often used (e.g., [74]). The asymptotic expansion of $S_{-2,1}(n)$ was also used for the evaluation of it in the old days (e.g., [76]). Therefore it seems quite natural to evaluate the higher harmonic sums with the asymptotic series expansions and the translation relations of them.

The asymptotic series rapidly converge for large n, in contrast badly diverge for small n. Additionally, in the complex domain, noting that the remainder error term of the expansions Eqs. (C.25) has a form such

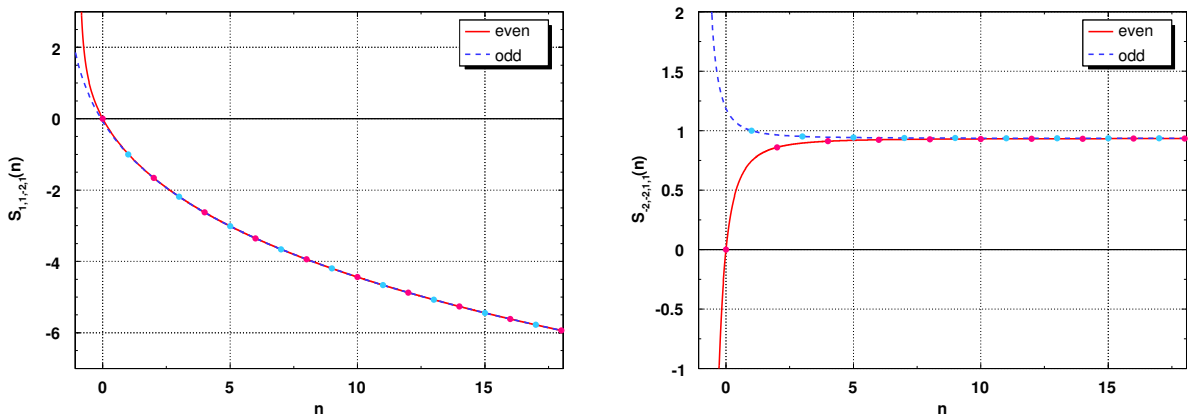

Figure C.1: Continued $S_{1,1,-2,1}(n)$ and $S_{-2,-2,1,1}(n)$ from their even/odd values.

as

$$|R| \lesssim (\text{const}) \times \int_0^\infty dx \left| \frac{1}{(n+x)^q} \right|, \tag{C.37}$$

we have to keep n off the negative real axis as well as zero in order to obtain the numerical values of the sum preciously as expected. Then, by using the translation relations Eqs. (C.24) recursively, one can make the connection between the values of the harmonic sums for small (or treacherous) n and that for sufficiently large (and safe) n. Therefore our algorithm for the evaluating the harmonic sums over the complex n-plane is simple:

- If $\mathrm{Re}(n) > n_0$ or $|\mathrm{Im}(n)| > n_1$, we use the asymptotic series expansions for the evaluation of the harmonic sums, where n_0 and n_1 are some sufficiently large real number (we take simply $n_1 = n_0$, i.e., keep n off the negative real axis equally to zero for safety when we use the asymptotic expansion for the evaluation). Choosing n_0 as some fixed (sufficiently large) integer, we can determine up to what order the expansion is needed for obtaining required accuracy.

- If n is not in the above region, we use the translation relation for shifting n recursively until $\mathrm{Re}(n) > n_0$.

As examples, the result for $S_{1,1,-2,1}(n)$ and $S_{-2,-2,1,1}(n)$ from even/odd values (i.e., $S^{\mathrm{even}}_{1,1,-2,1}(n)$, $S^{\mathrm{odd}}_{1,1,-2,1}(n)$, $S^{\mathrm{even}}_{-2,-2,1,1}(n)$ and $S^{\mathrm{odd}}_{-2,-2,1,1}(n)$) are presented in Fig. C.1.

The evaluation of the harmonic sums with this algorithm is of course rather slow for small n (especially for higher harmonic sums) but very fast for large n. However, what is more important is that this simple method can be applied to more higher harmonic sums in its entirety. The simplicity of the method allows us for the possibility of automatism of the construction of the program code to numerically evaluate the harmonic sums up to any weight over the complex plane. We plan to release a set of `FORTRAN` subroutines to compute any harmonic sums with a complex argument n (at least) up to weight 6 by using this algorithm [82].

References

[1] http://lhc.web.cern.ch/lhc/.

[2] http://www.linearcollider.org/cms/.

[3] T. F. Walsh, Phys. Lett. B **36**, 121 (1971).

[4] S. J. Brodsky, T. Kinoshita and H. Terazawa, Phys. Rev. Lett. **25**, 972 (1970);
H. Terazawa, Rev. Mod. Phys. **45**, 615 (1973).

[5] T. F. Walsh and P. M. Zerwas, Phys. Lett. B **44**, 195 (1973).

[6] R. L. Kingsley, Nucl. Phys. B **60**, 45 (1973).

[7] E. Witten, Nucl. Phys. B **120**, 189 (1977).

[8] W. A. Bardeen and A. J. Buras, Phys. Rev. D **20**, 166 (1979) [Erratum-ibid. D **21**, 2041 (1980)].

[9] A. Vogt, S. Moch and J. Vermaseren, Acta Phys. Polon. B **37**, 683 (2006).

[10] J. J. Sakurai, *Currents and Mesons*, (Univ. Chicago Press, 1969).

[11] T. Uematsu and T. F. Walsh, Phys. Lett. B **101**, 263 (1981).

[12] T. Uematsu and T. F. Walsh, Nucl. Phys. B **199**, 93 (1982).

[13] G. Rossi, Phys. Rev. D **29**, 852 (1984).

[14] K. Sasaki and T. Uematsu, Phys. Rev. D **59**, 114011 (1999); Phys. Lett. B **473**, 309 (2000); Eur. Phys. J. C **20**, 283 (2001).

[15] M. Glück, E. Reya and C. Sieg, Eur. Phys. J. C **20**, 271 (2001).

[16] H. Baba, K. Sasaki and T. Uematsu, Phys. Rev. D **65**, 114018 (2002).

[17] K. Sasaki, T. Ueda and T. Uematsu, Phys. Rev. D **73**, 094024 (2006).

[18] T. Ueda, T. Uematsu and K. Sasaki, Phys. Lett. B **640**, 188 (2006).

[19] W. A. Bardeen, A. J. Buras, D. W. Duke and T. Muta, Phys. Rev. D **18**, 3998 (1978).

[20] R. Nisius, Phys. Rept. **332**, 165 (2000);
M. Krawczyk, A. Zembrzuski and M. Staszel, Phys. Rept. **345**, 265 (2001);
I. Schienbein, Annals Phys. **301**, 128 (2002).

[21] T. Muta, *Foundations of quantum chromodynamics. Second edition*, (World Scientific, Singapore, 1998);
R. Brock *et al.* [CTEQ Collaboration], Rev. Mod. Phys. **67**, 157 (1995).

[22] a) V. M. Budnev, V. L. Chernyak and I. F. Ginzburg, Nucl. Phys. B **34**, 470 (1971);
b) V. M. Budnev, I. F. Ginzburg, G. V. Meledin and V. G. Serbo, Phys. Rept. **15**, 181 (1975).

[23] R. W. Brown and I. J. Muzinich, Phys. Rev. D **4**, 1496 (1971).

[24] C. E. Carlson and W. K. Tung, Phys. Rev. D **4**, 2873 (1971), [Erratum-ibid. D **6**, 402 (1972)].

[25] K. Sasaki, J. Soffer and T. Uematsu, Phys. Lett. B **522**, 22 (2001).

[26] K. Sasaki, J. Soffer and T. Uematsu, Phys. Rev. D **66**, 034014 (2002).

[27] P. Hoodbhoy, R. L. Jaffe and A. Manohar, Nucl. Phys. B **312**, 571 (1989).

[28] P. Mathews and V. Ravindran, Int. J. Mod. Phys. A **11**, 2783 (1996).

[29] H. Kolanoski, Springer Tracts Mod. Phys. **105**, 1 (1984).

[30] C. Berger and W. Wagner, Phys. Rept. **146**, 1 (1987).

[31] H. Fritzsch, M. Gell-Mann and H. Leutwyler, Phys. Lett. B **47**, 365 (1973).

[32] S. Weinberg, Phys. Rev. Lett. **19**, 1264 (1967).

[33] A. Salam, in *Proceedings of the 8th Novel Symposium*, ed. by N. Svartholm (Almqvist and Wiksells, Stockholm, 1968), 367.

[34] C. N. Yang and R. L. Mills, Phys. Rev. **96**, 191 (1954).

[35] L. D. Faddeev and V. N. Popov, Phys. Lett. B **25**, 29 (1967).

[36] W. Pauli and F. Villars, Rev. Mod. Phys. **21**, 434 (1949).

[37] G. 't Hooft, Nucl. Phys. B **61**, 455 (1973).

[38] D. J. Gross and F. Wilczek, Phys. Rev. Lett. **30**, 1343 (1973); Phys. Rev. D **8**, 3633 (1973).

[39] H. D. Politzer, Phys. Rev. Lett. **30**, 1346 (1973);
H. Georgi and H. D. Politzer, Phys. Rev. D **9**, 416 (1974).

[40] A. Zee, Phys. Rev. D **7**, 3630 (1973).

[41] S. R. Coleman and D. J. Gross, Phys. Rev. Lett. **31**, 851 (1973).

[42] K. G. Wilson, Phys. Rev. **179**, 1499 (1969).

[43] W. Zimmermann, "Lectures On Elementary Particles and Quantum Field Theory," Edited by S. Deser, M. Grisaru and H. Pendleton, (MIT press, 1970).

[44] N. H. Christ, B. Hasslacher and A. H. Mueller, Phys. Rev. D **6**, 3543 (1972).

[45] O. V. Tarasov, A. A. Vladimirov and A. Y. Zharkov, Phys. Lett. B **93**, 429 (1980).

[46] S. A. Larin and J. A. M. Vermaseren, Phys. Lett. B **303**, 334 (1993).

[47] E. G. Floratos, D. A. Ross and C. T. Sachrajda, Nucl. Phys. B **129**, 66 (1977) [Erratum-ibid. B **139**, 545 (1978)]; Nucl. Phys. B **152**, 493 (1979).

[48] W. L. van Neerven and E. B. Zijlstra, Phys. Lett. B **272**, 127 (1991);
E. B. Zijlstra and W. L. van Neerven, Phys. Lett. B **273**, 476 (1991); Nucl. Phys. B **383**, 525 (1992).

[49] S. Moch and J. A. M. Vermaseren, Nucl. Phys. B **573**, 853 (2000).

[50] S. Moch, J. A. M. Vermaseren and A. Vogt, Nucl. Phys. B **621**, 413 (2002).

[51] D. J. Gross and F. Wilczek, Phys. Rev. D **8**, 3633 (1973); Phys. Rev. D **9**, 980 (1974).

[52] H. Georgi and H. D. Politzer, Phys. Rev. D **9**, 416 (1974).

[53] G. Curci, W. Furmanski and R. Petronzio, Nucl. Phys. B **175**, 27 (1980);
W. Furmanski and R. Petronzio, Phys. Lett. B **97**, 437 (1980).

[54] R. Hamberg and W. L. van Neerven, Nucl. Phys. B **379**, 143 (1992).

[55] S. Moch, J. A. M. Vermaseren and A. Vogt, Nucl. Phys. B **688**, 101 (2004).

[56] A. Vogt, S. Moch and J. A. M. Vermaseren, Nucl. Phys. B **691**, 129 (2004).

[57] M. Fontannaz and E. Pilon, Phys. Rev. D **45**, 382 (1992).

[58] M. Glück, E. Reya and A. Vogt, Phys. Rev. D **45**, 3986 (1992).

[59] Y. Matiounine, J. Smith and W. L. van Neerven, Phys. Rev. D **57**, 6701 (1998).

[60] E. Remiddi and J. A. M. Vermaseren, Int. J. Mod. Phys. A **15**, 725 (2000).

[61] J. A. M. Vermaseren, Int. J. Mod. Phys. A **14**, 2037 (1999).

[62] J. A. M. Vermaseren, arXiv:math-ph/0010025.

[63] A. Zee, F. Wilczek and S. B. Treiman, Phys. Rev. D **10**, 2881 (1974).

[64] I. Hinchliffe and C. H. Llewellyn Smith, Nucl. Phys. B **128**, 93 (1977).

[65] D. W. Duke, J. D. Kimel and G. A. Sowell, Phys. Rev. D **25**, 71 (1982);
S. N. Coulson and R. E. Ecclestone, Phys. Lett. B **115**, 415 (1982); Nucl. Phys. B **211**, 317 (1983);
A. Devoto, D. W. Duke, J. D. Kimel and G. A. Sowell, Phys. Rev. D **30**, 541 (1984);
J. L. Miramontes, J. Sanchez Guillen and E. Zas, Phys. Rev. D **35**, 863 (1987).

[66] D. I. Kazakov and A. V. Kotikov, Nucl. Phys. B **307**, 721 (1988) [Erratum-ibid. B **345**, 299 (1990)].

[67] D. I. Kazakov, A. V. Kotikov, G. Parente, O. A. Sampayo and J. Sanchez Guillen, Phys. Rev. Lett. **65**, 1535 (1990) [Erratum-ibid. **65**, 2921 (1990)].

[68] J. Sánchez Guillén, J. Miramontes, M. Miramontes, G. Parente and O. A. Sampayo, Nucl. Phys. B **353**, 337 (1991).

[69] S. A. Larin and J. A. M. Vermaseren, Z. Phys. C **57**, 93 (1993).

[70] D. I. Kazakov and A. V. Kotikov, Phys. Lett. B **291**, 171 (1992).

[71] W. M. Yao *et al.* [Particle Data Group], J. Phys. G **33**, 1 (2006).

[72] A. V. Kotikov and V. N. Velizhanin, arXiv:hep-ph/0501274.

[73] a) J. Blümlein and S. Kurth, Phys. Rev. D **60**, 014018 (1999);
b) J. Blümlein, Comput. Phys. Commun. **133**, 76 (2000);
c) J. Blümlein and S. O. Moch, Phys. Lett. B **614**, 53 (2005).

[74] M. Glück, E. Reya and A. Vogt, Z. Phys. C **48**, 471 (1990).

[75] S. Moch, P. Uwer and S. Weinzierl, J. Math. Phys. **43**, 3363 (2002);
S. Weinzierl, J. Math. Phys. **45**, 2656 (2004).

[76] A. González-Arroyo, C. López and F. J. Ynduráin, Nucl. Phys. B **153**, 161 (1979).

[77] L. Euler, Novi Comm. Acad. Sci. Petropol. **20**, 140 (1775).

[78] D. Zagier, First European Congress of Mathematics, Vol. II, Birkhauser, Boston, 497 (1994).

[79] C. Costermans, J. Y. Enjalbert, Hoang Ngoc Minh and M. Petitot, ISSAC '05: Proceedings of the 2005 international symposium on Symbolic and algebraic computation, ACM Press, New York, 100 (2005).

[80] J. Blümlein and S. Kurth, arXiv:hep-ph/9708388.

[81] J. A. M. Vermaseren, A. Vogt and S. Moch, Nucl. Phys. B **724**, 3 (2005).

[82] T. Ueda, in preparation.